Design, development and validation of a multi-step plasma-based strategy for the direct functionalization of L605 cobalt chromium alloy for the grafting of bioactive molecules and its application in cardiovascular devices

Thèse

Sergio Agustin Diaz Rodriguez

Doctorat en génie des matériaux et de la métallurgie
Philosophiæ doctor (Ph. D.)

Québec, Canada

Design, development and validation of a multi-step plasma-based strategy for the direct functionalization of L605 cobalt chromium alloy for the grafting of bioactive molecules and its application in cardiovascular devices

Thèse

Sergio Diaz-Rodriguez

Sous la direction de :

Diego Mantovani, directeur de recherche

Résumé

Les maladies cardio-vasculaires sont la principale cause de mortalité dans le monde. Parmi celles-ci, et une des plus importantes, se trouve l'athérosclérose. Cette maladie se traduit par la formation d'une plaque sur les parois artérielles réduisant alors le diamètre luminal. La plaque d'athérome entrave la circulation du sang et peut se compliquer par la formation d'un thrombus artérielle pouvant provoquer un infarctus du myocarde. Une intervention capable de rétablir le flux (recanalisation) est alors nécessaire. Dans le cas des artères coronaires, l'intervention coronaire est percutanée (ICP) et consiste à amener et déployer jusqu'au site malade, une endoprothèse, appelé aussi stent. Un stent est un petit treillis métallique tubulaire qui permet de rouvrir la lumière de l'artère et de rétablir la circulation sanguine. Il sert aussi de support à l'artère malade pour empêcher son affaissement. Cependant, après implantation, certaines complications sont induites, telle que la resténose intra-stent (ISR) qui se caractérise par la réduction de la lumière de l'artère, reconduisant les problèmes créés par la plaque d'athérome. Ce phénomène est essentiellement dû à une prolifération excessive des cellules musculaires lisses, et qui résulte d'une lésion de l'endothélium lors de l'implantation. Afin de limiter cette complication, la première approche a été de changer les matériaux utilisés pour ces endoprothèses. Les principaux alliages utilisés pour fabriquer des stents sont l'acier inoxydable, les alliages de nitinol et ceux de chrome cobalt, plus particulièrement le L605. Ce dernier, dû à ses propriétés mécaniques, permet la fabrication de dispositifs plus minces, donc moins de métaux présents dans le corps humain, et a démontré induire moins de complications cliniques. Néanmoins, malgré la diminution des complications par rapport aux autres alliages, les endoprothèses nues en L605 ne s'intègrent que peu ou pas du tout dans le tissu artériel de l'hôte. Pour répondre aux exigences biologiques et cliniques, l'idéal serait d'avoir un dispositif qui favoriserait le recouvrement du dispositif par l'endothélium, ou « endothélialisation » et qui aurait un faible potentiel thrombotique et inflammatoire. L'approche couramment utilisée pour répondre à ces critères est de recourir à des dispositifs qui libèrent des médicaments anti-inflammatoires. Pour ce faire, il faut recouvrir les dispositifs métalliques avec des revêtements à base de polymères, en tant que couche intermédiaire, fonctionnalisée ensuite par des molécules bioactives. Toutefois, les dépôts de ces couches polymériques impliquent l'utilisation de chimie en solution incluant des solvants organiques. En outre, ces dernières démontrent avoir une faible adhésion au substrat métallique, dû au procédé utilisé, mais aussi un manque de cohésion. Lors de la procédure d'implantation, les stents subissent une déformation plastique, comme ces revêtements manquent de résistance, ils ont tendance à fissurer ou délaminer.

Ce projet de recherche s'insère donc dans cette problématique générale, et propose une nouvelle approche qui permettrait d'éviter ce revêtement polymérique, tout en apportant les propriétés biologiques recherchées. Pour ce faire, la modification de surface proposée implique la fonctionnalisation directe des surfaces métalliques par un procédé plasma. Ce procédé permet de ne pas modifier les propriétés de cœur du matériau, et de créer des

groupes fonctionnels en surface, ici des groupes amine réactifs (NH_2), qui servent de points d'ancrage pour le greffage ultérieur des molécules bioactives d'intérêt. En résumé, ce procédé original peut être divisé en 3 parties principales : a) préparation de la surface, b) fonctionnalisation par plasma et c) greffage de molécules bioactives. Tout au long de ce projet de recherche, l'optimisation de chaque partie a été réalisée en vue d'obtenir les propriétés adéquates et nécessaires pour l'application cardiovasculaire visée. Concernant la partie a), c'est-à-dire la préparation de la surface, les traitements suivants ont été testés : électropolissage, traitements thermiques et implantation ionique par immersion dans un plasma. Ces modifications ont été optimisées en vue d'obtenir une couche d'oxyde stable sous déformation présentant la meilleure résistance possible à la corrosion, tout en démontrant la plus haute efficacité d'amination directe par plasma pour la partie b). Enfin, en ce qui concerne le bloc c), le greffage de molécule bioactive, deux bras de liaison différents ont été étudiés pour évaluer leur impact sur la conformation et la performance biologique. Cette étude a été effectuée avec un peptide bioactif dérivé de la molécule d'adhésion des cellules endothéliales et des plaquettes (PECAM-1 ou CD31), en raison de ses propriétés anti-inflammatoire, anti-thrombotique et pro-endothélialisation. Les 2 bras d'ancrage testés sont un à chaine courte, l'anhydride glutarique (GA), contenant seulement 5 atomes de carbone, et un à longue chaine (600 atomes), le polyéthylène glycol (PEG) choisi aussi pour ses propriétés anti-adhérentes.

Tout d'abord, cette stratégie a été développée sur des échantillons plats, qui facilitaient grandement les analyses de surface, telles que XPS et ToF-SIMS, et donc les processus d'optimisation de chaque étape, comme la résistance à la déformation, corrosion et l'analyse des propriétés biologiques. Ceci a permis de démontrer que le prétraitement de surface optimal pour les substrats L605 était l'électropolissage, agissant sur sa couche d'oxyde passive pour une efficacité maximale lors de l'étape d'amination. Le bras de liaison qui a démontré le plus grand potentiel pour immobiliser le peptide d'intérêt est le PEG, avec une augmentation significative de la migration et viabilité des cellules endothéliales, par rapport au substrat métallique nu. De plus, le greffage du peptide sur le PEG ajoutait des propriétés anti-thrombotique et anti-inflammatoire par rapport aux échantillons électropolis. Ce procédé a été ensuite adapté à des stents, dont la configuration 3D est très complexe. Après optimisation, les stents pegylées + peptides biomimétiques (Plasma-P8RI) ont été testés in vivo par implantation dans les coronaires de porc porcin pendant 7 jours et 28 jours et leur potentiel de ré-endothélialisation et anti-resténotique ont été évalués. Il a été constaté que la stratégie proposée dans ce projet de recherche favorisait la ré-endothélialisation après 7 jours par rapport au DES (Drug Eluting Stent) commercial, et limitait l'adhérence des leucocytes et des plaquettes lorsque comparé au BMS (Bare Metal Stent). Après 28 jours d'implantation le diamètre luminal des artères n'était pas réduit sur le stent Plasma-P8RI, ce qui signifie que ces stents modifiés ne présentaient pas de risque de resténose, contrairement aux BMS.

Ce projet de recherche a permis de développer et de valider une stratégie prometteuse consistant à immobiliser directement des molécules bioactives sur des dispositifs cardiovasculaires en L605, alliage de chrome-cobalt.

A notre connaissance, cette approche n'a jamais été rapportée dans la littérature à notre connaissance. Cette stratégie originale, dépourvue des limites associées à l'usage des polymères et basée sur un procédé plasma, présente des avantages évidents et ouvre la voie vers le développement de dispositifs cardiovasculaires innovants.

Abstract

Cardiovascular diseases represent the leading cause of death in the world. Among them is atherosclerosis that characterizes by the formation of a plaque on the arterial walls that narrows the lumen diameter. This atherosclerotic plaque disrupts the blood flow and can be complicated by thrombosis which can ultimately lead to myocardial infarction. Efficient revascularization is mandatory to treat this disease and a percutaneous coronary intervention (PCI) is performed complemented with the deployment of a stent. Stents are tiny wire mesh that reopens the artery, re-establishing the blood flow whilst supporting the artery avoiding its collapse. Nevertheless, complications after stent implantation exist and in-stent restenosis (ISR) is one of the major concerns. This complication is characterized by the reduction of the lumen diameter, similar to an atherosclerotic plaque, and it is associated to the wound caused on the endothelium by the stent implantation followed by the over-proliferation of smooth muscle cells. One of the first strategies to decrease ISR involved the manufacture of stents using different alloys such as stainless steel, nitinol and cobalt chromium alloys (L605). The latest alloy, L605, has generated significant interest because it allows the fabrication of thinner devices, which have decreased post-implantation clinical complications. Nonetheless, despite the decrease in ISR, when compared to other alloys, the integration of L605 bare metal stents in the host tissue is minimal or inexistent. Thus, enhanced biological properties, such as endothelialisation, low thrombosis activity and anti-inflammatory behaviour represent mandatory requirements for clinical applications. To confer these properties onto metallic devices, polymeric-based coatings, as an intermediate layer to further functionalize with bioactive molecules, are often deposited. Nonetheless, major techniques to deposit these polymeric coatings involve the use of wet-chemistry and do not ensure total resistance during the stent implantation procedure due to lack of cohesion and delamination of the polymeric layer.

Thus, a novel approach that foregoes this previously mandatory coating step was developed in this research project. This novel approach involves the use of plasma-based techniques to create functional groups (reactive amine groups, -NH2), directly onto the metallic surface without modifying the bulk properties, that can be used as anchor points for the further grafting of bioactive molecules of interest. Briefly, this novel approach can be divided in 3 blocks: a) Surface preparation, b) plasma functionalization and c) bioactive molecule grafting. Throughout this research project the optimization of these main blocks was performed aiming for the desired cardiovascular application. Concerning block a), surface preparation, electropolishing, thermal treatments and plasma immersion ion implantations were performed to obtain an oxide layer deformation and corrosion resistant whilst demonstrating the highest direct plasma amination efficiency, for block b). Finally, as regards block c), bioactive molecule grafting, two different linking arms were studied to assess their impact on conformation, and the biological performance of a bioactive peptide derived from the platelet endothelial cell adhesion molecule (PECAM-1 or CD31) due to its pro-endothelialization, anti-inflammatory and anti-thrombotic potential: Glutaric

anhydride (GA), as a short chain spacer of 5 carbons, and polyethylene glycol (PEG), as a long chain spacer with antifouling properties.

Initially, this strategy was developed on flat samples where using a combination of high-resolution surface characterizations techniques, such as XPS and ToF-SIMS, and corrosion, deformation and biological tests it was confirmed that the optimal surface pre-treatment for L605 was electropolishing, due to its passive oxide layer and that it further allowed to obtain the highest amination efficiency. Furthermore, the best linking arm to immobilize the peptide was PEG, which demonstrated a significantly increase on endothelial cell viability with a faster migration, when compared to the bare metallic substrate. Moreover, peptides immobilized by PEG demonstrated that endothelial cells attached to the surface presented an anti-thrombotic and anti-inflammatory phenotype, when compared to electropolished samples. Thus, this biomimetic surface was selected for an in vivo trial in porcine model to evaluate its potential re-endothelialization and anti-restenotic activity. It was found that by directly attaching a CD31 agonist onto the bare metal stent by this strategy improved re-endothelialization after 7 days when compared to commercial DES, with further, low adhesion of leukocytes and platelets when compared to BMS. Moreover, after 28 days of implantation, Plasma-P8RI did not present a significant decrease on the lumen diameter, which was not the case for BMS that presented in-stent restenosis after this period.

Overall, this research project allowed the development and validation of a promising strategy to directly immobilize bioactive molecules onto L605 cobalt chromium cardiovascular devices, providing clear advantages of medical devices currently on the market. Furthermore, to the best of our knowledge, such plasma-based multi-step strategy has never been previously reported in literature.

Table of contents

List of Figures

List of Tables

Liste des abréviations, sigles, acronymes

AFM	Atomic force microscopy
BMS	Bare metal stent
CD31	Cluster of differentiation 31
CVDs	Cardiovascular diseases
DES	Drug eluting stent
EC	Endothelial cells
EDC	1-ethyl-3-(3-dimethylaminopropyl) carbodiimide hydrochloride
EP	Electropolished
FDA	Food drug administration
GA	Glutaric anhydride
HCAEC	Human coronary artery endothelial cells
HUVEC	Human umbilical vein endothelial cells
IL-6	Interleukyn-6
LA	Linking arm
LBB	Laboratory of bioengineering and biomaterials
LVTS	Laboratory for vascular and translational science
MC	Mean count
MW	Microwave
OCP	Open circuit potential
P23	23 amino acid peptide
P8FI	8 amino acid peptide forward
P8RI	8 amino acid peptide reversed
PBMA	Polybuthyl methacrylate
PBS	Phosphate buffer solution
PCI	Percutaneous coronary intervention
PDLLA	Poly-DL-Lactic acid
PECAM-1	Platelet endothelial cell adhesion molecule
PEG	Polyethilene glycol
PIII	Plasma immersion ion implantation
PLGA	Poly(lactic-co-glycolyc acid)
PLLA	Poly-L-Lactic acid
PMMA	Polymethyl methacrylate
Rq	Root mean square roughness
SEM	Scanning electron microscopy
SMC	Smooth muscle cells
SS316L	Stainless steel 316L
TFPI	Tissue factor pathway inhibitor
ToF-SIMS	Time of flight-secondary ion mass spectrometry
TT	Thermal treated
VCAM-1	Vascular cell adhesion molecule-1
WCA	Water contact angle
XPS	X-ray photoelectric spectroscopy

"En la autopista de la vida, si te saltas la salida hay que esperar…"

El Poeta Halley – Recorded by Love of Lesbian. 2016.

Para las 4 S. Por ayudarme a tomar las salidas correctas de esta autopista…

Acknowledgements

I would like to acknowledge my supervisor Diego Mantovani for the opening the doors of the laboratory of biomaterials and bioengineering allowing me to pursuit my PhD. To the members of the jury that reviewed this manuscript, for their discussion and suggestions to improve it: Marie Arsenault, Giuseppina Caligiuri, Marta Cerruti, and Frédéric Chaubet. To the director of the PhD program, Edward Ghali.

To all the administrative personal that were always present and willing to help me whenever I was in need, specially to: Andrée Lord and Karine Fortin.

To the people from the LBB who during these years helped me to improve my scientific discussion and that taught me how to overcome the different challenges that I faced throughout my project with a multidisciplinary approach: Rana Tolouei, Daniele Pezzoli, Caroline Loy, Lucie Levesque, Carlo Paternoster and Stephane Turgeon.

To my colleagues at the INSERM, specially to Giuseppina Caligiuri and Jules Mesnier for their patience and their help during my internship in their laboratory. To the colleagues at Université de Namur, specially to Laurent Houssiau and Céline Noël for their valuable contribution in this work and for the scientific discussions we had during these years.

I think it is also important to say that when someone leaves far away from their country and family, there is a necessity to stablish new bonds and relationships that could, somehow, fill this void. Thus, I want to really acknowledge the people that made this adventure to flow as easy as possible.

To all my families, present during these years in Quebec:

The LBB et al. – For all the coffees, card games, 5 a 7, picnics, going outs, conferences and activities. Samira, Majid, Jad, Loffredo, Ana Laura, Laurine, Alex, Simon, Geoffroy, Juliana, Clayton, Mahrok, Morgane, Caroline aka Pollo, Emilie, Ivan, el Champa and Natalia. Special shout out to *The Boss*, Pascale Chevallier. Without you, this journey would have been so much more difficult, professionally and personally speaking. Thanks for being there, for supporting me morally and not letting me down. For kicking and pushing me when I needed and for being one of the human beings I could always count with. I appreciate that a lot, sincerely.

The Europeans – For your hospitality, kindness and friendship no matter the distance nor how much time had passed since the first and last time we saw each other. Gabriela, Asier and Pablo: Mis hermanos de la madre patria. Anja and Max, the Germans. The frenchies: Ambre and Chloe, for their support and encouragement on the improvement of my French and for their honest friendship; Camille and Mihaela (considered French) for their

support during my stay in Paris; and finally Pauline, for who I have no words to describe how much your time and our deep discussions about everything and nothing helped me throughout this long journey. I am certain that we all will cross our paths again one day not so far from now.

Les Montréalaises – The neighbours who have being there whenever I pass around. Cary and Guillaume, for all the laughs, parties and chilling in the park. To Gagnon, Piston and Makita. Finally, to Salome, for always listening to me during my complains and for celebrating our achievements.

Para as brasileiras – Caro, Lety and Dimi. Muito obrigado por sua amizade e tudo que passamos juntos.

La familia mexa – A Astrid y a Linda, a mis compitas mexas. Solo tengo una cosa que decir: ¿Vas a cenar? Gracias infinitas, por los horoscopos, los cafes, los vinos rosas, el Mario kart y demás. Much love for you.

The 8-1155 crew – For sharing life with me, every single day, and being my closest family here in Qc. The oldschool 8-1155 aka the roomies: Ele, Ludi and Vane; Thanks for opening your home to me. The current 8-1155: Pancho, Astrid, Alessandra and Sara. For whom the only thing I have to say is thanks for always being there, for all the winters, concerts, festivals and most importantly, all the Novembers we were able to survive.

To the dream team – Gabriel, Max, Leodraccio, Pancho. The best team one can think about to chill around the city and for being some of the best colleagues I have ever had and whom I consider my brothers.

To my Destiny clan – Without you guys, I'm certain that this journey would have been in Heroic mode with extinguish modifier. Thanks for all the hours we have invested and shared during these years. Who would've thought that an online game could have given me some of my best friends? Special shout out to Koopa, Gnomie, Fabi, Nahtte, Seikrid, Gymlu, Napo, Javi, Rorro, JC and Lucho.

Furthermore, I would like to express a lot my gratitude to people that have supported me a lot: Sofi, Melis, Gloria, Saeideh and Lolo. Thanks a lot for your friendship, support, laughs and complains, deep discussions about the future of things.

To all the people I left behind in Mexico. To my lifetime friends, Angie and Moni, that after more than 20 years are still around. To Lorena, for everything we have passed together, for your unconditional friendship, understanding and support. I'm happy and lucky to still have you around me, nesh.

Y, para terminar, a mi verdadera familia, la biológica. A mis padres, por todo el sacrificio que han hecho durante todos estos años para realizarme profesionalmente. Por ser el mejor ejemplo y por haberme dado los valores que me han ayudado a ser quien soy. A mis hermanos, por ser una gran motivación para seguir adelante. Para

Abraham, quien me ha demostrado que a pesar de las adversidades que se puedan presentar en algún momento de la vida, no hay que agachar la cabeza y hay que salir adelante, en equipo. Para Gore, que a pesar de todo el tiempo que no hemos pasado juntos los últimos años, me ha escuchado en momentos en que lo necesito y por todas esas fotos de los perrhijos. A mi Madre, por creer en mí y nunca decir no a cualquier idea loca que se me ocurriera, por levantarme cuando lo necesito y por guiarme durante toda mi vida. Gracias infinitas.

Foreword

The present thesis has been developed at the *Université Laval* (Quebec, Canada) with strong collaborations with the *Université de Namur* (Namur, Belgium) and *Laboratory for Vascular Translational Science* (LVTS) at the INSERM U1148 (Paris, France). This research project was focused on the design, development and validation of novel strategy for the direct immobilization of bioactive molecules on L605 cobalt chromium alloy surface for cardiovascular applications. This strategy allows to avoid the previously mandatory polymeric coating deposition on the metallic substrate by creating *reactive amine groups* on the directly on surface that are further used as anchor points to immobilize bioactive peptides. These bioactive peptides confer the surface with "*biomimetic*" activity, promoting specific cellular response for the faster coverage of the metallic device from the biological medium.

Therefore, characterization techniques and the study of the *in vitro* and *in vivo* biological performance of the functionalized surfaces were as important as the development of this *multi-step plasma-based strategy*. Techniques, tests and materials selected for this project were related to the expertise of the three laboratories involved in this research project:

The **Laboratory for Biomaterials and Bioengineering (LBB)** at Université Laval is a multi-disciplinary laboratory with years of experience in the use of plasma processing for surface modification of biomaterials, specifically for cardiovascular applications. Furthermore, in this laboratory surface characterization by the means of different techniques, such as X-Ray Photoelectron Spectroscopy, Atomic Force Microscopy, Scanning Electron Microscopy and Water Contact Angle, was performed. Biological tests, involving endothelial cell adhesion, proliferation and migration and hemocompatibility studies, were also assessed in this laboratory.

The collaboration with the **Research Centre in Physics of Matter and Radiation (PMR)** at Université de Namur involved surface characterization by the means of ToF-SIMS and depth profile analysis. This research centre has developed several studies involving plasma modified surfaces and amino acid and protein coatings.

The **Laboratory for Vascular Translational Science (LVTS)** at the INSERM U1148 specializes in cardiovascular immunobiology. This research team is devoted to study the mechanisms through which the immune system interacts with diseased vessels and designing new vascular-protective immunointervention strategies. Their research program relies on skills and tools such as animal models, immunohistology and flow cytometry. Thus, the collaboration with this laboratory involved the in vitro studies of the interaction between human coronary artery endothelial cells and the developed surfaces, and in vivo tests in the porcine animal model.

Hence, the ensemble of expertise of these three groups allowed this project to have complementary investigations for the desired application.

This thesis is divided as follows: The **Introduction** presents the general problematic related to clinical complications after stent implantation. **Chapter 1** is focused on presenting the research project and the rationale behind the followed methodology. **Chapter 2, 3, 4** and **5** present the result and discussions obtained, which generated *4 scientific articles*, detailed bellow. **Chapter 6** presents a general discussion of the findings in this research project, with the limitations and perspectives. Finally, a conclusion is presented.

- **Chapter 2:** Low-pressure plasma treatment for direct amination of L605 CoCr alloy for the further covalent grafting of molecules

This first article explores the feasibility to directly functionalize with reactive amine groups the surface of L605 CoCr by the means of plasma treatments and the possibility to use them as anchor points for the further grafting of bioactive molecules.

Authors: Sergio Diaz-Rodriguez, Pascale Chevallier and Diego Mantovani

Article history:

Journal: *Plasma Processes and Polymers*

Submitted: November 2017

Accepted: March 2018

Published: April 2018

The experiments of this work were designed by all the authors. Diaz-Rodriguez carried out personally all the experiments and characterizations and a first analysis of the results, which were later discussed with the rest of the authors. This author redacted the full first draft of the paper which was corrected and modified by the rest of the authors. He was in charge of the final form of the paper including figures and tables.

- **Chapter 3:** Surface modification and direct plasma amination of L605 CoCr alloy: On the optimization of the oxide layer for application on cardiovascular implants

The second article focuses on the optimization of the L605 CoCr oxide layer, in terms of corrosion and deformation resistance, for its application on cardiovascular implants. This optimization was performed to select the surface pre-treatment suitable for the developed multi-step plasma-based strategy.

Authors: Sergio Diaz-Rodriguez, Pascale Chevallier, Carlo Paternoster, Vanessa Montaño-Machado, Céline Noël, Laurent Houssiau and Diego Mantovani

Article history:

Journal: *RSC Advances*

Submitted: October 2018

Accepted: December 2018

The experiments of this work were designed by Diaz-Rodriguez, Chevallier, Paternoster and Mantovani. Diaz-Rodriguez performed all the sample preparation and carried out all the experiments related to deformation and corrosion tests. Montaño-Machado performed the biological experimental part of this project. Noël (Université de Namur) provided technical support on ToF-SIMS analysis. Diaz-Rodriguez performed the first analysis of the results, which were later discussed with the rest of the authors. This author redacted the full first draft of the paper which was corrected and modified by the rest of the authors. He was in charge of the final form of the paper including figures and tables.

- **Chapter 4:** A comparison of the linking arm effect on the biological performance of a CD31 agonist directly grafted on L605 CoCr alloy by a plasma based multi-step strategy

The third article focuses on the optimization of the linking arm used for the direct grafting of a CD31 peptide onto the L605 CoCr surface. The study of the biological performance, peptide conformation and the feasibility to transfer this platform to commercial cardiovascular devices was assessed.

Authors: Sergio Diaz-Rodriguez, Caroline Loy, Pascale Chevallier, Céline Noël, Giuseppina Caligiuri, Laurent Houssiau and Diego Mantovani

Article history:

Journal: *Biointerphases*

To be submitted in June 2019

The experiments of this work were designed by Diaz-Rodriguez, Chevallier, Loy and Mantovani. Diaz-Rodriguez performed all the sample preparation and carried out most of the experiments and characterizations. The experiments involving biological tests were performed by Loy. ToF-SIMS analyses were performed by Chevalier and Noël. Diaz-Rodriguez performed the first analysis of the results, which were later discussed with the rest of the authors. This author redacted the full first draft of the paper which was corrected and modified by the rest of the authors. He is in charge of the final form of the paper including figures and tables.

- **Chapter 5:** Direct immobilization of a CD31 agonist improves in vitro and in vivo biological performance of CoCr coronary stents

The fourth article focuses on the study of the in vitro and in vivo biological performance of the Plasma-P8RI surfaces. In vitro performance was performed on flat samples, whilst in vivo performance, in coronary porcine model, was evaluated on bare metal stents modified by the novel strategy.

Authors: Sergio Diaz-Rodriguez, Jules Mesnier, Pascale Chevallier, Giuseppina Caligiuri, and Diego Mantovani

Article history:

Journal: *Biomaterials*

To be submitted in July 2019

The experiments of this work were designed by Diaz-Rodriguez, Chevallier, Caligiuri and Mantovani. Diaz-Rodriguez performed all the sample preparation and carried out the in vitro experiments and characterizations. In vivo experiments were performed by Mesnier and Caligiuri. Diaz-Rodriguez performed the first analyses of the results, which were first discussed with Caligiury and later discussed with the rest of the authors. This author redacted the full first draft of the paper. He oversees the final form of the paper including figures and tables.

Note to the jury: As it can be observed, chapters 5 and 6 present the manuscripts for two articles in process of publication. At this moment, a discussion about an agreement is ongoing among the authors from different institutions regarding the protection of the intellectual property for this work. Nevertheless, the author of this thesis considers that the discussion of this research project would be incomplete if these two chapters were removed. However, this thesis report meets the requirements for the initial deposit.

Introduction

Cardiovascular diseases and atherosclerosis

Cardiovascular diseases (CVDs) represent the leading cause of death in the world, in 2012 from the total of 56 million deaths in the world 17.5 million of them were due to CVDs [1]. These deaths happen mainly in countries with low- and middle-income countries. The numbers of deaths related to CVDs has increased worldwide throughout the years and it is expected to continue with the same tendency. One of these CVDs is atherosclerosis which is a leading cause of decease in North America [2,3,4].

Atherosclerosis, general information

Atherosclerosis is a CVD that characterizes for the deposition of a plaque that narrows the arterial diameter. This plaque is mainly formed of fatty substances, such as cholesterol, cellular waste products and calcium. As observed in Figure 1, the presence of this plaque causes blood flow interruptions that could lead to heart attacks [3,5].

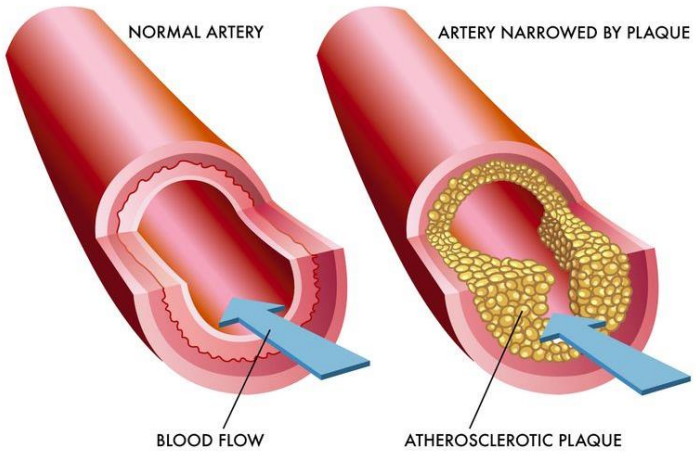

Figure 1 Representation of a healthy artery (left) against an atherosclerotic artery (right) [6]

Nowadays there are different programs to prevent atherosclerosis; they consist mainly in having a controlled and healthy diet, being physically active and specially avoiding smoking. However, once the plaque has been formed medical intervention is necessary: An angioplasty with a stent implantation is performed [7].

Clinical treatments and complications

An angioplasty is a percutaneous endovascular procedure which treats the narrowed artery with the help of a balloon catheter, generally made of PET, which is expanded in the damaged zone pushing the narrowing plaque to the arterial walls reopening the blood flow. However, if the artery is severely damaged it is necessary to

implant a stent, a tiny wire mesh that functions as a scaffold. The device is implanted as shown in Figure 2, where the catheter and the stent are placed in the narrowed area, once there the balloon is inflated the stent is expanded and deployed where it will rest permanently. The presence of this device not only re-establishes the blood flow towards the heart muscle but also avoids the collapse of the arterial walls.

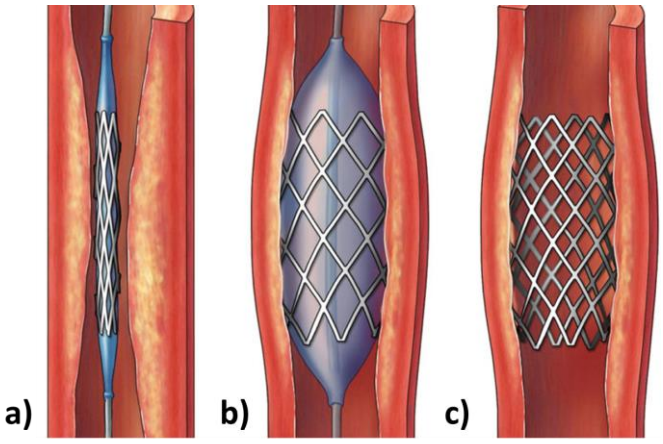

Figure 2 Schematic of the deployment of a stent in an artery. The stent is introduced to the diseased zone on a catheter (a), which is inflated to expand the device (b), fixing it onto the arterial wall, reopening the narrowed area (c) [8].

Stents: general information and properties

Nowadays millions of stents are implanted worldwide and even though there is an improvement of health after implantation, compared with angioplasty alone, clinical complications are still observed. These complications are related to the aggressive implantation of the device in the host [9,10]. One of the most important is restenosis, which, similarly to atherosclerosis, generates a reduction on the arterial diameter. The difference between both diseases is the time it takes to develop; Atherosclerosis can take up to decades to develop whilst restenosis develops during the first three months after implantation [11,12]. Figure 3 schematically presents the process of in-stent restenosis after implantation.

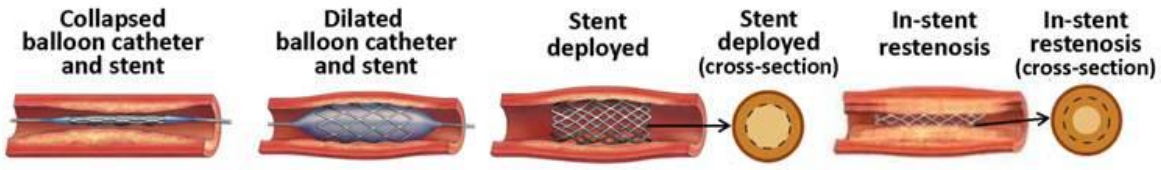

Figure 3 General schematic of a percutaneous coronary intervention and the deployment of a stent. First, the device is introduced on a balloon catheter to the narrowed area where it is inflated and deployed. Finally, the schematic representation of in-stent restenosis, and with the reduction on the arterial diameter, as observed in the cross section. [12]

The mechanism behind the formation of the narrowing plaque in restenosis has not been fully understood there are some factors that promote the formation of this disease: (1) There is a major injury related to the removal of

endothelial cells after balloon angioplasty/stent implantation. (2) Inflammation responses proportional to the penetration of the stent's struts on the arterial walls. (3) Adsorption of proteins on the surface of the biomaterial immediately after implantation, these proteins can lead to unfavorable interactions with leucocytes, platelets and coagulation factors. (4) Smooth muscle cells (SMC) play an important role in the reduction of the lumen diameter, proliferation is promoted in zones where the endothelium is removed. Furthermore, other complications such as late thrombosis or in-stent calcification can also occur after stent deployment.

In the last decades different generations of stents have been developed as a strategy to mainly decrease in-stent restenosis rate, as schematically presented in Figure 4. The main three generations of stents are: Bare metal stents (BMS), drug-eluting stents (DES) and, bioresorbable stents. The use of these BMS has helped to reduce the incidence of restenosis from 30–40% in coronary surgery. DES, which consisted of stents coating with anti-proliferative agents, were introduced as a strategy to minimize restenosis and requirement for re-intervention. Despite clinical outcomes, long-term stent thrombosis remained. The third generation, the bioresorbable stents, made of biodegradable polymer or resorbable metals, have emerged and have been accepted in European market in 2012, whereas FDA has approved the first one in 2016 [13].

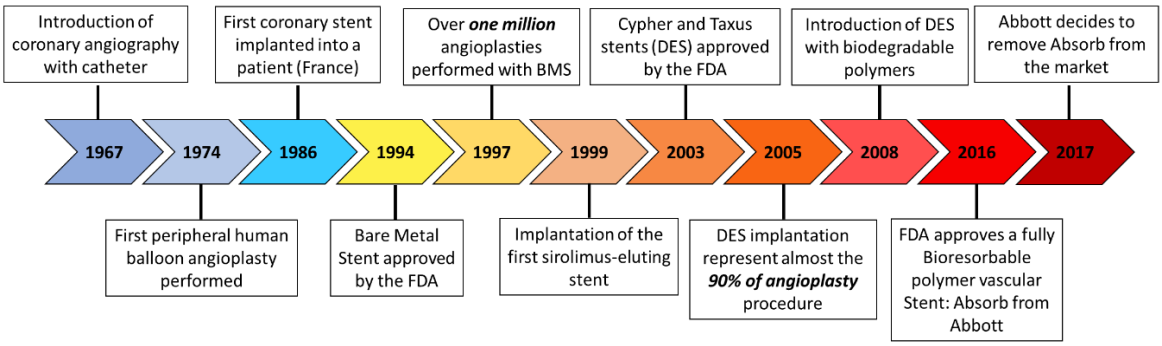

Figure 4 Timeline of important events on the development of coronary stents.

Despite the advances of generations in stents, long-term stent thrombosis remains on DES compared to BMS and moreover, once drugs are completely released from a DES the remaining implanted device is a BMS, which can be made of stainless steel or CoCr alloys. Therefore, it is of interest to modify and enhance the surface properties of BMS, with the aim of lowering complications after implantation. Section 1.2.1 discusses about the general properties of different BMS materials.

Bare Metal Stents (BMS)

Different materials have been studied and commercialized; these materials include titanium based, nickel, stainless steels and cobalt based alloys. Table 1 gives a general panorama of the characteristics and properties

of different alloys used in bare metal stents. Due to the process of implantation a stent is exposed, there is a challenge in finding a material with good biocompatibility and proper mechanical properties.

Table 1 Stent materials, strengths and weakness. Adapted from [14].

Material	Strengths	Weaknesses
Stainless Steel	-Commonly used in stents. -Good mechanical properties. -Corrosion resistant	-Potential release of Ni, Cr and Mo.
Nitinol	-Shape memory -Visible in fluoroscopy -49-52% of Ni	-Potential release of Ni that could cause toxic effects.
Cobalt-Chromium alloys	-Mechanical properties alloy to make ultra-thin struts. -Radiopaque -Corrosion resistant	-Cr can cause allergic reactions
Titanium	-Excellent biocompatibility -Excellent corrosion resistance	-Low tensile strength -Low ductility -Risk of fracture

One of the most important characteristics in a stent to assure a successful deployment and a long stay in the host are the mechanical properties. The environment where stents are exposed is highly aggressive: more than 35 million pulsations per year causing physical stress additional to the blood cells and components of the surrounding tissue which have the abilities to biochemically degenerate any foreign material [15]. As shown in Figure 2, stents suffer compression and expansion processes during the implantation procedure, therefore elastic properties have an important role while deciding the stent material. Table 2 shows the mechanical properties of metals that are commonly used in the fabrication of stents.

Table 2 Mechanical properties of metals used in stents. Adapted from [14].

Metal/alloy	Elastic modulus (GPa)	Tensile strength (Mpa)	Yield strength (Mpa)	Density (g/cm^3)
316L Stainless Steel	190	586	331	7.9
Tantalum (annealed)	185	207	138	16.6
Cp-Titanium (F67; 30% cold worked)	110	760	485	4.5

Nitinol (austenite phase)	83	895	195-690	6.7
Nitinol (martensite phase)	28-41	895	70-140	6.7
Cobalt Chromium	210	951-1220	448-648	9.2
Pure Iron	211.4	180-210	120-150	7.87
Mg alloy (WE43)	44	250	162	1.84

Stainless steel 316L, introduced in the mid-80s, was one of the most used metals in the industry of stents due to its mechanical properties and corrosion resistance given by the presence of chromium in its composition. Nevertheless, the stent industry has been focusing towards the use of different alloys such as cobalt chromium L605, as consequence of the low flexibility and thick struts, on stainless steel devices, that lead to higher rates of in-stent restenosis. L605, first approved by the FDA in 2011, possesses better mechanical properties than stainless steel, as observed in Table 2. This alloy allows the creation of stents with thinner struts, Figure *5* Comparison of stent's struts made of Stainless Steel and chromium alloys. Taken from [], which has lowered the percentage of complications after implantation [16,17]. Nowadays, L605 has replaced the use of other alloys, such as SS316L and nitinol, as the base alloy for stents.

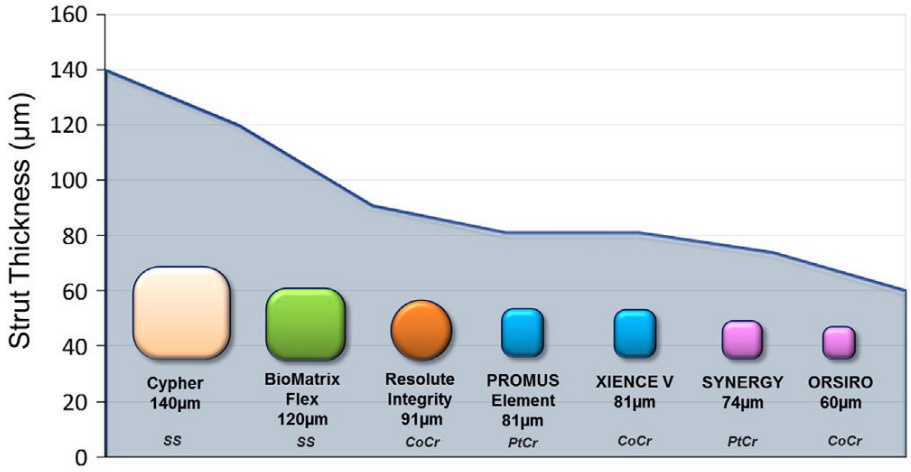

Figure 5 Comparison of stent's struts made of Stainless Steel and chromium alloys. Taken from [18]

Drug Eluting Stents (DES)

Despite the help to reduce the incidence of restenosis in coronary surgery by the implantation BMS, complications persist. As observed in Figure 4, a new strategy was introduced in 1999 with the development of drug-eluting stents (DES) that combine the use of stent coatings with anti-proliferative agents that minimize these complications and avoid a subsequent chirurgical intervention. These devices are composed of a) a drug carrier, which can be a bioresorbable layer of poly(lactic-co-clycolic acid) (PLGA), poly-L-lactic acid (PLLA) or poly-DL-lactic acid (PDLLA), or a porous matrix to elute the drug; b) The active compound which the most

common on DES are Sirolimus, Paclitaxel and c) a metallic wire mesh comprising the stent. Table 3 presents a general panorama of available coronary drug eluting stents in the market.

Table 3 Available drug eluting stents on the market, their materials, characteristics and productors. Adapted from [26].

Stent name	Materials	Characteristics	Produced by
Bx Velocity	316 L stainless steel: drug eluting form (CYPHER™) or with covalently bound heparin	Balloon expandable; slotted tube. First DES approved by FDA in 2000. It presented high rate of restenosis. Cypher stent had a Parylene tie-layer and polyethylene-co-vinyl acetate (PEVA) and poly-n-butyl methacrylate (PBMA) polymer with a sirolimus coating.	Cordis, a Johnson and Johnson Company, USA
-TAXUS Express²™ (DES).	316 L stainless steel drug eluting version: poly(styrene-b-isobutylene-b-styrene) with paclitaxel coating	Balloon expandable; slotted tube. The modular ring strut pattern consists of two separate module designs: short, narrow sinusoidal MicroTM elements linked via straight articulations to long, wide sinusoidal MacroTM elements. FDA approved 2002.	Boston Scientific, MA, USA
Axxess	Nitinol covered with PDLLA charged with Biolimus A9	Clinical study: DIVERGE Self-expanding platform. Dedicated to bifurcation. Abluminal coating adsorbed in 6-9 months.	Biosensors, Singapore
BioMime	Cobalt chromium covered with PLLA/PLGA charged with sirolimus	30-days eluting kinetics. Coating of 2um thickness. electro-polishing technique eliminates surface nickel oxides.	Biosensors, Singapore
BioMatrix	316 L stainless steel covered with PDLLA charged with Biolimus A9	Absorbed after 6 to 9 months. Largest cell opening.	Biosensors, Singapore
Combo	316 L stainless steel covered with PDLLA/PLGA charged with Biolimus A9	Luminal endothelial progenitor cells coating. Complete polymer degradation in 90 days.	OrbusNeich, Honk Kong
DESyne BD	Cobalt chromium covered with PLLA charged with novolimus	The thickness of the polymer coating is thinner (3 μm) than other (5–8 μm) stents.	Elixir Medical, CA, USA
Infinium	316 L stainless steel coated with PLLA, PLGA, PCL, PVP charged with placitaxel	Exhibited safety and efficacy in SIMPLE II clinical trials.	Sahajanandi Medical, India
MiStent	Cobalt chromium coated with PLGA charged with crystalline sirolimus	Polymer fully adsorbed in 90 days but SES sirolimus is maintained in a microcrystalline matrix and elution is sustained up to 9 months. Thin struts of 64 μm.	Micell, NC, USA
Nobori	316 L stainless steel coated with PDLLA charged with Biolimus A9	It contains an ultra-thin non-degradable parylene coating between the stent and bioadsorbable polymer.	Terumo, Japan
Orsiro	Cobalt chromium coated with PLLA charged with sirolimus	Ultrathin strut (60–80 μm) with an amorphous hydrogen-rich silicon-carbide layer, which can reduce iron release. Sirolimus can be released within 12–14 weeks, with PLLA degrading within 12–24 months.	Biotronik, Germany

Supralimus	Cobalt chromium coated with PLLA, PLGA, PCL, PVP charged with sirolimus	Coating thickness is 4-5 μm. Sirolimus is released within 48 days. It has been effective in reducing reintervention.	Sahajanandi Medical, India
Synergy	Platinum chromium coated with PLGA charged with everolimus	The polymer is degraded shortly after the drug is completely eluted at about 3 months.	Boston Scientific, MA, USA
Ultimaster	Cobalt chromium coated with PDLLA/PCL charged with sirolimus	Strut thickness of 80 μm. Coating abluminal and gradient. Polymer degradation and drug release in 3 to 4 months.	Terumo, Japan
Yukon stent	316 L stainless steel coated with sirolimus	Microporous stainless steel surface which can be coated with sirolimus without necessity of a carrier polymer	Translumina, Hechingen, Germany
Yukon Choice PC	316 L stainless steel coated with PLLA charged with sirolimus	Strut thickness of 87 μm. Balloon marker material of platinum/iridium. Micro-porous surface.	Translumina, Hechingen, Germany
Endeavor resolute	Cobalt chromium and phosphorylcholine charged with zotarolimus	Platform with thinner struts. Better results in terms of restenosis and repeat revascularization than a bare metal stents.	Medtronic Vascular, CA, USA
Promus Element Plus	Platinum chromium charged with everolimus	Helical, two-connector design. Denser than SS and Co-Cr.	Boston Scientific, MA, USA
Xience	Cobalt chromium charged with everolimus	Co-axial positioned system. A compliant, tapered balloon, with two radiopaque markers.	Abbott Vascular, CA, USA
Cre8	Cobalt chromium coated with carbon charged with amphilimus	Nanoparticle polymer-free drug eluting stent.	CID Vascular, Saluggia, Italy
BioFreedom	316 L stainless steel charged with Biolimus A9	Metal platform with a microstructure abluminal surface. is attached to the abluminal surface without a polymer.	Morges, Switzerland
Amazonia Pax	Cobalt chromium charged with paclitaxel	Metal platform with paclitaxel applied as microdrops on the abluminal surface by crystallization, and the drug can be released within 30 days.	Minvasys, Gennevillieres, France
VESTAsync	316 L stainless steel coated with hydroxyapatite charged with sirolimus on microporous pores	The hydroxyapatite dissolves gradually within one year.	MIV Therapeutics, GA, USA
OPTIMA	316 L stainless steel charged with tacrolimus	Metal platform without a polymer, and tacrolimus coated into grooves as a reservoir on the stent abluminal surface	CID, Saluggia, Italy
CoStar	Cobalt chromium alloy and PLGA polymer with paclitaxel	It uses laser drilling technology to create drug-filled holes on the stent surface in order to avoid long-term exposure of the polymer to the vessel wall.	Conor MedSystems, CA, USA

In order to produce a DES with the desired performance whilst avoiding side effects the device must be designed to control the drug release before and after the implantation. Other important criteria for a successful design of a DES are a) minimal thrombus formation, b) stability of the stent/coating in the arterial wall after deployment, c) compatibility between the carrier and the drug during the coating deposition and d) stability and proper degradation (if necessary) of the carrier after the deployment of the device. Nevertheless, despite the advances

of DES, complications after implantation and in long-term persist mainly due to the drug pharmacology. As a consequence of the low specificity of the bioactive agent, there is not only an inhibition of SMC proliferation but for EC too. Thus, the need for a combination of different strategies to lower the probability of further complications for example with a dual antiplatelet strategy up to 16 months, as recommended by the American College of Cardiology [19]. Therefore, current research for the developing of new stents focuses on the development of novel strategies that can modulate specific biological responses without compromising the performance of the device at short and long term.

Current strategies to improve the performance of cardiovascular devices

When developing a new biomaterial, in this case a cardiovascular stent, mechanical properties play a crucial role in the performance of the device, nevertheless, not only these properties should be taken in consideration when designing a new device. Biological properties that can increase the integration of the device and therefore avoid complications after implantation are mandatory for clinics. Regarding stents, the main desired properties aim to obtain a device with anti-inflammatory and anti-thrombotic activities, that promotes endothelialization and avoids the release of potential toxic ions from the composition of the metallic alloy. Different strategies to achieve these properties involve the modification of the surface in order to conserve its mechanical properties.

Surface modification

When choosing among the modification treatments for a specific material, factors such as the application and the structure of the device should be taken into consideration. Regarding stents, a complex 3D wire mesh that is introduced compressed on a catheter, guided through the vascular system up to a narrowed zone and expanded up to a 25% to reopen the arterial flow and depositing the device to avoid the collapse of the artery. Therefore, modification procedures for cardiovascular application aim for the modulation of surface properties avoiding the modification of bulk properties, thus not compromising the mechanical performance of the device. Overall, surface modification of the device can be performed involving two different strategies: by depositing a coating that confers new properties and allows a further modification or by working directly on the material surface.

Surface properties such as corrosion resistance, to avoid the release of potential cancerogenic ions such as nickel, chrome or others [20], surface chemical composition, morphology, charge, surface wettability and roughness have an impact in the biological activity, as observed in Table 4, and therefore the performance of the device can be modulated [21]. These surface properties influence mainly the in vitro performance of materials. As regards in vivo performance, it has been found that the reaction of the body to a foreign material is independent from simple surface chemistry, mainly due to non-specific adsorption of proteins. Therefore, the

manufacture of surfaces that focus on the emulation of the interactions in the body, such as ligand-enzyme reactions for example [25].

Table 4 Effect of the modification of different parameters on the biological activity of implants.

Parameter	Response/Outcome	Reference
Chemical composition	Polar and non-polar groups can affect the different proteins that can adhere to the substrate. Functionalization with $-CH_3$, $-NH_2$, -COOH, -OH groups influence this behaviour.	[22]
Surface wettability	Water is one of the main components of blood. Wettability affects the way a biomaterial interacts with a device. Modifying the hydrophobic character of a surface certain kinds of cells and extra cellular proteins can interact and adhere to the substrate. This property can be modified by chemical meanings, using functional groups, or physical strategy modifying the topography.	[23]
Topography	It has been found that increasing the surface roughness leads to the promotion of the adhesion of proteins and cells. This property can be either modified by polishing the surface, either mechanical or electropolishing, depending the desired roughness and homogeneity, or by creating patterns using different techniques.	[24]
Molecule grafting	Modifying the surface to control protein interaction by adding signaling molecules to mimic specific molecular interactions. Two main strategies: a) non-fouling surfaces, that are resistant to protein adsorption, b) by the grafting of molecules targeting specific protein interaction/response.	[25]

One of the main strategies to modify the surface properties without interfering the bulk is the deposition of coatings. These coatings can be used to smooth the surface whilst also modifying the surface energy or directly influence desired biological responses to decrease post-implantation complications. In general, coatings can be classified by the nature of their material: inorganic, polymeric and biological coatings; or by their activity: passive or bioactive [13, 26]. Table 5 presents a general overview from the different coatings for stent application.

Table 5 Different coatings developed for stent application [13].

Coating	Characteristic	Classification
Gold	Deposited on stainless steel stents of less than 80 μm to enhance their fluoroscopic visibility due to its high radiopacity. No improvement on restenosis rates reported in vivo. Promotes activation of platelets.	Inorganic, passive

PTFE/CF_x	Hydrophobic surface. Not significant different in restenosis rate after six months follow up between BMS and coated stent.	Polymeric, antifouling
Iridium oxide	Iridium oxide is considered a biocompatible substrate. Used to promote fast endothelialization by preventing the formation of free oxygen radicals, that can affect the adhesion and proliferation of EC. Lunar stent (Inflow Dynamics Germany) is a 316L stent coated with gold and a layer of iridium oxide.	Inorganic, passive
Diamond like carbon (DLC)	In vitro results show an improved biocompatibility compared to stainless steel. No significant advance on restenosis rate in vivo. Considered as an "inactive" coating due to these results.	Inorganic, passive
Silicon Carbide (SiC)	Silicon carbide coatings produce antithrombotic surfaces. In vitro, it reduces the deposition and activation of platelets, leukocytes and monocytes. Nevertheless, in vivo it does not present satisfactory results.	Inorganic, passive
PLGA, PLLA, PDLLA	Generally used as a polymeric carrier for drug eluting stents for sirolimus and paclitaxel, considered as bioactive coatings for this reason. Scaffolds of these materials have also developed as biodegradable stents.	Polymeric, bioactive

Deposition techniques for these coatings have advanced from simple adsorption of molecules onto the surface to multi-step procedures with complex solutions, as observed in Table 6. Nevertheless, despite the advances on these techniques, one of the main concerns for these coatings is the stability when applied on cardiovascular devices, a complex 3D structure. Cracks and delamination can be present mainly related to the lack of adhesion and cohesion between the coating and the substrate [24]. Therefore, a novel strategy needs to be explored in order to promote the biological properties of cardiovascular devices. Thus, working directly onto the surface of the metallic device represents a promising strategy to explore.

Table 6 Deposition techniques for stent application. Adapted from [26]

Methodology	Description
Adsorption	Simple methodology largely used for proteins and biomolecules. Performed at 37 °C to avoid denaturation of proteins. This technique does not assure the stability of the coating in vivo.
Dip coating	Simple and fast technique used for charged polymers. Performed as a layer-by-layer deposition. Similar to adsorption, this technique does not assure the stability of the coating in vivo and after deployment of stents.
Spin coating	Simple, cheap, fast deposition technique for polymers. Nevertheless, the lack of homogeneity compromises the stability of the coating.
Spray coating	A solution is pulverized on the surface. It allows to obtain thin films of polymers. Low adherence can be observed.
Plasma treatment	Long-term application, control of surface properties. Solvent-free. High adhesive and cohesive coatings depending on the feeding gases. Nevertheless, this technique can be expensive and often involves multi-step procedures.

Grafting	Immobilization of bioactive molecules onto the surface. Generally obtained after the combination of different procedures. Requires a previous surface functionalization that can be achieved by plasma treatment or chemical procedures.

Chapter 1 A novel alternative: Design, development and validation of a plasma-based strategy for the direct grafting of bioactive molecules on L605 CoCr stents

As discussed in the previous chapter, complications after implantation of BMS exist and in-stent restenosis remains as one of the leading concerns. Furthermore, the development and use of DES, by eluting anti-proliferative drugs to prevent restenosis do not present a significant improve due to the compromise of endothelium healing. In fact, the Canadian Association of Interventional Cardiology and the Canadian Cardiovascular Society have given statements about the use of DES in Canada, which no significant improvement in restenosis and stent thrombosis was found after 30 days and up to 12 months compared to BMS [27]. A novel strategy that can enhance the properties of these devices needs to be developed.

Thus, this research work focuses on the development of a novel strategy that can increase the biological integration of L605 BMS. By combining different surface modification techniques, this strategy allowed the creation of functional groups, used as anchor points to covalently graft biomolecules. By the immobilization of these biomolecules, with the potential to mimic specific molecular interactions, the biological response can be modulated to produce an anti-inflammatory surface that also promotes the endothelialization of the arterial wall.

Following subsection detail the rationale, objectives, methodology and the strategy followed throughout the project.

1.1 Rationale of the project

Coronary stents are used for the treatment of arterial stenosis. Their implantation procedure involves the navigation through tortuous arterial beds, deployment, and fixation in the diseased artery. Complications after implantation exist. A general trend to overcome them and to increase the integration of a metallic cardiovascular device is the use of coatings that can be further functionalized with bioactive molecules to increase their performance, as observed in Figure 6a. Nevertheless, these coatings, generally polymeric based, can present cracks and delamination due to the complex structure and implantation procedure of the device. A different approach, Figure 6b is to directly work on the metallic substrate to directly functionalize the oxide layer with reactive groups that act as anchor points for the immobilization of bioactive molecules.

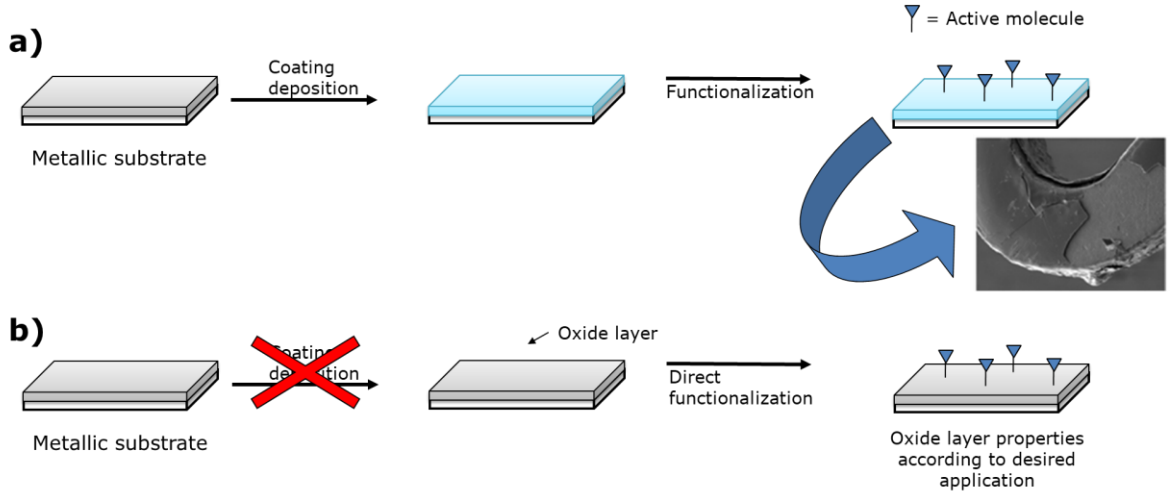

Figure 6 Strategies to functionalize a metallic surface with bioactive molecules: a) using polymeric-based coatings and b) directly working onto the metallic surface. Stent coated with a multi-layer of PLGA and Fucoidan with detachment of the coating taken from [28]

Different functional groups, such as hydroxyl, phosphonate, carboxylic, amine and epoxy, can be created onto metallic surfaces via two different kind of treatments: wet-based or dry strategies. Main concern about using wet-based techniques, such as acid/base or solvent dipping, on cardiovascular devices is the potential residues that can be present on the surface and the use of high temperatures to promote certain groups on the surface that can alter the bulk properties of the devices. As regards the second approach, one of the most important dry technique is plasma treatment, which has already been used for the modification and sterilization of many biomaterials [29].

1.1.1 Plasma based treatments

Briefly, this technology excites a gas, such as ammonia, oxygen, acetylene, helium or argon, via an energy source, such as electric discharge, alternating/direct current, radio-frequency energy, microwaves, or heat, thus leading to partial ionization of the gas into charged particles, electrons, and neutral molecules [30]. These high-energy species are then used to bombard the material surface, resulting in energy transfer and modification of surface chemical and physical properties [31]. Some of the advantages of plasma treatments are [29, 30]:

- ✓ Enables the surface functionalization without the generation of chemical waste.
- ✓ Less degradation and surface roughening than wet-based techniques (chemical etching).
- ✓ Surface properties can be modulated without altering bulk properties.

Plasma processing, depending on the parameters and the application, can be divided in four main groups: 1) coating deposition, 2) etching, 3) ion implantation, and 4) surface functionalization [31, 32], and onto different materials as summarized in Table 7.

Table 7 Plasma processing of different substrates.

Substrate	Process	Plasma treatment conditions	Reference
Polymers	- Add new functional groups (-NH_2, -COOH, -OH) - Reticulation of polymers - Antibacterial properties - Sterilization	- MW and RF are used in amination (N_2/H_2 or NH_3) - PIII of Cu	[33,34]
Metals	- Deposition of thin-layer coatings - Corrosion resistance - Wear resistance - Ion implantation (N, O, etc.) - Etching	- RF Plasma (CFx, DLC for ex) - PIII (O_2, Cu, N_2 for ex)	[29, 35, 36]

Coatings deposited by plasma treatments present high adherence, complex molecular structure (high reticulation and crosslinked chains) when compared to coating deposition techniques discussed in section 1.3 [37, 38]. Even if this technology is considered substrate-independent, the main challenge on this technique is the homogeneous coating deposition onto complex structures such as stents [39]. Plasma etching is a procedure where the reactive species generated in the gas discharge are used to selectively remove a layer of atoms or patterns [40]. Its main applications involve the fabrication of patterns on microelectronics and the cleaning of surfaces [41]. As regards ion implantation, also known as plasma immersion ion implantation (PIII), can produce changes both on the surface and in the internal structure, leading to an amorphous oxide layer, due to the acceleration of ions into the metallic substrate by the application of a bias [24, 42]. Finally, during the surface functionalization by plasma treatment, reactive species, created inside the plasma, bombard the surface of the substrate, resulting in a change in the physical and chemical properties of the surface. Plasma functionalization is generally performed onto inert polymers but the interest to create functional groups onto metallic surface exists. The following subsection develops the surface functionalization by plasma treatments.

1.1.2 Surface functionalization by plasma treatments

The surface chemistry of an implanted device plays a role on the cellular response. The use of plasma treatments that allow the modification of the surface chemistry by introducing new functional groups without compromising the integrity of the material's bulk properties whilst avoiding the generation chemical waste represents an alternative to conventional techniques (wet-based). These functional groups can be used to modulate specific

surface properties, thus, the biological response of a biomaterial [29, 43, 44, 45]. Among the different functional groups that can be obtained by this strategy the most important are: Hydroxyl (-OH), carboxylic (-COOH) and primary amine groups (-NH_2). A summary of these functionalities, how they are obtained by plasma treatment and their effect onto a biomaterial is shown in Table 8.

Table 8 Surface properties of different functional groups obtained by plasma.

Functional group	**Properties**	**Feeding gases**	**References**
Hydroxyl **-OH**	- Increases the hydrophilicity of a surface. - Promoting cell colonization - Low chemical reactivity (high water affinity) - Physisorption of small peptides	Ar + O_2 O_2	[46, 47]
Carboxylic **-COOH**	- Support for cell anchorage - Platform for interfacial immobilization of bioactive molecules with amine groups (-NH_2) - Plasma treatments can create crosslinking on the substrate	O_2 CO CO_2	[48, 49, 50]
Amines **-NH_2**	- Promotes cell colonization - Platform for interfacial immobilization of molecules with terminal (-COOH) - Increases the hydrophilicity of a surface	NH_3 NH_3 + H_2 N_2 + H_2	[46, 51, 52]

In general, these functionalities can be introduced onto the surface by two ways: directly or indirectly. Direct way is obtained after a plasma treatment with feeding gases that will promote the functionalization with the desired group, as observed in Table 8. Direct functionalization is usually performed onto polymeric substrates. On the other side, the indirect functionalization involves the plasma polymerization of a precursor that contains the functionality. For example, for hydroxyl groups: methanol [53, 54], ethanol [53] and allyl alcohol [55]; for carboxylic groups: acrylic acid [55, 56, 57] and propanoic acid [58]; and finally, for amine groups: allyl amine [57, 55], butyl amine [59] and 1-3 diaminopropane [60]. Indirect functionalization is mainly performed onto metallic substrates. As regards this project, only the direct functionalization is considered for the previously discussed advantages over the coating strategies for stent applications. Furthermore, among the previously mentioned functionalities, primary amines have an increased interest due to their feasibility to immobilize bioactive molecules onto the surface, thus, next subsection is focused on developing plasma amination and the immobilization strategy.

1.1.3 Plasma amination for molecule immobilization

Primary amine groups, due to their high reactivity, can act as anchor points to immobilize covalently molecules onto the surface of a material thus, enhancing the performance of the implant. This reaction, known as carbodiimide chemistry, takes place between the surface amine groups and carboxylic groups present on the biomolecule of interest. As observed in Figure 7, the reaction leads to the formation of interfacial amide bonds by activating the terminal carboxylic group of molecule 1 that reacts with the terminal amine group of molecule 2. This strategy not only enhances the surface with properties such as anti-inflammatory, pro-endothelialisation, depending of the molecule grafted, but also assures the stability of the molecule from detachment by the creation of a chemical bond, compared to physical techniques, such as adsorption. Some of the molecules grafted by this carbodiimide chemistry onto aminated plasma treated surfaces are: DNA [61, 62], heparin [63], hyaluronic acid [64], enzymes [65], proteins [66], antibodies [67], lysozymes [68], dextran [69].

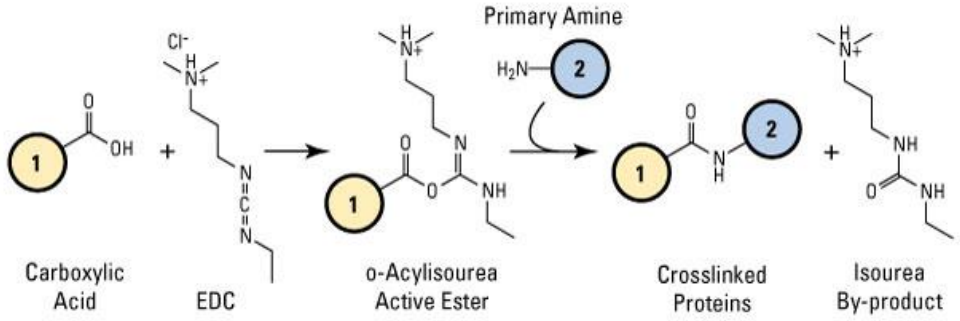

Figure 7 Carbodiimide crosslinking reaction scheme. Carboxyl-to-amine crosslinking with the popular carbodiimide, EDC. Molecules (1) and (2) can be peptides, proteins or any chemicals that have respective carboxylate and primary amine groups. When they are peptides or proteins, these molecules are tens-to-thousands of times larger than the crosslinker and conjugation arms diagrammed in the reaction. Image taken from ThermoFisher Scientific resource library [70]

Ideally, the immobilization of molecules onto a surface must present the next properties [34]:

- ✓ Covalent bond between the molecule and the surface to avoid its loss in the biological media
- ✓ The active site of the immobilized molecule must face the biological medium
- ✓ After the binding, the immobilized molecule must not be denatured nor change its conformation
- ✓ Carbodiimide chemistry must be specific between the surface and the molecule of interest

As observed, some of the concerns of this technique is to preserve the activity of the immobilized molecule. The use of different spacers, or linking arms, have been studied in order to avoid the denaturation of the bioactive molecule and to grant freedom to the preserve its conformation [68]. Table 9 presents some of the linking arms that have been used to immobilize molecules by carbodiimide chemistry. As regards the immobilization of

proteins/peptides, it is recommended to use linking arms with terminal carboxylic groups that when activated react with the free amine groups of the bioactive molecule. This avoids the risk of auto condensation of the protein/peptide, thus losing its bioactivity when immobilized. For instance, Glutaric anhydride (GA) and polyethylene glycol bis carboxyl (PEGb) are suitable for this strategy due to their terminal carboxylic groups. Furthermore, as observed in Table 9, these linking arms have already been used to covalently immobilize different molecules without affecting their biological properties.

Table 9 General properties and molecules that have been grafted by PEG and GA as linking arms.

Linking arm	Properties	Previously grafted molecules	References
Polyethylene glycol	- Different chain length - Anti-fouling molecule - Highly hydrophilic - Terminal groups can be modulated, single or double groups (-COOH or $-NH_2$)	- Poly L-Lysine - RGD - Heparin - Hyaluronic acid - Chitosan	[24, 56, 71,72, 73, 74]
Glutaric anhydride	- 6 carbon chain - Synthetized by the body - Terminal -COOH	- Poly L-Lysine - RGD - Fibronectin - Chitosan	[73, 75, 76, 77]

In literature, this direct amination by plasma, for further biomolecule grafting, has been extensively used for polymeric materials but, to our best of knowledge, never on metallic surfaces. Indeed, most of the plasma processing on metals is focused on enhancing the corrosion and wear resistance by PIII of oxygen and nitrogen [23, 78, 79]. As L605 alloy is the most important nowadays on stent manufacture, the feasibility to create primary amine groups onto its surface, without the use of any polymeric coating, represents a challenge to overcome.

Therefore, the main hypothesis for this project is that using plasma treatments, at low pressure, primary amines can be created directly onto the surface of the alloy. These reactive groups can be used as anchor points for the grafting of different molecules: first a spacer to preserve the activity of the bioactive molecule, to be grafted on a second step. The biomolecule of interest in this project, aiming cardiovascular applications, is a peptide derivative from the transmembrane receptor Platelet Endothelial Cell Adhesion Molecule (PECAM-1), also known as CD31. It has been found in endothelial cells, platelets and leukocytes, where it plays a role in adhesion [80, 81, 82]. This specific fragment used herein has been patented and have exhibited anti-inflammatory, pro endothelialisation and anti-stenotic behaviors, which are key properties for stent applications [83]. Thereby, these functional surfaces are expected to improve the performance of BMS by decreasing the rate of restenosis whilst promoting the endothelial cell survival, migration on the substrate.

1.2 Project objectives

Therefore, this project aims on the development of a novel platform that allows the ***direct immobilization*** of bioactive molecules onto L605 CoCr alloy by using primary amine groups, created by plasma treatments, as anchor points in order to enhance the bioactivity of this metallic substrate. This strategy avoids the use of any polymeric based interlayer to support the bioactive molecule on the metallic substrate.

In order to develop and optimize this platform four main questions needs to be answered focusing on the feasibility to create primary amine groups, optimization of the surface, of the grafting and the biological performance. In Figure 8, a general schema of how the project is divided to answer these questions, the key experiments to answer them and general tools is presented.

The first block consists on studying the feasibility of functionalizing the alloy and grafting a biomolecule. The second block is focused on the modification and optimization of the surface (oxide layer) in order to obtain the most suitable in terms of corrosion, deformation resistance and amination efficiency for a stent application. The third block is oriented on the study of the grafting of the peptide using different linking arms on the previously optimized oxide layer. Finally, the fourth block is focused on the in vitro and in vivo performance of the functionalized surfaces, both flat and stents, in a collaboration with the Laboratory for Vascular and Translational Science (LVTS), under Professor Giuseppina Caligiuri's supervision.

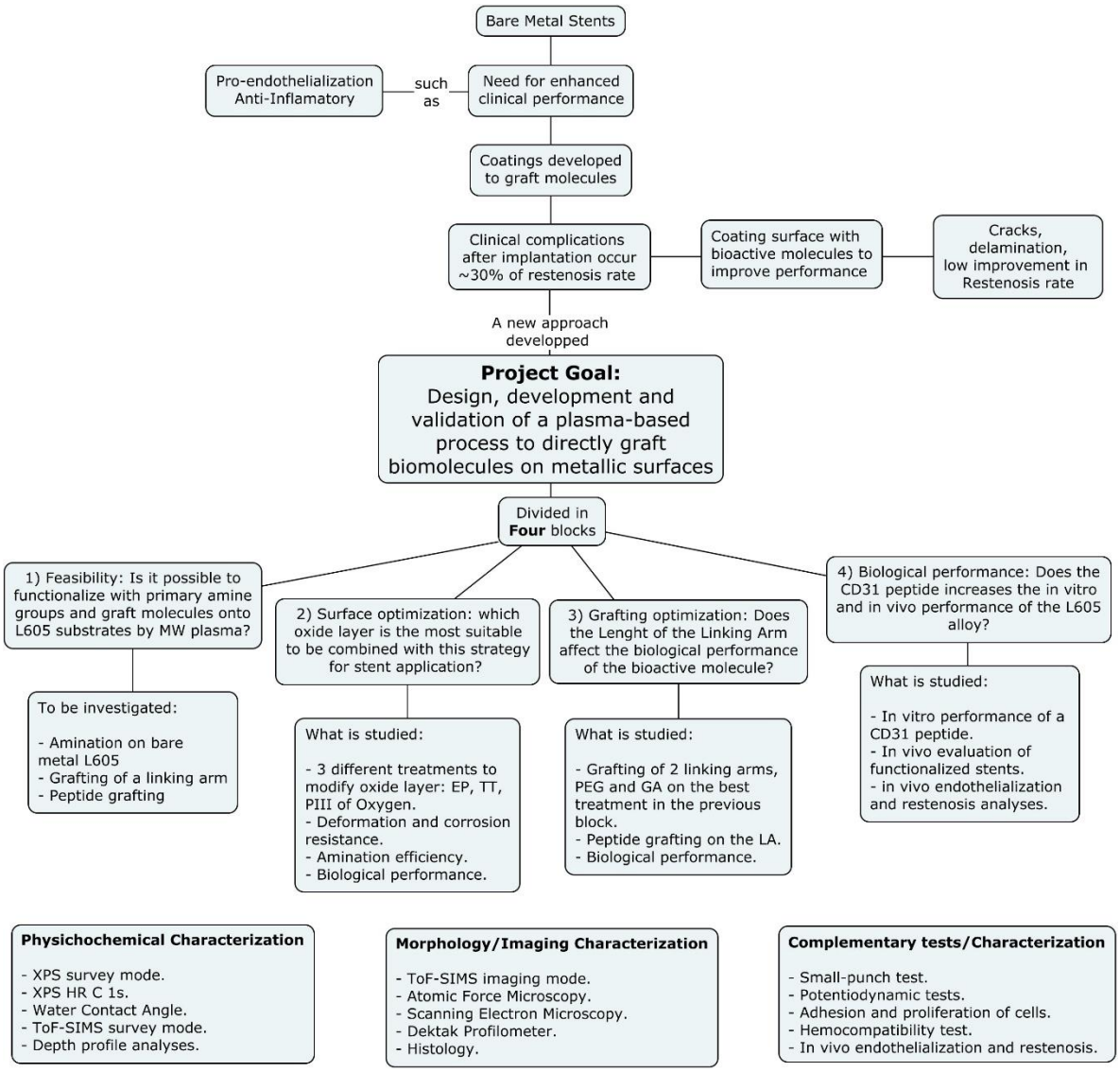

Figure 8 General schema of the project.

1.3 Direct functionalization of L605 CoCr alloy and biomolecule grafting: From flat model to cardiovascular devices

A multi-step procedure has been proposed in order to directly graft bioactive molecules on cobalt chromium surfaces. This procedure is composed of 3 main steps: 1) Surface optimization, where the as received alloy is electropolished to remove any contaminant and to homogenize the composition of the oxide layer; 2) MW Plasma functionalization, where the primary amine groups are created to be used as anchor points in the last block, 3) Biomolecule grafting that consists on the bonding of a linking arm and the peptide of interest.

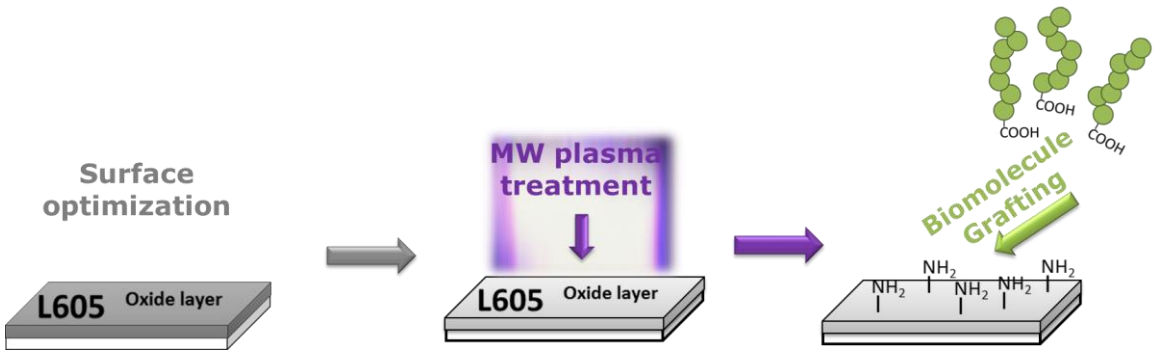

Figure 9 General methodology for the multi-step plasma functionalization of L605 and the direct biomolecule grafting

Regarding surface preparation, three surface modifications are proposed to study: Electropolishing, to clean the as received alloy and to homogenize the oxide layer; Thermal treatments to modify the oxide layer with a diffusion process; and Plasma immersion ion implantation (PIII) of oxygen, as a physical modification of the oxide layer. Modifying the native oxide layer with these treatments can create an interphase capable of resisting deformation, corrosion and that can be suitable for MW plasma amination, moreover, surface properties and topography play an important role during protein adsorption/cell interaction processes [25, 84].

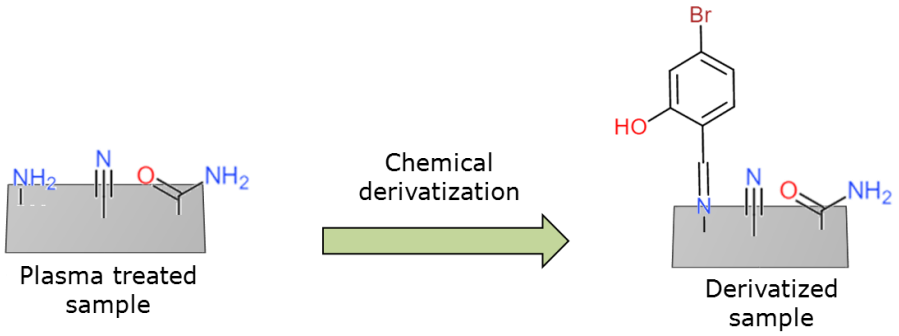

Figure 10 Schema of the reaction for the characterization of primary amine groups by chemical derivatization.

Once the oxide layer has been optimized the plasma treatments to modify the chemical composition are carried out. This step focuses on the functionalization of the surface with primary amine groups using only plasma-based treatments. During this step, proper confirmation of the primary amine groups needs to be performed, since, as observed in Figure 10, other nitrogen species can be formed but are not useful to react with the linking arms or bioactive molecules of interest. For this reason, a chemical derivatization is performed to quantify the useful amine species. Once the functionalization with primary amine groups on metallic surfaces is done, the third step of this procedure is performed.

Primary amine groups can be used as anchor points mainly using two different strategies, as shown in Figure 11. Upper route consists on activating the carboxylic groups of the CD31 peptide, nevertheless, this strategy has a potential problematic as auto-condensation of the bioactive molecule due to its activation in solution, which

can lead thereafter to losing its biological properties. The lower route, the strategy that will be used in this project, consists in the reaction of the amine groups with two different linking arms that will work as spacers between the peptide and the metallic surface. After the reaction between the LA and the primary amine groups of the metallic substrate, the resulting terminal carboxylic group is activated. By activating this terminal carboxylic group, that is already immobilized on the surface, the auto-condensation of the biomolecules is avoided. This reactive intermediate will react with the free amine groups of the peptide. This strategy assures the no auto-condensation of the molecule of interest, its grafting efficiency to the surface, thus, leading to a potentially less risk of losing its bioactive properties. Following subsections detail the methodology followed in each block of the project.

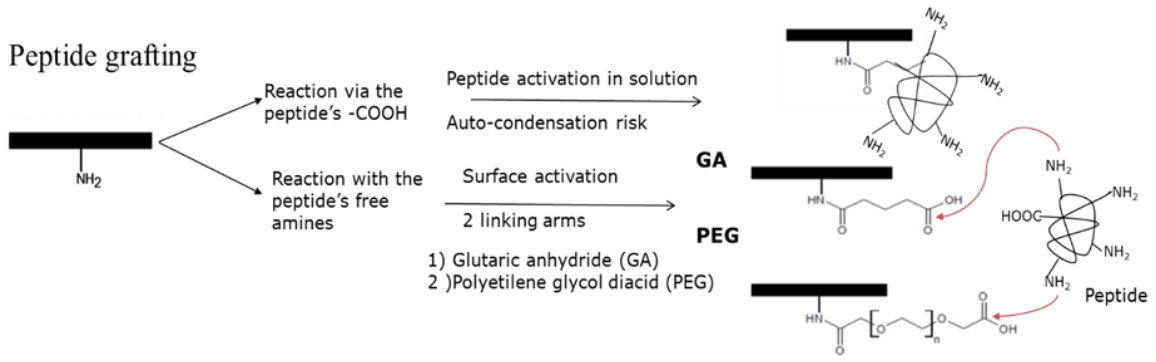

Figure 11 Schematic of the possible reaction pathways to covalently graft a peptide onto primary amine groups on a surface.

1.3.1 Feasibility: Is it possible to functionalize and graft molecules onto L605 substrates using MW plasma treatments?

The first block of this project represents an exploratory work of the multi-step procedure proposed in previous sections, to confirm the feasibility of the plasma functionalization with primary amine groups on L605 surfaces and that effectively, these functional groups can be used to further graft other molecules of interest. Figure 12 shows a general methodology for this exploratory block.

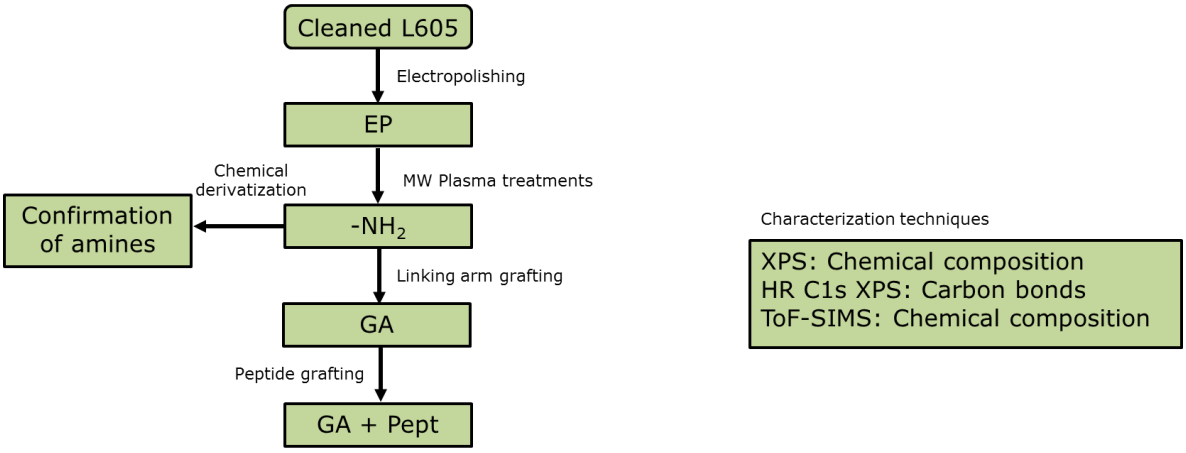

Figure 12 General methodology for the study of the feasibility of direct plasma amination on cobalt chromium alloys

During this block the selected technique for the surface preparation was electropolishing, this treatment allowed to the removal of the native oxide layer from the as-received specimens and allowed the creation of a homogeneous, controlled and reproducible new oxide layer with a nano-smooth roughness with a mirror like finishing [85, 93]. Furthermore, due to the presence of chromium in the alloy (Table *10*), electropolishing L605 surface creates a passive oxide layer that can decrease the corrosion, thus, the release of toxic ions into the blood stream [86, 87].

Table 10 Chemical composition of the L605 alloy, also known as Haynes 25. Values reported as wt %.

L605	*Co*	*Cr*	*W*	*Ni*	*Fe*	*Mn*	*C*
Max	Balance	21.0	16.0	11.0	3.0	2.0	0.15
Min		19.0	14.0	9.0	-	1.0	0.05

Once the surface has been electropolished the plasma functionalization is performed, using a MW plasma reactor with nitrogen and hydrogen as feeding gases leading to primary amine groups (confirmed by chemical derivatization [88]) that were used as anchor points to graft a linking arm and a peptide.

Important parameters that must be taken into consideration for promoting the presence of primary amine groups are shown in Table 11. These parameters have been studied on polymeric surfaces, therefore the creation of primary amine groups onto the surface of metallic substrates is a challenge and an optimization should be performed.

Table 11 Parameters influencing the plasma amination efficiency on polymers. Information adapted from [89, 90, 91]

Parameter	**Conditions**	**Outcome**
Gas mixture	Main combinations used: NH_3 N_2/H_2	High density of primary amine groups by ammonia treatments

Time	Short time treatments (seconds) Treatments of 5 min or more.	Long-time treatments insert more nitrogen on the surface, therefore a post treatment is necessary
H_2 Post treatment	Post treatment used to promote amination	Reduces other nitrogen species to primary amine groups.

1.3.2 Surface optimization: Which oxide layer is the most suitable for a stent application?

Several surface treatments are proposed to modify the properties of the interface and impact the following steps on the grafting of biomolecules directly on metallic substrates. These surface treatments were selected to obtain a different chemical composition, with a suitable corrosion resistance and able to deformation up to a 25%, as expected on a stent implantation. The selected surface modifications were Electropolishing, Thermal Treatment and Plasma Immersion Ion Implantation (PIII) with oxygen.

Electropolishing is an electrochemical procedure that removes the contaminations that come from the alloy as received. As previously mentioned, this treatment creates a homogeneous oxide layer with a metallic mirror-like finishing with a passivated oxide layer [92, 93]. Electropolished samples will be further modified either by a Thermal treatment in an open atmosphere oven or by PIII with oxygen. These two treatments are performed in order to modify the oxide layer composition. Thermal treatment can modify the composition of the electropolished sample due to the diffusion of ions in the alloy to the outmost layers as an effect of temperature, achieving homogeneous changes on the chemical and structural composition [92, 24]. PIII consists in the bombardment of the surface with highly energetic oxygen ions that break the crystalline network of the outer nanometers of the alloy producing an amorphous oxide layer [94, 95].

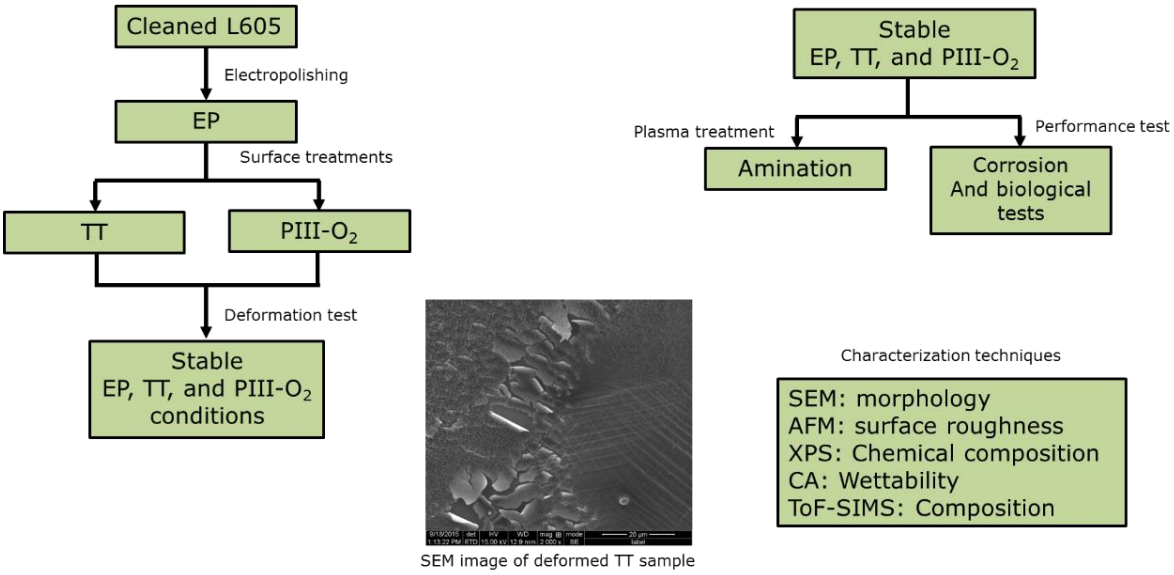

Figure 13 General methodology for the optimization and direct plasma amination of the oxide layer of cobalt chromium alloys for stent applications

The general strategy for this block is shown in Figure 13 where the first part, left side, focuses on finding a stable oxide layer from the proposed conditions of each treatment, whilst the second part, right side, focuses on the performance of the selected surface modifications and the plasma treatment of the samples. Characterization of this block is mainly composed of SEM where the morphology of the surfaces is analysed in order to find cracks or delamination after deformation, AFM to observe the surface roughness and topography, XPS to follow surface chemical composition changes between the treatments and before and after amination, and depth analyses were also performed using ToF-SIMS.

By using these different surface treatments, it is expected to have oxide layers that differ not only from their chemical composition but also in properties such as corrosion and deformation resistance and hydrophobicity. The performance of these optimized treatments will be evaluated in order to find the most suitable oxide layer for a stent application, that will be used as base surface treatment in the following blocks of this strategy.

1.3.3 Grafting optimization: does the length of the linking arm affect the biological performance of the bioactive molecule?

Once the alloy surface has been functionalized with amino, the grafting of the biomolecules of interest can be performed. In order to covalent graft the peptide two molecules were selected as a linking arm between the substrate and the peptide: Glutaric anhydride and PEG. PEG is a molecule that has anti adhesive properties and has a long chain (~600 carbons), it has been studied and grafted on other substrates as linking arm [23, 71, 72], on the other side glutaric anhydride is a short chain of just 6 carbons that has already been used to graft proteins by a similar strategy on Teflon and CF_x substrates [75, 76, 77].

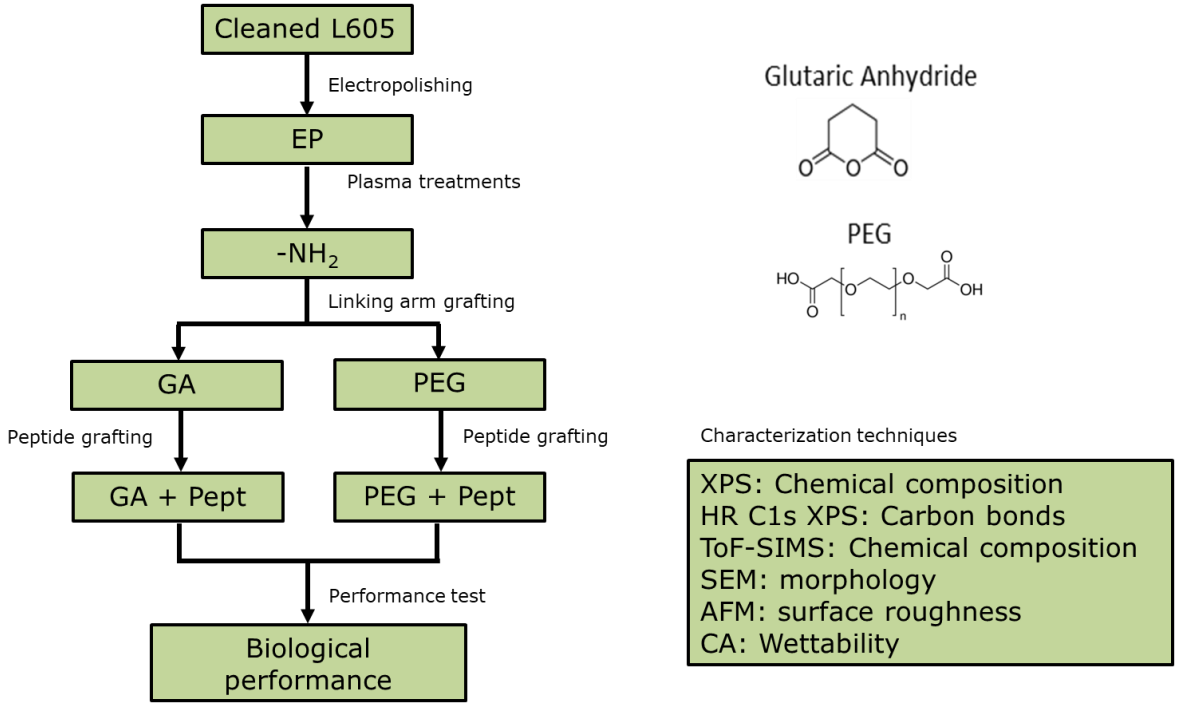

Figure 14 General methodology for the optimization of the linking arm to be used in this multi-step strategy

These linking arms are activated by their terminal carboxylic groups in order to create a covalent bonding with the selected biomolecule. This molecule is a synthetic peptide that has been patented for its anti-inflammatory, pro endothelialisation and anti-stenotic properties, which is a fragment of the transmembrane receptor PECAM-1. This receptor, also known as CD31, has been found in endothelial cells, platelets and leukocytes, where it plays a role in adhesion. The fragment of interest is a 23 amino acid peptide that contains free amino groups, as lysine and arginine, that are used to react with the previously activated carboxylic groups of the linking arms. The sequence of P23, expressed in the single-letter amino acid code detailed in Table *12*, is:

H-**N**HASSVP**R**S**K**ILTV**R**VILAPW**KK**-OH

It is expected that after the grafting this peptide conserves the desired properties. [96,97,98,99,100].

Table 12 Single-letter code of the amino acids of interest for this project. Furthermore, the ToF-SIMS fragments in positive mode with their respective m/z is also presented for further references. [101]

Letter	Amino acid	Tof-SIMS fragment	m/z
N	Asparagine	C_3H_4NO, $C_3H_7N_2O$, $C_3H_6NO_2$ and $C_4H_4NO_2$	70, 87, 88 and 98
H	Histidine	$C_4H_5N_2$, $C_4H_6N_2$ and $C_5H_8N_3$	81, 82 and 110
A	Alanine	C_2H_6N	44

S	Serine	C_2H_6NO and $C_3H_3O_2$	60 and 71
V	Valine	$C_4H_{10}N$ and C_5H_7O	72 and 83
P	Proline	C_4H_6N and C_4H_8N	68 and 70
R	Arginine	CH_3N_2, $C_2H_7N_3$, $C_4H_{10}N_3$, $C_4H_{11}N_3$ $C_5H_8N_3$ and $C_5H_{11}N_4$	43, 73, 100, 101, 112 and 127
K	Lysine	$C_5H_{10}N$	84
I	Isoleucine	$C_5H_{12}N$	86
L	Leucine	$C_5H_{12}N$	86
W	Tryptophan	C_9H_8N, $C_{10}H_{11}N$ and $C_{11}H_8NO$	130, 159 and 170
F	Phenylalanine	$C_8H_{10}N$ and C_9H_7O	120 and 131

1.3.4 Biological performance: does the CD-31 peptide increases the in vitro and in vivo performance of the L605 CoCr alloy?

The last block of this project focuses on the evaluation of the performance in vitro and in vivo of the functionalized L605 CoCr alloy. In vitro tests are performed mainly for flat samples whilst in vivo focuses on the implantation of functionalized stents (Multi-link by Abbott) in pig model. Nevertheless, compared with the previous block, smaller peptide sequence than P23 are used, P8RI and P8FI. Both are peptides with 8 amino acids chains with the same composition only that P8RI is a reversed chain and P8FI is the "forward" chain. The 8 amino acids that compound the peptide chain are:

RVFLAPW**K**

These peptide sequences have been isolated from the previous one (P23), and have exhibited the same biological properties, meaning anti-inflammatory, anti-restenosis and pro-endothelialization. By using smaller peptides, steric hindrance and 3D conformation are lower, thus the losing of biological properties is limited. Still, the presence of arginine and lysine, that have free amino groups, can react with the linking arm. Therein, due to the complexity of in vivo studies, and based on preliminary tests on flat samples where peptides grafted via PEG have exhibited lower inflammatory response, only PEG was used for this block. Figure 15 shows the general methodology for this block.

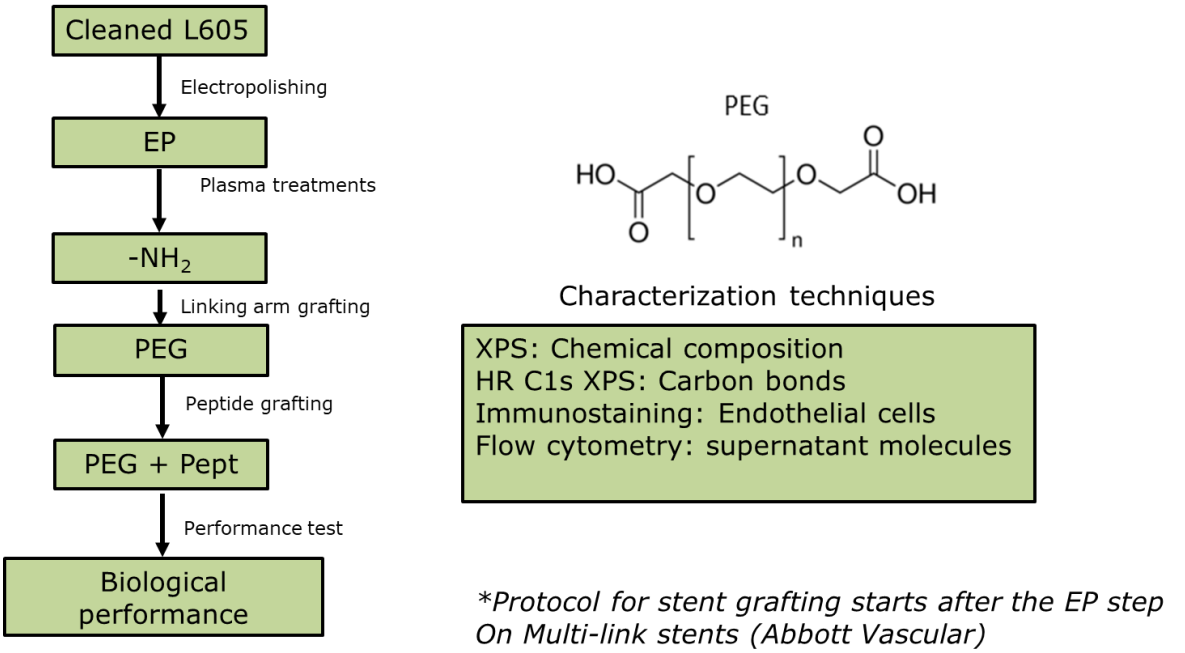

Figure 15 General methodology for the sample preparation for the in vitro and in vivo evaluation of different peptides in flat and commercial bare metal stents

Also, regarding the transfer of the plasma functionalization from flat to 3D structures, the feasibility of functionalizing stents and the parameters for the plasma treatments must be adapted and optimized.

1.3.5 Characterization techniques

Due to the nature of this project, characterization techniques play an important role in the understanding of the surface modification, the molecule grafting and to predict the further interaction of the device with the organism. The proposed multi-step procedure modifies the first layer of atoms of the oxide layer of the alloy and introduces functional groups and bioactive molecules. Therefore, the scale of work represents a challenge and a need for adequate and sensible characterization methods to understand the chemical changes throughout the procedure. A combination of different characterization techniques should be performed in order to obtain the complete information of the surfaces. Thus, allowing to understand the functionalization and predict the interactions between the surfaces and the different tests. Characterization techniques with their specific application on this project are shown in Table 13.

Table 13 Characterization techniques with their specific application in this research project.

Characterization method	Applications
XPS	Allows the study of the atomic composition and the nature of the chemical bonds present on the surface by using the high-resolution spectra of specific atoms.

	XPS allows the study of the composition of the oxide layer, the confirmation of nitrogen and primary amine groups obtained after plasma treatments. The presence of the linking arm and peptide grafting onto the alloy surface can be studied by XPS.
Water Contact Angle	Allows to study the wettability of the surface and their changes throughout the multi-step procedure. The addition of functional groups can be correlated to an increase or decrease of this property.
TOF-SIMS	Surface characterization technique that allows the study of the first layer of atoms of a material. Study of the chemical composition of the surface by irradiating the surface with energetic ions. Allows the study of depth profile, imaging mode and static mode. ToF-SIMS plays an important role in this project for the quantification of primary amine groups on the surface (static mode), conformation of the grafted molecules (static and imaging mode), confirmation of the transter of the platform to cardiovascular devices (imaging mode) and for the study of the oxide layer modifications by depth profile. Table 12 shows some of the fragments of interest for this project.
SEM	Scanning electron microscopy allows the study of the topography of the surface. It can confirm the presence of cracks or delamination after the deformation test on the oxide layer of the alloy.
AFM	Atomic force microscopy measures the roughness and morphology of a substrate. It allows to understand the changes on the surface after the plasma treatments and how the linking arms or the peptides grafted onto the surface modifies the surface roughness.
Fluorescent microscopy	Allows the study of cells after immunostaining. It can be used to observe the difference on the cellular interaction between the different peptides.

1.3.6 Biological performance and characterization

Further than just the characterization of the surface, due to the application of this multi-step procedure it is essential the assessment of the biological properties of the functional surface in vitro and in vivo. the use of pertinent biological tests to correlate the properties with the material composition is crucial for this work. Due to the nature of the peptide and the application, biological tests focus on the study of the cellular and inflammatory response and hemocompatibility of surfaces. Furthermore, thanks to the collaboration with the INSERM and the LVTS it was possible to study the in vivo performance of the functionalized device. A list of these techniques with their specific application on this project are shown in Table 14.

Table 14 Biological tests and their specific application in this research project

Characterization method	**Applications**
Cell proliferation	Allows the study of the cell viability in contact with a surface. Cellular counting is commonly performed at 1, 3 and 7 days of contact with a surface, depending on the desired information. As regards this project, cell viability essays can give information about the toxicity of the different oxide layers in the surface optimization block, after the linking arm grafting to identify the one with the best performance or when comparing different bioactive molecules grafted by this methodology.
Cell adhesion and migration	Allows to obtain information about the behaviour of the cells when in contact of a surface. The use of immunostaining with phalloidin to observe the attachment of the cells on the metallic substrate can be performed. Furthermore, migration essays of endothelial cells can be performed to simulate the re-endothelialization procedure after the implantation in vitro.
Inflammation response	The analysis of the supernatant after the incubation of endothelial cells can be performed to study the presence of different metabolic products. As regards this project, it is desired to find low concentration of pro-inflammatory factors (IL-6 and VCAM-1) and a high concentration of anti-thrombotic factors

	(TFPI). The comparison of these analytes can be used to select the best surface with the best potential for in vivo studies.
Hemoglobin free: hemolysis rate	Blood compatibility of the surfaces is investigated using the hemoglobin free technique. This technique measures the quantity of free hemoglobin after the contact with a sample for a fixed time. Higher the hemoglobin free, higher hemocompatibility.
In-stent restenosis	Restenosis rate evaluated after 28 days of implantation in porcine model. This model was selected due to its similarities to the human heart regarding the distribution of the coronary arteries, coagulation system and platelet activity [102]. Explanted arteries were further characterized by histology and fluorescent histology. Furthermore, angiographies can be used to obtain information about restenosis whilst still in the body.
Re-endothelialization	Re-endothelialization studies after 7 days of implantation in porcine model. Further characterization is performed by SEM imaging.

Chapter 2: Low-pressure plasma treatment for direct amination of L605 CoCr alloy for the further covalent grafting of molecules

Authors: Sergio Diaz-Rodriguez[1], Pascale Chevallier[1], Diego Mantovani[1]

[1] Laboratory for Biomaterials and Bioengineering (CRC-I) Department of Min-Met-Mat Engineering and the CHU de Québec Research Center, Laval University, PLT-1745G, Québec, QC Canada G1V 0A6

Keywords: amination; biomolecule grafting; cobalt chromium alloy (L605); metallic substrate; plasma functionalization

This chapter has been published in Plasma Polymers and Processes.

Diaz-Rodriguez, S.; Chevallier, P.; Mantovani, D. *Plasma Process. Polym.* **2018**, e1700214. DOI: 10.1002/ppap.201700214

2.1 Résumé

Les plasmas à basse pression permettent de modifier la surface des matériaux de multiples façons grâce à leurs grands nombres de paramètres variables, ce qui fait d'eux une plateforme très polyvalente. Cependant, lorsqu'il s'agit de substrats métalliques, l'approche utilisée pour greffer des biomolécules, est le dépôt préliminaire de revêtements polymères, suivi d'une activation. L'approche originale proposée dans ce travail est de s'affranchir de cette couche polymère, via un procédé en plusieurs étapes qui consiste en une préparation de la surface, suivi de l'amination directe par plasma, puis le greffage de la biomolécule. Les résultats obtenus par XPS et ToF-SIMS confirment la faisabilité de ce procédé. En effet, le greffage du peptide sur le substrat métallique est effectif et homogène. Au meilleur de nos connaissances, il s'agit de la première étude à présenter une procédure d'amination directe, par plasma à basse pression, sur des substrats métalliques. Cette technique innovante a le potentiel de greffer des biomolécules facilement et directement sur des métaux, et ouvre ainsi la porte à de nouvelles avancées dans le développement de dispositifs fonctionnels.

2.2 Abstract

Low-pressure plasma represents a versatile platform for material surface modifications. As regards metallic substrates, the deposition of polymeric coatings generally constitutes an added step prior to biomolecule grafting. An original multi-step approach involving surface preparation, direct plasma-amination, and biomolecule grafting was explored in the present study. Overall results, supported by XPS and ToF-SIMS analyses, confirm the successful and homogeneous grafting of peptide onto the metallic substrate. To the best of our knowledge, this is the first study to present a successful low-pressure plasma amination procedure in metal. This innovative technique has the potential to easily graft biomolecules and thus creates opportunities for advances in the development of novel functional devices.

2.3 Introduction

Metallic alloys, such as CoCr, stainless steels, and titanium have been used in a wide range of applications owing to several excellent mechanical and surface properties, including tensile strength, ductility, corrosion resistance, and chemical composition. [103] In the realm of biological applications, alloys are used primarily as prostheses for the fixation of fractures or intravascular implants. In the latter application, stainless steel and cobalt chromium (L605) represent the most popular alloys in the vascular medical device industry. L605 has generated significant interest because of its potential in the fabrication of thinner devices, thereby decreasing post-implantation clinical complications. [16] Nevertheless, due to a lack of integration with the host, bare metallic devices, such as stents, lead to failure after implantation. Thus, enhanced biological properties, such as antibacterial activity, endothelialization, low thrombosis, and anti-inflammatory response, constitute mandatory requirements for clinics. [25] In order to confer such properties to metallic substrates, polymeric-based coatings, as an intermediate layer, are usually deposited to be further functionalized with bioactive molecules and proteins. Indeed, the major techniques currently in use for this purpose are wet-chemistry based: dip coatings, atomic layer-by-layer casting depositions, solvent evaporation, and spray coatings. However, the procured polymeric coating stability does not ensure total resistance during the implantation procedure (navigation through tortuous arterial beds, deployment, and fixation), as well as cracks, delamination, and coating breakages, which are often observed. [24]

To address these issues, a highly adherent polymeric-based coating deposited by plasma polymerization on electropolished metallic substrates has emerged. Specifically, a highly-adherent fluorocarbon-based plasma interlayer has been investigated, from its deposition to deformation and from its stability to fluidity under static and dynamic conditions with grafted proteins.[76, 104, 105, 106] In the present work, a novel approach that foregoes the polymeric coating step [28, 107, 108, 109, 110] is proposed, involving the direct functionalization of the first layers of the metal surface by plasma-based techniques to further graft biomolecules of interest. To the best of our knowledge, such a multi-step strategy has not yet been reported in the literature.

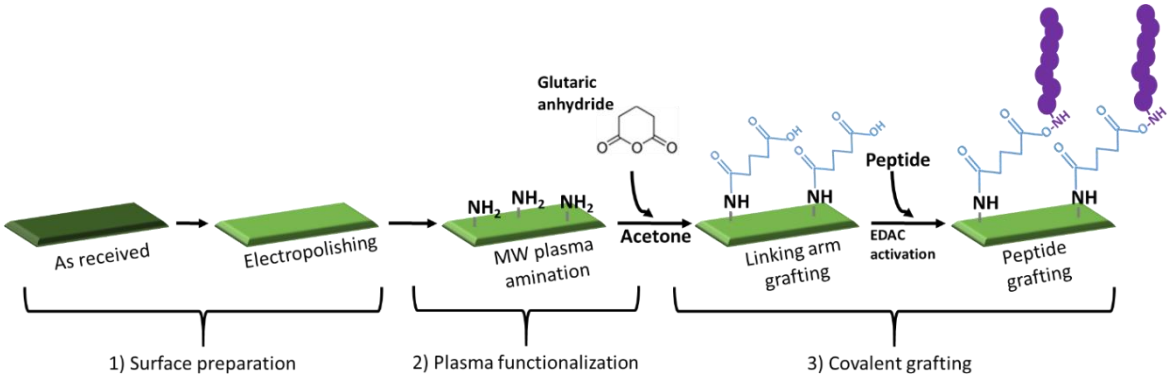

Figure 16 Multi-step procedure for the covalent grafting of molecules on bare metallic L605 CoCr alloys based on a MW plasma amination. The procedure consisted of three main steps: surface preparation, plasma functionalization, and covalent grafting of molecules onto the metallic surfaces.

In this work, we report on the feasibility of grafting biomolecules onto L605 metallic substrates through direct plasma amination. Using an innovative multi-step procedure as shown in Figure 16, a biomolecule, in this case a peptide, was successfully grafted onto the surface of the metal. Briefly, this process houses three main steps: (1) surface preparation by electropolishing (EP) to remove the native oxide layer from as-received specimens and to create an homogeneous, controlled, and reproducible new one; followed by (2) plasma functionalization by nitrogen/hydrogen microwave (MW) plasma leading to functional primary amine groups which, due to their high reactivity, are used as anchor points for further reactions;[75] and finally (3) the covalent grafting of molecules, including a linking arm, i.e., glutaric anhydride (GA) [24, 77] and/or a biomolecule. One of the main advantages of this multi-step technique is that primary amine groups can be directly created onto metallic surfaces by means of plasma treatment, without the use of wet chemistry. [111] The effects of each step of the procedure, such as changes in chemical composition, were carefully assessed by X-ray Photoelectron Spectroscopy (XPS) analyses. In addition, Time of Flight Secondary Ion Mass Spectroscopy (ToF-SIMS) was used to investigate specific fragments associated with surface functionalization as well as the grafting homogeneity.

2.4 Materials and Methods

2.4.1 Materials

L605 alloy sheets (wt %: Co 51%, Cr 20%, W 15%, Ni 10%, Fe ≤ 3%, C ≤ 0.15%) were purchased from Rolled alloys Inc. (QC, Canada). Acetone and methanol (ACS grade, respectively) were purchased from Fisher Scientific. Phosphoric acid (85%), sulfuric acid (ACS grade), and hydrofluoric acid (48%) were purchased from Laboratoire MAT (QC, Canada). From Sigma-Aldrich the following reagents were purchased: Sodium hydroxide (≥ 97%, pellets), Glutaric anhydride (GA, 95%), MES (2-(N-morpholino)ethanesulfonic acid, ≥ 99%), and EDC (1-ethyl-3-(3-dimethylaminopropyl) carbodiimide hydrochloride, ≥ 98%). PBS (phosphate buffered solution, 1 X

powder) was purchased from Fisher Scientific. For the grafted molecules, custom peptides, containing lysine in its structure, and a modified peptide, with a terminal tyrosine with iodine, Tyr(3I), were purchased from Mimotopes (MN, USA) and GeneCust (Dudelange, Luxembourg), respectively.

2.4.2 Methods

To remove the impurities, round 1 cm^2 specimens punched from L605 alloy sheets were first cleaned in three successive 10 min ultrasonic baths of acetone, nanopure water, and methanol, subsequently air dried, and finally stored under vacuum until use. After cleaning, the samples were electropolished. The samples were treated three times for 2 min with a 3 A current in a solution containing 67% phosphoric acid, 20% sulphuric acid, 10% nanopure water (18.2 MΩ·cm at 25 °C), and 3% hydrofluoric acid at 10 °C in an ice bath. Thereafter, the samples were cleaned in three successive 10 min ultrasonic baths of nanopure water, sodium hydroxide 2 N, and nanopure water, respectively.

Plasma amination of the substrates was performed in the after-glow region (7 cm) of MW plasma (Plasmionique Inc., Varennes, QC, Canada) by means of a two-step process using a mixture of N_2 and H_2 (grade 4.8 and 5.0, respectively, Linde, QC, Canada) as the feeding gases. The first stage was carried out at 150 W during 10 min at 100 mTorr, 5/5 sccm of N_2/H_2, while the second was performed at 150 W during 30 s at 300 mTorr, 10 sccm of H_2. This short plasma treatment using hydrogen was performed to promote the amination, by using the H radicals created during the plasma as potential reducing agents for other nitrogen species other than amines (amides, imides, etc).

For the covalent grafting step, plasma-treated samples were immersed in acetone and GA (0.1 g mL^{-1}) was added thereafter at 0, 20, and 40 min. After 1 h of reaction, the samples were washed three times with acetone and five times with deionized water under vortex, and finally air dried. GA was used as a linking arm to further graft the peptide of interest through its lysyl moieties through a stable covalent binding. For this purpose, samples grafted with GA were activated in MES (2-(N-morpholino)ethanesulfonic acid) buffer (pH 4.75), with 3 mg mL^{-1} of EDC (1-ethyl-3-(3-dimethylaminopropyl) carbodiimide hydrochloride) added every 10 min, for three times, until the reaction was complete (30 min). Following activation, the samples were covered with 500 µL peptide solution (2.5 x 10^{-5} M in phosphate buffer saline) and left to react for 3 h. Thereafter, the grafted samples were washed five times with deionized water under vortex, air dried, and characterized.

The surface chemical composition was assessed using X-ray Photoelectron Spectroscopy (XPS -PHI 5600-ci Spectrometer-Physical Electronics, USA), at a pressure under 10^{-8} Torr, with an achromatic Al X-ray source while high resolution spectra of C1s were obtained using an achromatic Mg X-ray source. The detection was performed at 45° with respect to the surface normal and the analysed area was 0.5 mm^2. The ToF-SIMS

analyses were performed using a ToF-SIMS IV spectrometer (ION-TOF GmbH, Munster Germany) with a pulsed 25 keV Bi^{3+} ion beam over a 250 × 250 μm^2 area. The total ion fluence was kept under 10^{12} ions/cm^2, and the secondary ions were extracted at a 2 kV acceleration voltage.

2.5 Results and Discussion

The first step of this procedure consisted on the surface preparation of the L605 alloy, where the homogeneity and composition of the oxide layer were modified by electropolishing to increase the functionalization with -NH_2 groups implanted during the second step of the procedure. Following electropolishing, the samples displayed a mirror like finish, and for the chemical composition, XPS surface analyses (depth: 5 nm, Table 15) confirmed that the oxide layer was mainly composed of chromium oxide. The detected carbon percentage on the surface can be related to the presence of carbides on the metallic surface grain boundaries after electropolishing, known to increase the alloy resistance to abrasion. As electropolishing noticeably removed the impurities from the as received samples, it was ascertained that the nitrogen detected in subsequent analyses unequivocally resulted from surface modifications.

Table 15 Surface chemical composition of L605 CoCr substrate after each modification step, assessed by XPS survey analyses. Expressed as the mean ± standard deviation. Analyses performed on 3 different samples with 3 points per samples (n=9).

	METALLIC ELEMENTS		OTHER ELEMENTS		
SAMPLES	**%Cr**	**%Co**	**%O**	**%C**	**%N**
L605 AS RECEIVED	6.8 ± 0.4	3.9 ± 0.8	46.4 ± 1.1	40.8 ±1.6	2.4 ± 0.6
EP	4.8 ± 0.2	-	51.9 ± 1.4	42.9 ± 1.1	-
NH_2	10.3 ± 0.2	4.7 ± 0.1	40.3 ± 0.5	25.3 ± 0.4	10.4 ± 0.5
GA	8.8 ± 1.4	1.3 ± 0.5	41.4 ± 1.6	35.7 ± 3.9	6.3 ± 0.9
PEPTIDE	5.9 ± 0.6	1.2 ± 0.4	35.4 ± 1.0	44.6 ± 0.7	8.2 ± 0.7

After plasma functionalization, cobalt was detected on the surface by XPS survey analyses, related to a potential etching of the metallic surface. XPS analyses confirmed the presence of nitrogen, 10.4 ± 0.5%, as shown in Table 15. An estimation of the primary amine groups on the substrate was thus assessed by vapor phase chemical derivatization with 5-bromosalicylaldehyde, selected by its specific affinity to amine groups than to other nitrogen species. [88] Furthermore, no bromine from the chemical derivatization agent was detected on the electropolished surface, used as control. The surfaces were found to be successfully functionalized, with 1.5 ± 0.4% of primary amine groups detected on the substrate following plasma treatment. The selectivity of the MW plasma treatment, namely, the ratio between the primary amines and initial nitrogen amount detected (%NH_2/%N), was 14.4%. Nevertheless, there is an ongoing debate for the use of chemical derivatization as a valid quantification method for primary amine groups, therefore the need for supplementary surface characterization. [112] The presence of primary amine groups was also confirmed by ToF-SIMS analyses in static negative mode, with the characteristic fragment NH_2^- (m/z 16.095) displaying a NH_2^-/total peak ratio of 2.2

$x10^{-4}$ after amination, as compared to 2.7 $x10^{-6}$ before, confirming the plasma functionalization. These moieties were used thereafter as anchor points to graft molecules, at which point GA was selected as the linking arm and the grafting of a peptide took place as the next stage of the procedure.

The GA grafting was confirmed by XPS analyses, with an observed increase in the amounts of carbon and oxygen associated with the bonded GA structure (-NH-CO-$(CH_2)_3$-COOH), while the metallic and nitrogen relative percentages decreased (Table 15). The efficiency of the GA grafting on primary amines was also confirmed by XPS HR of C1s, as presented in Figure 17a. Indeed, compared to NH_2 sample, the contribution of the C-C/C-H bonding at 285 eV increased, as did the oxygen bonding, with C-O/C-N and C=O (related to COOH/CONH) at 286.5 and 288.3 eV, respectively. This successful grafting was also highlighted by ToF-SIMS analyses in static positive mode (Figure 17b) showing the appearance of a GA-characteristic fragment $C_2H_5O^+$ (m/z 45.033).

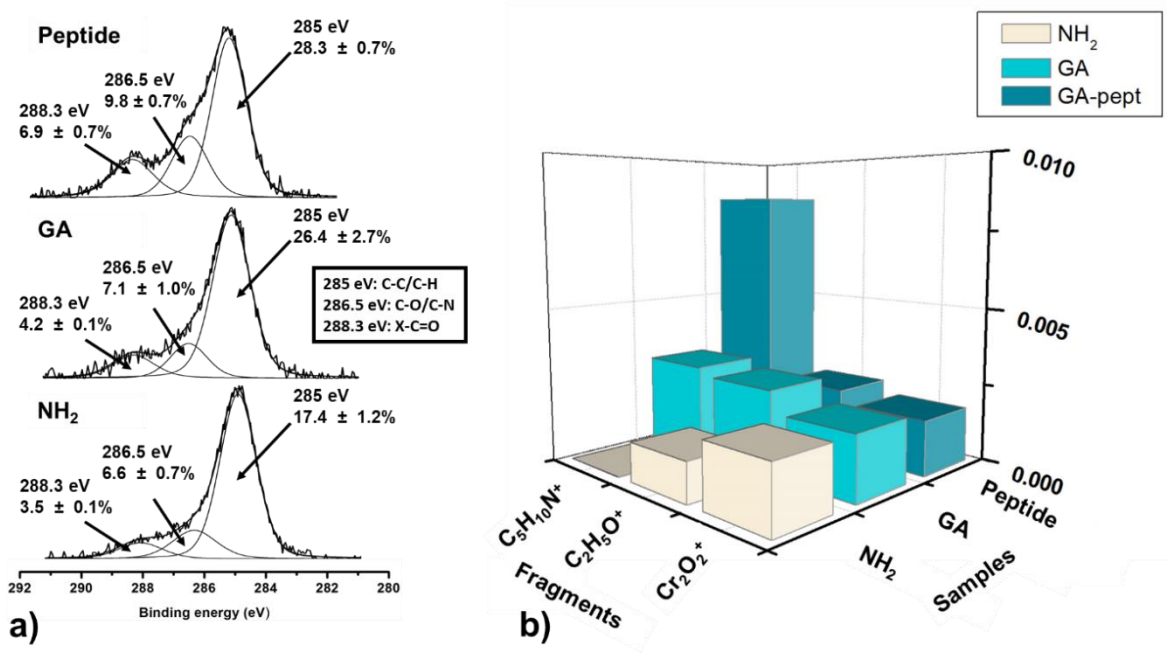

Figure 17 (a) HR-XPS of C1s on an aminated (NH_2), GA (-NH-CO-$(CH_2)_3$-COOH) and peptide grafted sample, reported as mean value ± standard deviation, n=9. X = -OH, -NH_2, -NH. (b) Static ToF-SIMS results, in positive mode, based on the relative peak intensity of the different characteristic fragments: $Cr_2O_2^+$, m/z 135.871 (L605 metallic surface); $C_2H_5O^+$, m/z 45.033 (GA grafting); and $C_5H_{10}N^+$, m/z 84.085 (peptide lysyl moieties).

Chemical composition, as assessed by XPS (Table 15), confirmed the covering of the metallic substrate, with a decrease in the percentage of metallic elements associated with the peptide grafting. Meanwhile, elements of the peptide composition, namely, carbon and nitrogen, increased as expected. The grafting was also evidenced by HR-XPS C1s spectra (Figure 17a) emphasising the significant increase of the band at 288.3 eV, associated with the peptide bond (-NH-C=O). Furthermore, due to the structure of peptide, a slight increase of C-O/C-N at

286.5 eV and C-C/C-H bonding at 285 eV were observed. The efficiency of the peptide grafting was further highlighted by ToF-SIMS analyses in static positive mode through the specific lysine fragment ($C_5H_{10}N^+$ m/z 84.085), as evidenced in Figure 17b, which presented a significant increase compared to the GA surface. The presence of this fragment on GA could be related to another fragmentation present after the GA grafting for example $C_4H_6ON^+$. The direct MW plasma amination of bare L605 metal surfaces after the removal of their native oxide layer by EP was clearly achieved using this multi-step procedure. This oxide layer, achieved after EP, was composed mainly by chromium oxide, as evidenced in XPS survey analyses. Chromium oxide fragments (Figure 17b) present throughout the multi-step procedure confirm a direct metal functionalization, rather than a coating deposition. In addition, the anchor points created on the substrate with MW plasma (the primary amine groups) were stable under the different conditions under study, namely, acetone, buffer aqueous solution, under agitation, and under vortex. Well-defined grafting efficiency was assessed by XPS analyses in both the survey and the high-resolution spectra of C1s, as well as by static ToF-SIMS analyses. Moreover, homogeneity of the grafted material was examined because of its relevance for eventual medical device applications. For this purpose, ToF-SIMS analyses and imaging were performed by using a specific heteroatom added to the peptide to ascertain that the associated signal unequivocally resulted from the peptide grafting. In this case, modified peptide with iodide was considered. The ToF-SIMS findings clearly evidenced that the peptide was successfully grafted (Figure 18). On the left, the relative intensity of the amino acid fragments related to the peptide composition: alanine ($C_2H_6N^+$, m/z 44.0501), proline ($C_4H_8N^+$, m/z 70.071), valine ($C_4H_{10}N^+$, m/z 72.083), lysine ($C_5H_{10}N^+$, m/z 84.085), leucine/isoleucine ($C_5H_{12}N^+$, m/z 86.097) and the sum of these fragments are shown.[19] It can be observed the significant increase on the relative intensity of these fragments after the grafting of the peptide. Moreover, the iodine-specific fragment, I^-, m/z 126.904 was not detected on the GA sample (Figure 18b) but was found on the iodide peptide-grafted specimen (Figure 18c) and was found to be homogenously distributed on the surface.

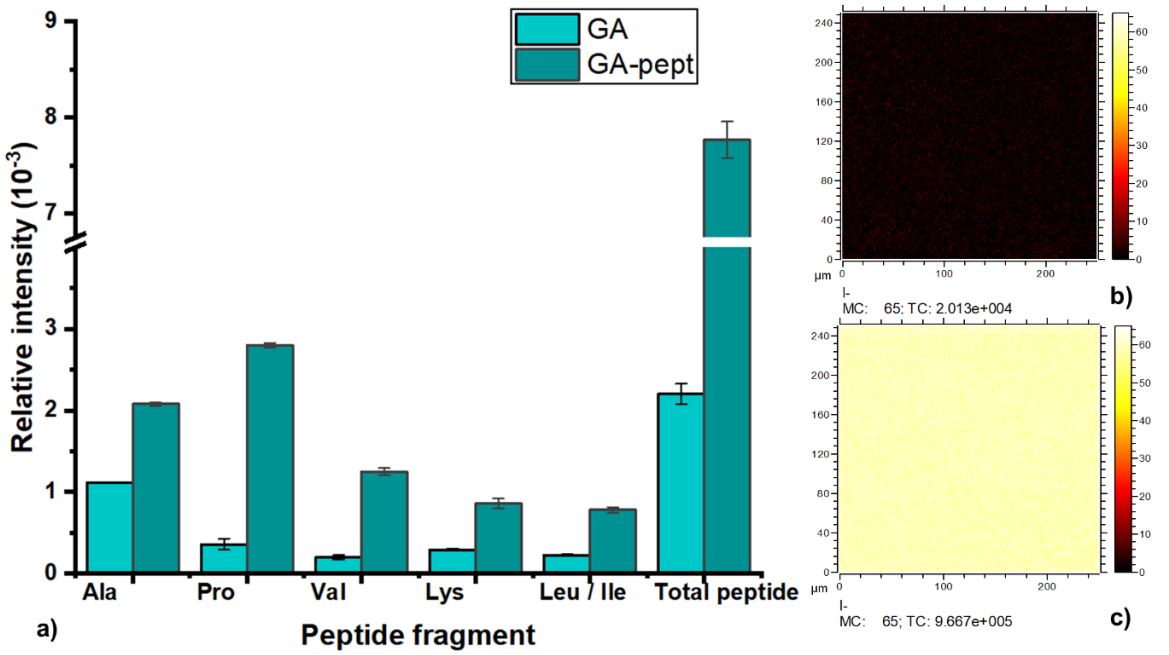

Figure 18 ToF SIMS analyses of the GA surface, prior and after peptide grafting. (a) On the left, relative intensity of the amino acid fragments related to peptide composition: alanine, proline, valine, lysine, leusine/isoleusine and a total sum of these fragments. On the right, ToF-SIMS images 250 µm x 250 µm of fragment I^-, m/z 126.904. (b) GA sample, as the control, without the iodine peptide, and (c) the grafting surface which exhibited a homogeneous distribution of the Peptide-I.

2.5 Conclusion

In summary, a multi-step procedure based on MW plasma was successfully used to functionalize amine groups on bare L605 cobalt chromium alloy surfaces. These amine groups were found to be stable under various conditions, such as solvent, temperature, and vortex rinsing. Further to this, GA was grafted onto these amine groups and was used as a linking arm to bond the peptide. This novel approach has the potential to directly functionalize metals without the use of a polymeric-based coating and simplify the procedure to create new bioactive surfaces and provide clear advantages for the functionalization of medical devices. To the best of our knowledge, such a plasma-based strategy has never been reported.

2.6 Acknowledgements

This work was supported by the Natural Sciences and Engineering Research Council of Canada (NSERC) and the CHU de Québec Research Center. Sergio Diaz-Rodriguez is a recipient of a PhD scholarship from the NCPRM (www.ncprm.ulaval.ca). The ToF-SIMS analyses were performed by Céline Noël, under the supervision of Laurent Houssiau, PhD, at the Laboratoire Interdisciplinaire de Spectroscopie Éléctronique (LISE), Namur University, Belgium. The authors wish to express their gratitude to Frédéric Chaubet, PhD, Stéphane Turgeon, PhD, and Carlo Paternoster, PhD, for their help, guidance and strategic input.

Chapter 3 Surface modification and direct plasma amination of L605 CoCr alloy: On the optimization of the oxide layer for application on cardiovascular implants

Authors: Sergio Diaz-Rodriguez[1], Pascale Chevallier[1], Carlo Paternoster[1], Vanessa Montaño-Machado[1], Céline Noël[2], Laurent Houssiau[2], Diego Mantovani[1]

[1] Laboratory for Biomaterials and Bioengineering (CRC-I) Department of Min-Met-Mat Engineering and the CHU de Québec Research Center, Laval University, PLT-1745G, Québec, QC Canada G1V 0A6

[2] Laboratoire Interdisciplinaire de Spectroscopie Electronique, Namur Institute of Structured Matter, University of Namur, 61 Rue de Bruxelles, 5000 Namur, Belgium

Keywords: cobalt chromium alloy (L605); metallic substrate; plasma functionalization, oxide layer modification, corrosion,

This chapter has been submitted to RSC Advances on 12-Oct-2018.
Manuscript accepted on 08-Dec-2018.

3.1 Résumé

Les stents sont des dispositifs cardiovasculaires métalliques, utilisés pour traiter l'athérosclérose. Ils sont implantés et déployés dans les artères malades, rétrécies par des dépôts, et permettent de rouvrir la lumière biologique. Néanmoins, des complications après implantation sont encore observées dans 10 à 14% des cas. Par conséquent, l'intérêt de fonctionnaliser ces dispositifs avec des molécules actives pour améliorer leurs interactions avec les tissus environnants, permettrait d'avoir un plus grand taux de succès. Pour cela, un procédé original pour greffer directement des biomolécules à la surface de surface métallique, par traitement plasma à basse pression, sans aucun revêtement polymère, a été précédemment développé. Cependant, il faut s'assurer que cette modification est stable lorsque soumise à la déformation plastique, telle que celle générée lors de l'implantation, aussi qu'elle n'induise pas un processus de corrosion. Cette étude explore donc l'influence de différents prétraitements de surfaces, tels que i) le polissage électrolytique; ii) traitements thermiques, et iii) implantation d'ions par immersion dans le plasma d'oxygène, sur la composition chimique de la couche d'oxyde, sa rugosité, sa mouillabilité, son influence sur l'efficacité du procédé d'amination au plasma, sa stabilité sous déformation, et sa résistance à la corrosion. Pour répondre à cela, des analyses en XPS, AFM, ToF-SIMS imagerie et profil, angle de contact, MEB et des tests potentiodynamiques ont été effectués. Les propriétés biologiques ont été aussi évaluées via des tests d'hémocompatibilité, et de viabilité cellulaire. Les résultats ont démontré que les prétraitements influençaient grandement la composition chimique de la couche d'oxyde : EP est principalement à base d'oxyde de chrome, PIII d'oxyde de cobalt et TT d'un mélange des deux oxydes. De plus, EP, versus les autres prétraitements, a démontré une plus grande efficacité quant au processus d'amination et une plus grande résistance à la corrosion. L'électropolissage apparait donc comme le prétraitement le plus approprié pour la fonctionnalisation de stent.

3.2 Abstract

Stents are cardiovascular devices used to treat atherosclerosis, deployed into the narrowed artery and implanted by expansion to reopen the biological lumen. Nevertheless, complications after implantation are still observed in 10-14% of the implantation. Therefore, the interest to functionalize these devices with active molecules to improve the interfacial effects with the surrounding tissue strongly impact their success. A plasma-based procedure to directly graft biomolecules to the surface of cobalt chromium alloy, without any polymeric coating, has been recently reported. Assuring the stability of the coating during the plastic deformation generated during the implantation whilst avoiding the corrosion of the surface is crucial. Therefore, this study explores different surface treatments to be used as pre-treatment for this novel procedure. The effects of i) electropolishing; ii) thermal treatments, and iii) plasma immersion ion implantation of oxygen on the chemical composition, roughness, wettability and the efficiency on the plasma-amination procedure whilst avoiding cracks after deformation thus maintaining a corrosion resistant behaviour were investigated by XPS, AFM, ToF-SIMS imaging and depth profile, WCA. Furthermore, hemocompatibility and cytotoxicity of the surfaces were also assessed. Results showed that all treatments create a different surface chemical composition, EP mainly of chromium oxide, PIII with a layer of cobalt oxide and TT with a mixture of oxides, as observed by XPS and ToF-SIMS. Moreover, EP was the process that generated a surface with the highest efficiency to amination and the most corrosion resistant among the treatments, and it appeared as the most suitable pre-treatment for stent functionalization.

3.3 Introduction

Atherosclerosis is a cardiovascular disease characterized by the formation of a plaque that narrows the arterial walls leading to thrombus formation and ultimately heart strokes [5]. Once progressed at late stages, this disease is surgically treated by the implantation of a stent which is a metallic wire mesh. This device is introduced with a catheter to the narrowed zone and expanded up to a 25 % deformation to reopen the arterial flow, deploying the device whilst avoiding the collapse of the artery [107, 113]. Among the materials used for bare metal stents (BMS), there is cobalt chromium L605 alloy, which has interesting mechanical properties and it is covered with a passive oxide layer that protects the surface from potential corrosion. Furthermore, this alloy allows the fabrication of thinner devices with smaller struts that have been correlated to lower clinical post-implantation adverse effects [16]. Nevertheless, complications on BMS remain, indeed, in-stent restenosis, thrombus formation, endothelium damage, still occur due to the invasive procedure of stent deployment [12]. Although, drug eluting stents (DES) have been developed to counter these complications by releasing drugs from a polymeric coating (deposited on the surface). Nonetheless, cracks and delamination of this coating have been observed due to lack of adhesion and cohesion between the surface and the coating [13, 85]. This finding can be related to the complex geometry of stents and the deposition techniques of the polymeric layer (dip coating, spray coating, layer by layer coating, etc.) that can not assure the coating stability during the deployment of the device [114].

Therefore, a novel procedure that allows the direct covalent grafting of active molecules, without any intermediate layer to enhance the biological performance of cardiovascular devices has been developed. Briefly, this procedure focuses on the direct functionalization with primary amine groups, known for their high reactivity [115], on the surface of the L605 alloy that act as anchor points for the further grafting of molecules of interest. Assuring the stability and the properties of the surface (oxide layer) thus appears crucial for the application of this strategy on cardiovascular devices. This oxide layer must resist the deformation related to the deployment of the device, corrosion resistant to avoid the release of toxic ion in the blood stream whilst being biocompatible [13, 94, 116]. Among the different strategies to modify the oxide layer and finishing of metallic substrates, procedures can be divided in mechanical treatments, thermal treatments, ion implantation and chemical treatments [35]. All these treatments can modulate properties such as chemical composition, surface roughness, corrosion and deformation resistance, wettability, blood compatibility and cytotoxicity.

Though all of these treatments can modify the surface of metallic substrates, nevertheless regarding the stent application, mechanical treatments (mechanical polishing for example) are not suitable due to the complex geometry of the device. Therefore, thermal treatments, ion implantation and chemical treatments represent suitable modification procedures. For instance, thermal treatments in a controlled atmosphere can be used to achieve homogeneous changes on the chemical and structural composition [24, 35]. As regards ion implantation

processes, such as plasma immersion ion implantation (PIII), can produce changes both on the surface and in the internal structure, producing an amorphous oxide layer, due to the acceleration of ions into the metallic substrate [94, 95, 117, 118]. Finally, chemical treatments, for example by electropolishing, allow the removal of any surface contaminant and the passivation of the surface whilst obtaining a nano-smooth surface with a mirror like finishing [116, 35, 119].

This study focuses on the surface preparation step of the L605 alloy for its direct plasma amination. Three different surface treatments on L605 CoCr alloy to modify the oxide layer are proposed: Electropolishing (EP), as a base treatment, followed by either thermal treatment (TT) or PIII of oxygen. The specimens were thoroughly characterized by X-ray Photoelectron Spectroscopy (XPS), Time of Flight-Secondary Ion Mass Spectrometry (ToF-SIMS), Atomic Force Microscopy (AFM), Scanning Electron Microscopy (SEM) and Water Contact Angle (WCA) to study their chemical composition, topography and wettability. Furthermore, the influence of these properties on the plasma amination efficiency of the surface was assessed. The deformation resistance and the corrosion behaviour were also determined along with the biological performance of the surface (hemocompatibility and cytotoxicity). These biological properties were selected to study the potential effect on wound healing of the endothelium and the thrombus formation of the device.

3.4 Materials and Methods

3.4.1 Materials

L605 alloy sheets (nominal composition wt %: Co 51%, Cr 20%, W 15%, Ni 10%, Fe ≤ 3%) were purchased from Rolled alloys Inc. (QC, Canada). Acetone and methanol (ACS grade, respectively) were purchased from Fisher Scientific (NJ, USA). Phosphoric acid (85%), sulfuric acid (ACS grade), and hydrofluoric acid (48%) were purchased from Laboratoire MAT (QC, Canada). From Sigma-Aldrich, the following reagents were purchased: sodium hydroxide (≤ 97%, pellets), Calcium chloride (99.99%) and 5-Bromosalicyladehyde (98%). PBS (phosphate buffered solution, 1 X powder) was purchased from Fisher Scientific.

3.4.2 Sample preparation

3.4.2.1 Sample cleaning

To remove impurities, round 12.7 mm diameter specimens cut from L605 alloy sheets were first cleaned in three successive 10 min ultrasonic baths of acetone, nanopure water (18.2 MΩ·cm at 25 °C), and methanol. Samples were air-dried after each cleaning and stored under vacuum until further use.

3.4.2.2 Electropolishing

All samples underwent a three-cycle electropolishing procedure; each cycle was performed for 2 minutes with a fixed current density of 2.4 A/cm^2 in a solution containing 67 vol.% phosphoric acid, 20 vol.% sulfuric acid, 10

vol.% nanopure water and 3 vol.% hydrofluoric acid at 10 °C in an ice bath with a round L605 specimen as cathode. After electropolishing samples were cleaned in three ultrasonic baths for 10 min each using nanopore water, sodium hydroxide 2 N and nanopure water, respectively.

3.4.2.3 Surface treatments

To modify the composition of oxide layer and to study its effect on the direct plasma amination, EP samples were further treated by two different surface modifications: by thermal treatment and by PIII of oxygen. For the thermal treatments, samples were placed in an air furnace at atmospheric pressure at three different temperatures and two different times: 400, 500 and 600 °C during one or two hours. On the other side, samples modified by PIII of oxygen were implanted using a Plasmionique Inc. (QC, Canada) reactor with gas flow of 10 sccm of O_2, a pulse of 50 ms and a frequency of 100 Hz at 5 mTorr, 300 W of power; during 60 min at -10 kV, -1 kV or -0.1 kV as bias; or for 15 min, 30 min at -10 kV bias.

3.4.3 Stability tests

3.4.3.1 Deformation test

Treated samples were deformed up to a 25% using a custom-made small punch test device, mounted on a SATEC T20000 testing machine (Instron, Norwood, USA), which has been already described elsewhere [120]. Deformations were performed at room temperature with a displacement rate of 0.05 mm s□1 with a maximal load of 2800 N, adapted for L605, and further characterized.

3.4.3.2 Corrosion test

Corrosion tests were carried out using a standard 3 electrode electrochemical set up using large carbon electrodes as counter electrodes and a saturated calomel electrode as reference in a 1 L corrosion cell. The selected solution was PBS at 37 ± 1 °C under mechanical stirring. Open circuit potential analyses were performed for one hour followed by potentiodynamic analyses. Corrosion rate calculations were performed following the ASTM G102-89, as previously described [104]. Briefly the corrosion rate was calculated based on Faradays law (equation 1).

$$Corrosion\ rate = 0.00373\ Icorr\ \frac{Ew}{d}$$

where 0.00372 is the conversion factor (mm/mA year), Icorr is the corrosion current density, expressed in mA/cm^2, and EW the equivalent weight of the alloy (26 g) and d is the density of the L605 alloy (9.134 g/cm^3). Measurements were performed with Model K47 Corrosion Cell system and Versa-STAT 3 Potentiostat controlled via Versa-Studio software (AMETEK Princeton Applied Research, TN, USA).

3.4.4 Plasma functionalization

3.4.4.1 Plasma amination

The direct plasma amination was performed in a microwave plasma (Plasmionique Inc., QC, Canada) through a two-step procedure: the first step used a mixture of N_2 (grade 4.8, Linde, QC, Canada) H_2 (grade 5.0, Linde, QC, Canada) as feeding gases; at 150 W during 10 min at 100 mTorr with a 5/5 sccm flow [115]. The second step was carried out at 150 W during 30 s at 300 mTorr with a 10 sccm flow of hydrogen. This short plasma treatment using hydrogen was performed to promote the formation of amine groups and reducing the presence of other nitrogen species [52]. During both steps samples were placed in the after-glow (~7 cm). Amination efficiency was assessed by chemical derivatization with 5-Bromosalicylaldehyde as described by Chevallier et al. [88] immediately after the plasma treatments. This molecule was selected due to its specific selectivity to primary amine groups.

3.4.5 Biological tests

3.4.5.1 Cell viability

Human umbilical vein endothelial cells (HUVEC) were isolated from an umbilical cordon with the previous consent of donor mothers as previously described [121]. Cells from third to sixth passages were used to evaluate the interaction with the surfaces. 40000 cells in M199 (Thermo Fisher, 11150-067) culture media containing serum and penicillin-streptomycin (Gibco, 15140-122) were deposited on surfaces and incubated at 37 °C. After adhesion for 24 h, cells were rinsed with PBS in order to eliminate all rests of culture medium. 300 mL of solution of resazurin on culture medium (1:10) was then added to the samples and let react during 4 h. 150 mL were taken from each sample and fluorescence was measured at 570 nm using a spectrophotometer ELISA reader (BioRad mod.450, ON, Canada).

3.4.5.2 Haemolysis rate

In order to study the hemocompatibility of the different surfaces, the hemoglobin free methodology was assessed [69]. Briefly, 120 µL of recalcified citrated blood were dropped onto the surfaces were added immediately. Samples were incubated at 37 °C and after 20 min, 2 mL of distilled water were added to each surface. Red blood cells not entrapped in a thrombus were hemolyzed. Free hemoglobin molecules were measured using a spectrophotometer ELISA reader at 540 nm. The test was performed 3 independent times with 2 samples per condition each time. Blood from different donors was used for each experiment.

3.4.6 Surface Characterization

3.4.6.1 X-Ray Photoelectron Spectroscopy (XPS)

The chemical composition of the different surfaces was assessed by XPS (depth analysis of ~5 nm). The analyses were carried out using an X-Ray Photoelectron Spectrometer (XPS-PHI 5600-ci Spectrometer-Physical

Electronics, MN, USA). Survey spectra (0-1400 eV) were acquired with standard aluminium X-ray source (1486.6 eV) at 300 W. Charge neutralization was not applied for the analyses. The detection was performed at 45° with respect to the surface normal and the analyzed area was 0.005 cm^2.

3.4.6.2 Time of Flight Secondary Ion Mass Spectroscopy (ToF-SIMS)

All analyses were performed using a ToF-SIMS IV spectrometer (ION-TOF GmbH, Münster Germany) with, for the surface spectra and images, the following operating conditions: A pulsed 25 keV Bi_3^+ ion beam (current = 0.3-0.4 pA; pulse width = 20 ns; pulse width after bunching = 1.0 ns; repetition rate = 10 kHz) was rastered during an acquisition time of 100 s over a 250 x 250 μm^2 area. The total ion fluence was kept under 10^{12} ions/cm2 in order to guarantee static conditions. The secondary ions were extracted at a 2 kV acceleration voltage. Positive and negative spectra were calibrated to the CH_3^+, $C_3H_3^+$ and $CrOH^+$ peaks and to the C_2^-, CrO^- and CoO_2^- peaks, respectively. ToF-SIMS spectra were acquired from 0 to 880 m/z.

During ToF-SIMS depth profiling, the analysis beam (as previously described) and the erosion beam (Cs^+ at 500 eV, current: 40-45 nA), rastered over a 500 x 500 μm^2 area to avoid border effects, were operated in non-interlaced mode with one analysis frame (1.6384 s) and 5 s erosion per cycle, both with a 45° incidence angle to the sample surface.

3.4.6.3 Scanning Electron Microscopy

The sample surfaces were imaged by SEM using a FEI Quanta 250 (FEI Company Inc. Thermo-Fisher Scientific, OR, USA), with a tungsten filament and an acceleration voltage in the range of 10-30 kV in secondary electron mode.

3.4.6.4 Atomic Force Microscopy

Surface texture investigations were performed using the tapping mode on a DimensionsTM 3100 Atomic Force Microscope (Digital Instruments/Veeco, NY, USA) with an etched silicon tip (model NCHV, tip radius = 10 nm, Bruker). Areas of 20 x 20 μm^2 were recorded and analyzed using the NanoScope Analysis software (Bruker). Surface roughness was assessed with NanoScope Analysis (Bruker Corporation, MA, USA) and reported as the root mean square roughness (Rq).

3.4.6.5 Water Contact Angle

Surface wettability was assessed by water contact angle measurements with a video contact angle system VCA-2500 XETM (AST products Inc., MA, USA) in static mode before and after plasma functionalization. A 1 mL droplet of nanopure water was used.

3.4.6.6 Statistical analyses

For XPS, WCA, hemoglobin free, cell viability and corrosion tests, the data were represented as the mean ± standard deviation of 9 measurements, corresponding to 3 independent experiments with each condition in

triplicate. For all tests, significant differences were determined running a one-way ANOVA followed by Tukeys post-hoc method to test all possible pairwise comparisons and determine where the differences lied. A p-value < 0.05 was considered significant (*).

3.5 Results

3.5.1 Selection of conditions

Due to the importance of the mechanical stability of the oxide layer during the deployment of a stent, a deformation test was performed in order to evaluate resistance of the different treatments. As observed in Figure 19, conditions such as 600 °C for 1 h for TT and on the case of PIII, -10 kV for 1 h, presented cracks and peelings on their oxide layer. Therefore, such conditions were discarded. From the remaining conditions, only one for each treatment was selected for the complete study. The selected conditions are EP as a base treatment, TT at 400 °C for 1 h and PIII -0.1 kV for 1 h.

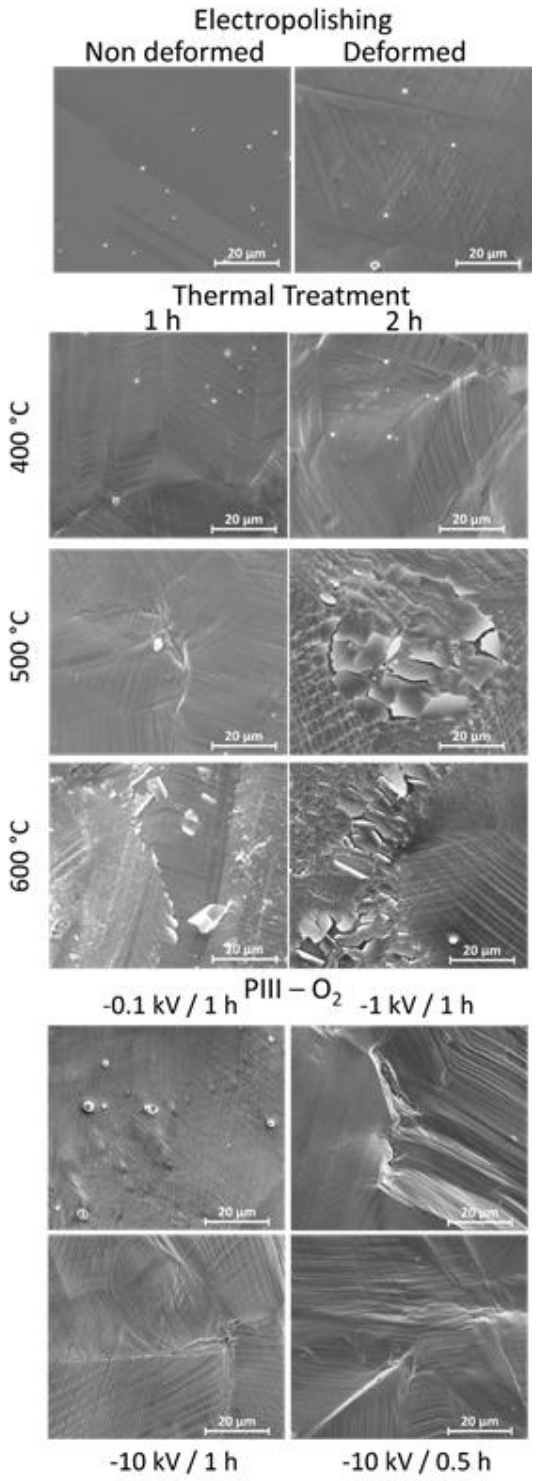

Figure 19 SEM images of surfaces after small punch test to simulate a deformation up to 25%. Cracks and delamination were observed in some TT and PIII conditions. Selected conditions for the further steps of the study were EP, as a base surface, 400 °C for 1 h for TT and -0.1 kV for 1 h for PIII. Magnification of 2000x in all the images. TT and PIII images were all obtained after deformation.

3.5.2 Surface treatments

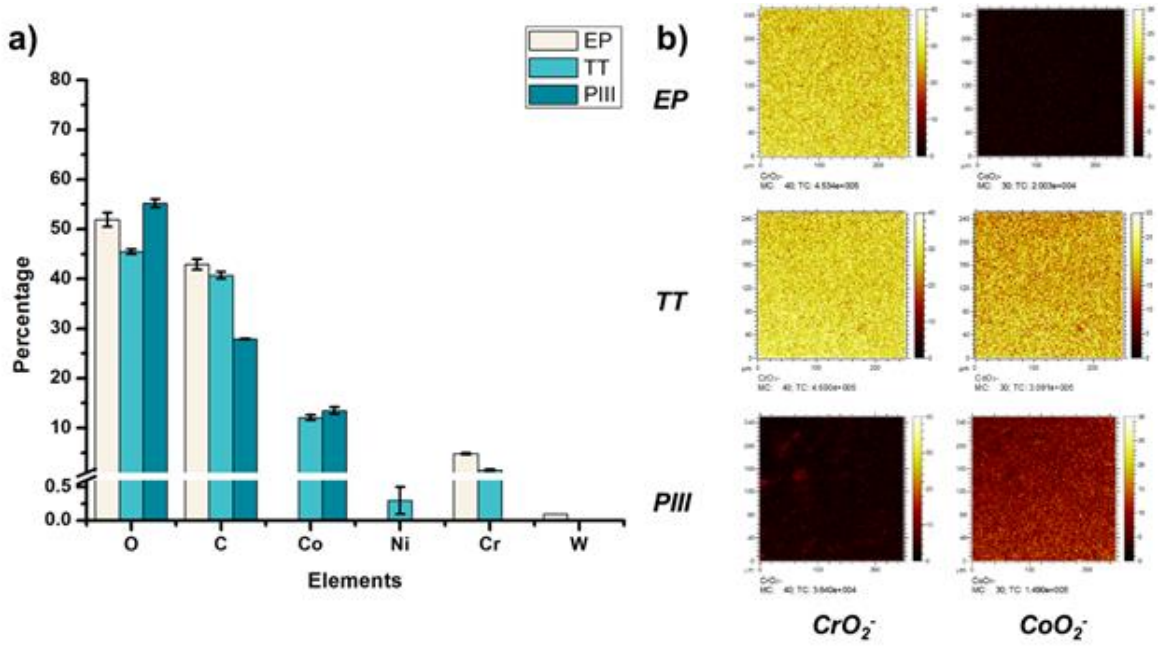

Figure 20 Chemical composition of the studied surfaces. a) XPS survey analyses and b) ToF-SIMS imaging mode of the surface of the specific metallic oxide fragments, for chromium CrO_2^- (84 m/z) and for cobalt CoO_2^- (91 m/z).

Chemical composition of the oxide layers, assessed by XPS survey analyses, in Figure 20a, showed that the first few nanometers of the oxide layer of the EP sample surface are composed mainly of chromium (%Cr = 4.8 ± 0.2); on the contrary, PIII sample surface is composed of cobalt (%Co = 13.5 ± 0.7 %); and finally, TT sample surfaces shows the presence of both cobalt and chromium oxides (%Cr = 1.5 ± 0.2, %Co = 12.1 ± 0.5) with traces of other metals such as nickel. Moreover, the distribution of CrO_2^- and CoO_2^- ions was studied for each of the metallic oxides by ToF-SIMS imaging in negative mode (Figure 20b). It confirmed what was observed in XPS survey results, where it was found that the composition of the outmost layer of EP, TT and PIII follows the same trend. ToF-SIMS depth profile analyses were also performed to obtain information about the depth distribution of the different elements of the oxide layers. Figure 21 shows the obtained profiles where it was found that the EP oxide was the thinnest of them all (~50 s of sputtering) and is composed mainly of chromium oxide. PIII on the other side, has a thicker oxide layer that is composed of a topmost cobalt oxide layer on a chromium oxide sublayer (~150 s and ~350 s of sputtering respectively). Finally, TT has a thick oxide layer composed of both cobalt and chromium oxides on the topmost layer of the surface (~600 s of sputtering). It is worthy noticing that SRIM simulations have been performed to estimate the sputter yields of chromium and cobalt oxides under Cs bombardment and that their similar values (2.4 and 2.6 atoms/ion, respectively) allowed us to safely compare the sputter times between the profiles and equate them with depths.

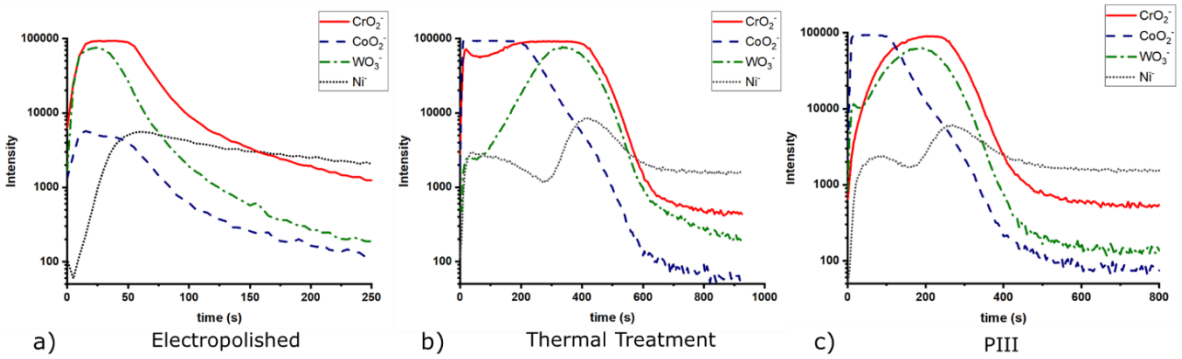

Figure 21 ToF-SIMS Depth profile of surface treatments. a) EP, thin layer composed mainly of chromium oxides, b) TT, thicker layer composed of both oxides on the same depth, c) PIII two layers, first Cobalt oxides then Chromium oxide.

The morphology of the substrate surface was evaluated through AFM (Figure 22). It can be observed on the EP surface the presence of grain boundaries, but not as visibly as on the TT surface, whereas on PIII grain boundaries are not clearly present. Regarding the surface roughness, Rq, it was found that the smoothest surface among the different treatments was EP and that after the surface modification this value increased significantly on both TT and PIII.

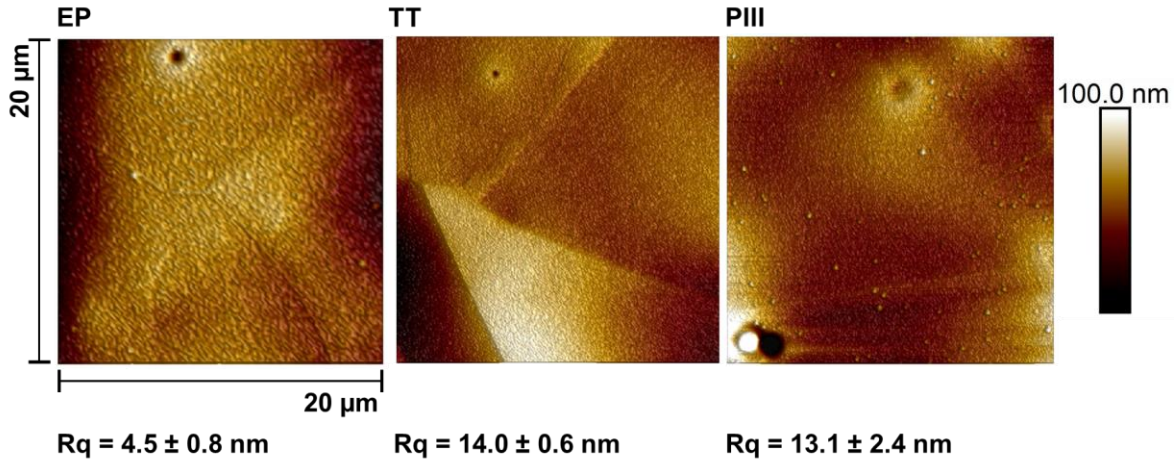

Figure 22 AFM images (20 x 20 µm^2, height mode) of the different samples with their respective roughness values. It can be observed that EP is significantly smoother than the other two surface treatments. TT and PIII present no significant difference among them.

To investigate the corrosion behaviour of the different surface treatments, OCP and potentiodynamic polarization analyses were performed. Regarding OCP (Figure 23a) it was found that TT, composed of a mixture of chromium and cobalt oxides has the lowest open circuit potential, the less noble oxide layer or the most susceptible to corrosion, compared to the other surfaces, whilst PIII was the one with the most positive potential, the noblest oxide layer. Potentiodynamic curves (Figure 23b) allowed the calculation of the corrosion rate where it was found that, as observed in the OCP curves, TT was the surface treatment with the highest corrosion rate, followed by

PIII and finally EP with a ~20x decrease compared to TT. These values and a summary of the results are shown in Figure 23c.

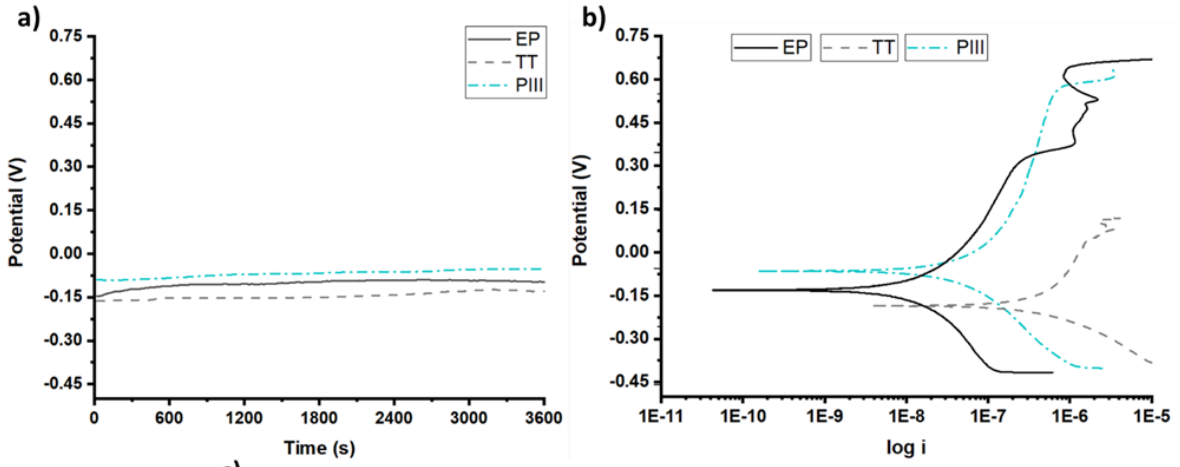

c)

Sample	E_{oc} mV	E_{corr} mV	i corr µA/cm²	Corrosion Rate µm/year
EP	-97.1 ± 12.5	-84.3 ± 9.9	0.013 ± 0.005	0.12 ± 0.05
TT	-150.2 ± 11.5	-125.7 ± 33.5	0.27 ± 0.14	2.55 ± 1.29
PIII	-66.4 ± 11.9	-74.8 ± 16.7	0.05 ± 0.03	0.47 ± 0.29

Figure 23 Corrosion rate of surface treatments. It was found that EP is the most corrosion resistant, followed by PIII and finally TT the less resistant. Potentiodynamic tests performed in PBS at 37 °C.

3.5.3 Plasma functionalization

After the complete characterization of the different oxide surfaces, direct plasma amination was carried out. For the characterization of the surface, chemical derivatization was performed in order to confirm the presence of the amine groups [88]. XPS survey analyses results show that on the TT and PIII surface there is a significantly higher percentage of nitrogen on the surface compared to EP, Figure 24a. Moreover, there was significant difference of percentage of NH_2 on EP with the other two surface treatments, but not between TT and PIII. Finally, regarding the efficiency of the functionalization (%NH_2/N) it was found that EP is the one with the highest efficiency, close to 15%, compared to the other surface treatments, around 9%, as observed in Figure 24a.

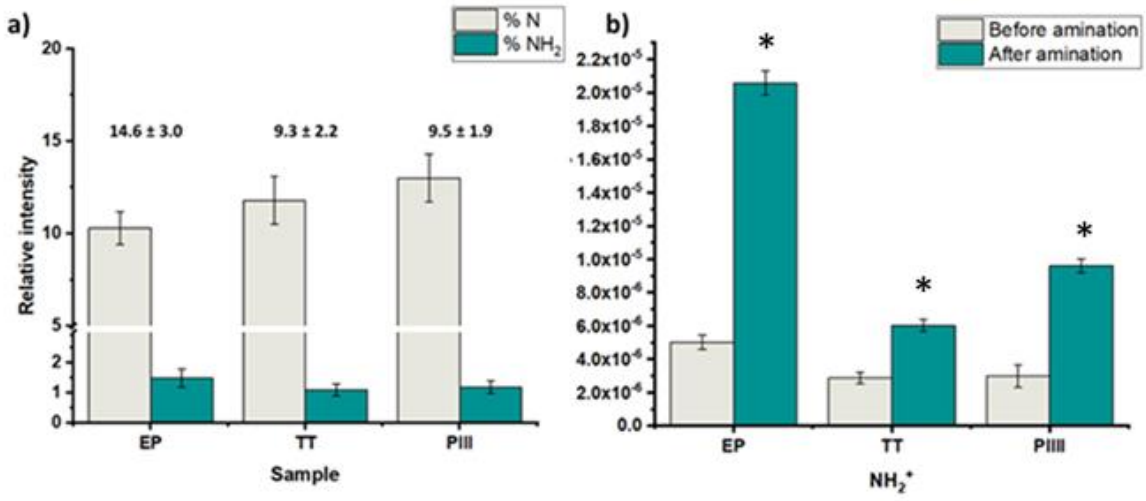

Figure 24 Nitrogen and amine quantification after plasma treatment of the surfaces. a) percent of nitrogen and percent of amine groups after chemical derivatization, obtained by XPS survey analyses with the amination efficiency on top of each sample %(NH_2/N) and b) Comparison of the presence of the NH_2^+ fragment on the different surfaces, before and after amination, performed by ToF-SIMS where EP showed the highest presence of the fragment compared to the other surfaces similar to results obtained after XPS analyses. It should be noticed that the intensity of the fragments was normalized by all of the total signal in order to be able to compare the results. Significant differences were determined running a one-way ANOVA followed by Tukey's post-hoc method, p-value < 0.05 was considered significant (*).

Due to the present debate for the use of chemical derivatization as a valid quantification method for primary amine groups, supplementary surface characterization was performed [112]. Complementary results obtained from ToF-SIMS static mode analyses for the fragment NH_2^+ confirmed that EP has a higher relative concentration of this fragment, followed by PIII and then TT with the lowest signal, as observed in Figure 24b. Another characterization technique that was performed was contact angle, where it was found that the wettability of all surface treatments changed from a relatively hydrophobic behaviour to a more hydrophilic surface after the plasma amination, as observed in Figure 25.

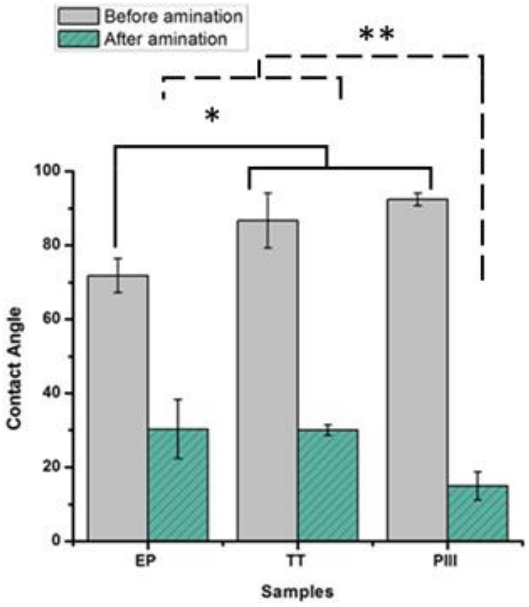

Figure 25 Water contact angle of the surfaces before and after plasma amination. It was found that after the functionalization all of the surfaces presented a hydrophilic behaviour. Significant differences were determined running a one-way ANOVA followed by Tukey's post-hoc method, p-value < 0.05 was considered significant (*).

3.5.4 Biological performance

Further characterization of the surfaces was performed in order to evaluate the biological performance of the different conditions. The viability of HUVEC was studied after 24 h of contact with the samples. As observed in Figure 26a, significantly higher cell viability was observed in EP condition (> 80%) when compared to the PIII one (> 60%), while TT presented an intermediate behaviour with no significant difference with TT nor with EP (> 70%). Hence, EP exhibited the higher viability of all samples. Regarding the evaluation of the hemocompatibility, neither of the samples presented thrombus formation after 20 min of contact with whole blood (Figure 26b). TT condition seemed to present the higher amount of free hemoglobin therefore the best hemocompatibility. However, no significant differences were found among the different conditions after statistical analysis, mainly because of the high variations observed.

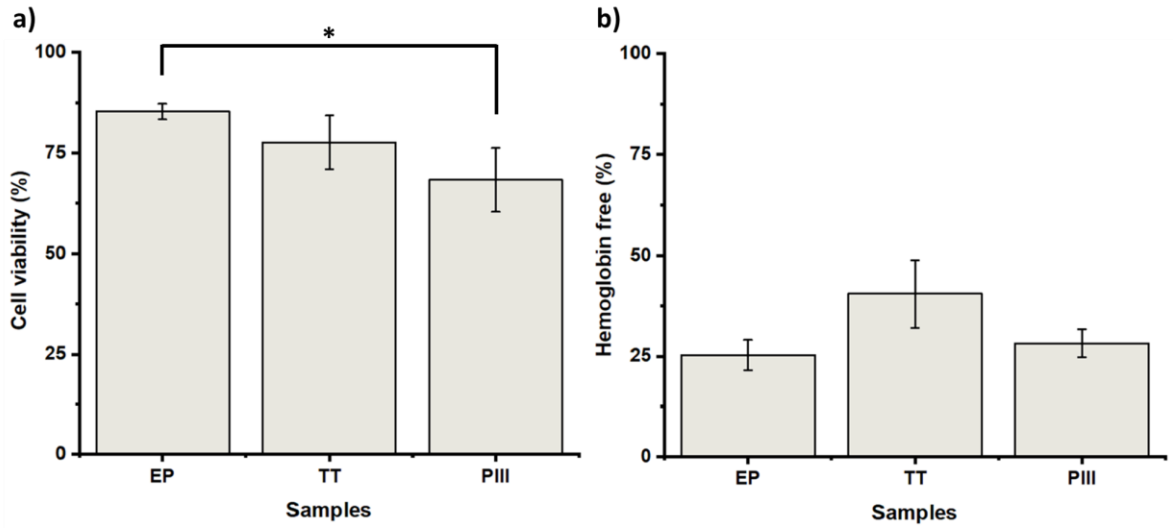

Figure 26 Biological performance of the different treated surfaces. a) HUVEC viability, normalized to polystyrene well. No significant difference among samples, except EP with PIII, but viability higher than 60% of cells. b) Hemocompatibility test, normalized to haemolysed blood, where no significant difference between samples after haemoglobin free test. Significant differences were determined running a one-way ANOVA followed by Tukey's post-hoc method, p-value < 0.05 was considered significant (*).

3.6 Discussion

The aim of this work was to study different surface treatments on L605 CoCr alloy with potential application on cardiovascular devices. In order to find the most suitable oxide layer, properties such as deformation and corrosion resistance, efficiency towards direct functionalization (therein amination) and biological performance in terms of cytotoxicity and hemocompatibility were studied.

Therefore, one of the initial properties to assure for these oxide layers is the resistance to deformation, without showing neither cracks nor delamination. After deforming them up to a 25%, similar to a stent deployment [120], some of the initially proposed conditions exhibited cracks and delamination, as observed in Figure 19, meaning that their oxide layers were unstable and not suitable for the application. This may be explained by the formation of brittle or too thick oxide layers that were not able to sustain deformation. Regarding thermal treated samples, only the oxide layer obtained at 400 °C for 1 h did not exhibit cracks and delamination (Figure 19), despite its thick oxide layer, approximately 10 times more than the EP one, as observed by ToF-SIMS depth-profile results (sputter time 600 s versus 60 s, respectively - Figure 21). The failure of thermal treatments at higher temperature and longer time could be related to the formation of bigger oxide crystals (as seen in Figure 19 for 500 °C 2 h, 600 °C 1 h and 2 h). Similar observations have been already described by Grisaffe et al. where they found that during thermal treatments L605s surface had a low resistance to oxidation resulting in a thicker oxide layer as a function of temperature and time [122]. Moreover, considering the mechanism for cracks and delamination proposed by Wang et al., which involves the formation of microcracks/voids and a high density of oxide particles on the grain boundaries in the near surface area that propagate parallel to the alloy surface with deformation

[123]. These features create a less ductile surface than the underlying bulk leading to peeling, cracks and delamination. This mechanism explains what was observed at higher temperatures of thermal treatments (Figure 19), making these conditions not suitable for the desired application.

In the case of PIII treatments, a higher bias voltage (-1 kV and -10 kV) appeared to induce a thicker oxide layer unstable to deformation, without formation of crystals compared to TT, as observed in Figure 19, whereas the oxide surface obtained at the lowest bias, -0.1 kV, sustained the deformation. It is known that oxygen implantation doses can modulate the crystalline structure (hexagonal Co-oxygen rich phase), the oxide layer thickness, thus changes in the mechanical properties (hardness) [42, 124]. The ion doses are higher when the bias voltage applied on the sample is more negative leading to the acceleration of positive ions which are thus more implanted (increase of the oxide thickness). Thus, -1 kV and -10 kV should create a thicker oxide layer than the one obtained at -0.1 kV, which already needed a sputter time of 400 s (Figure 21, ToF-SIMS depth profile). Moreover, as it can be observed in Figure 19, the failure of the PIIIs oxide layer is mainly due to delamination than to the formation of cracks, as seen in thermal treatments. This behaviour might be related to the amorphization of the oxide layer after the implantation of the oxygen ions [42]. Hence, due to their performance to deformation, only EP, as a base surface treatment, TT at 400 °C for 1 h and PIII with a bias of -0.1 kV for 1 h of implantation of oxygen will be considered.

Another desired surface property for the stent application is corrosion resistance. Due to the composition of the alloy, the concern of the release of potential cancerogenic ions, such as nickel and chromium, into the blood stream is latent. It is known that alloys such as L605 are resistant to corrosion due to its percentage of chromium oxide [23, 87], but modifying its surface composition can influence its corrosion resistance. To have a better idea of the oxide layer stability and resistance to corrosion both Open Circuit Potential (OCP) and potentiodynamic tests have been done (Figure 23). As shown in this figure, EP, the treatment with the thinnest oxide layer (Figure 21) composed of chromium oxides on the surface, based on XPS and ToF-SIMS analyses (Figure 20), was the most corrosion resistant compared to the other ones. This can be attributed to the formation of a passive layer by the Cr_2O_3 surface, similar to what Sojitra et al. observed on stainless steels [93]. Furthermore, corrosion rate for PIII was not far from EP, this could be associated to the ”bilayer” composition of the oxide layer of the PIII treatment. The topmost composed mainly by cobalt oxides then followed closely by chromium oxides, as observed via ToF-SIMS depth analyses (Figure 21c). This change in both composition and corrosion is similar to what was found by Lutz et al. [78]: a diffusion of cobalt to the topmost layer of the alloy. This increases the dissolution of this ion during the initial step of corrosion, followed by a decrease on the corrosion rate by the presence of the passive layer conferred by Cr_2O_3. Moreover, as observed in Figure 23, PIII exhibited the highest Eoc meaning that this oxide layer behaves as the noblest surface compared to the 2 other samples. However, all the samples exhibited a stable oxide layer as no increase nor decrease were observed during the 1 h of OCP.

Finally, on the TT surface, a combination of chromium and cobalt oxides are present on both the surface and in depth (Figure 21b). In fact, this surface chemical composition could be related to a potential formation of a spinel ($CoCr_2O_4$) which has been described previously in literature [122, 125]. Furthermore, after thermal treatments at higher temperatures a dark blue colour, characteristic of this compound, was observed under polarized light (image not shown). The formation of this spinel added to the increase on the roughness of the surface, as observed by AFM (Figure *22*), and the lowest values of both Eoc and Ecorr (Figure 23), lead to a surface more prone to corrode thus an increase of the corrosion on the surface.

Regarding the direct amination of the different oxide layers by plasma functionalization, it was found that all of the surfaces changed their hydrophobic behaviour after the plasma treatment to a more hydrophilic surface as noticed by contact angle (Figure *25*). This can be related to the nitrogen species formed after the plasma treatments since surfaces functionalized with amine groups can lower the contact angle of the oxide layers via hydrogen bond interactions [71]. Furthermore, nitrogen content incorporated on the surfaces was assessed by XPS survey analyses (Figure *24*a). Among the proposed surface treatments, EP was the one with the less percentage of nitrogen on the surface with around 10%, whilst TT and PIII are both around 15%. However, the percentage of primary amine groups on the surfaces on metallic substrates is around 1.5% with no significant difference between the surfaces. When evaluating the efficiency of the direct plasma amination, $\%NH_2/N$, EP is the surface treatment with the highest efficiency as observed in Figure *24*a. Moreover, this observation is furthermore confirmed by ToF-SIMS analyses on static mode of the NH_2^+ fragment related to the primary amine group (Figure *24*b). Indeed, similar to XPS survey analyses, EP is the oxide layer that shows the highest concentration of this specific fragment, on the first layer of its atomic composition, followed by PIII and finally TT has the less presence of this fragment on the surface. The main hypothesis for this preferential formation of amines on the EP surface, could be explained by a substitution reaction of $-NH_2$ on surface hydroxyl groups (-OH), which are already present in the surface of L605 alloy and generated during the basic bath performed just after the electropolishing [126]. Nevertheless, when performing the thermal treatment and the ion implantation these -OH groups could be lost by re-oxidizing the surface and therefore decreasing the amination efficiency.

The biological performances of the different samples were also assessed to ensure that the proposed surface treatments were suitable for the stent application. Therefore, the interaction of the samples with blood and endothelial cells was evaluated. The decreasing cell viability observed in the samples as EP > TT > PIII, as observed in Figure 26a, can be explained with the chemical composition of the surfaces. As it was previously stated, EP sample has mainly chromium at the surface, PIII has mostly cobalt, while TT has a mixture of both elements. Hence, our results are coherent with previous works comparing the behaviour of different cell types in the presence of chromium and cobalt. Indeed, Rushton et al. compared these two elements when in contact

with osteoblasts-like cells, proving that cobalt has the most negative effect when compared to chromium and to an alloy of both elements [127]. Other groups have also evaluated the negative effect of the presence of cobalt in the proliferation and collagen production of osteoblast-like cells [128, 129, 130]. Moreover, Maffi et al. also proved higher endothelial cell viability when cobalt-chromium alloys were enriched with Cr at the surface [131]. However, chromium, and specifically Cr6+, has also been proved to reduce cell survival, which explains the limited difference among all samples, as well as the decrease of cell viability when compared to the positive control. These finding are also coherent with an intermediate behaviour of TT between EP and PIII, mainly because TT has both Cr and Co at the surface. When it comes to hemocompatibility, Figure 26b, all samples presented promising results with no thrombus formation after 20 min of contact with the samples. These results are coherent with previous clinical studies comparing several alloys used in biomaterials where cobalt-chromium presented high hemocompatibility [129, 132]. The different treatments performed had no significant impact on the hemocompatibility of the samples.

3.7 Conclusions

In this study, different surface treatments have been explored in order to reach the most suitable surface, regarding oxide layer stability towards deformation and corrosion, and for amination efficiency. Some surface treatment conditions have been discarded as after deformation, their surfaces have shown cracks or delamination. The other treatments have led to different oxide layer composition and thickness as evidenced by XPS and ToF-SIMS depth profiling analyses. Indeed, EP surface is mainly composed of a thin layer of chromium oxide, whereas PIII surface oxides exhibit a bilayer arrangement, with essentially cobalt oxides on the outermost layer followed by chromium oxides underneath, and finally, TT displays the thickest oxide layer of a mixed chromium and cobalt oxides on the surface. Corrosion performance showed that among the three proposed surface treatments EP was the surface with the lowest corrosion rate, followed by PIII and finally TT with the highest corrosion rate, ~20 times more than EP. Then, regarding biological tests, the different surface oxide exhibited no significant difference among them, appeared to be non-cytotoxic, cells viability was higher than 60%, and to not induce thrombus formation as evidenced by the hemocompatibility tests. Concerning direct plasma functionalization, it was found that all the surfaces could be directly functionalized with primary amine groups no matter of initial oxide layer composition. However, regarding the amination efficiency, EP oxide composition seemed to promote amine formation as evidenced by XPS and ToF-SIMS analyses.

Therefore, among the different surface treatments, EP oxide surface displayed the best corrosion resistance as well as the highest amination efficiency, to be non-cytotoxic nor to induce thrombus formation. Thus, EP treatment appeared as the most suitable metallic interface for further grafting of biomolecule. This direct amination of metallic substrate and grafting of biomolecule, without any intermediate layer, emerges as a potential approach for a new generation of bioactive cardiovascular devices, aiming to lower post implantation

complications. Future studies will investigate different grafting strategies of peptides on EP aminated samples, their stability under pseudo-physiological conditions as well as their biological performances.

Chapter 4 A comparison of the linking arm effect on the biological performance of a CD31 agonist directly grafted on L605 CoCr alloy by a plasma based multi-step strategy.

Authors: Sergio Diaz-Rodriguez[1], Caroline Loy[1], Pascale Chevallier[1], Céline Noël[2], Giuseppina Caligiuri[3], Laurent Houssiau[2] and Diego Mantovani[1]

[1] Laboratory for Biomaterials and Bioengineering (CRC-I) Department of Min-Met-Mat Engineering and the CHU de Québec Research Center, Laval University, PLT-1745G, Québec, QC Canada G1V 0A6

[2] Laboratoire Interdisciplinaire de Spectroscopie Electronique, Namur Institute of Structured Matter, University of Namur, 61 Rue de Bruxelles, 5000 Namur, Belgium

[3] Institut National de la Santé et de la Recherche Médicale U1148, Department of Cardiology, Bichat Hospital, Paris, France.

Keywords: cobalt chromium alloy (L605), stent, plasma functionalization, plasma amination, biomolecule grafting; ToF-SIMS, peptide conformation, in vitro tests

Chapter to be submitted to Biointerphases in July 2019.

4.1 Résumé

Une nouvelle approche permettant le greffage direct de molécules bioactives sur des dispositifs en cobalt-chrome (alliage L605) a été développée. Cette stratégie originale implique la fonctionnalisation directe de la surface métallique, basée sur un procédé par plasma, avec des amines primaires (-NH_2). Ces groupes agissent comme points d'ancrage pour greffer de manière covalente la biomolécule d'intérêt, en l'occurrence un peptide dérivé de CD31 (P23) ayant des propriétés pro-endothélialisation et anti-thrombotiques. Cependant, l'activité biologique du peptide dépend fortement de sa conformation lorsque greffé. Cette étude porte donc sur l'influence de bras d'ancrage, ici l'anhydride glutarique (GA), un bras à chaîne courte, et un polyéthylène glycol (PEG) de chaîne plus longue et doté de propriétés anti-adhérence. Le greffage covalent du peptide d'intérêt sur L605, via les 2 bras d'ancrage, a été confirmé par XPS et ToF-SIMS. Les performances biologiques de ces surfaces fonctionnalisées ont montré que, par rapport à l'alliage nu, greffer le P23 peu importe le bras d'ancrage permet d'augmenter l'adhésion et la prolifération des cellules endothéliales. De plus, ces dernières forment une monocouche complète à la surface de l'échantillon empêchant ainsi la formation de caillots. Par conséquent, cette approche originale permet de fonctionnaliser directement par plasma l'alliage L605, de greffer un peptide dérivé du CD31, et d'obtenir les propriétés souhaitées pour des applications cardiovasculaires.

4.2 Abstract

Stents are cardiovascular devices implanted in atherosclerotic patient that aid to reopen the narrowed artery, sustain and avoid its collapse. Nevertheless, post-implantation complications remain, and the risk of the renewal of the plaque subsists. Therefore, enhanced properties are mandatory requirements for clinics. For that purpose, a novel approach allowing the direct grafting of bioactive molecules on Cobalt-Chromium devices (L605 alloy) has been developed. This original strategy involves the direct functionalization of metallic surface, based on a plasma-process, with primary amines ($-NH_2$). These groups act as anchor points to covalent graft the biomolecule of interest, herein a peptide derived from CD31 (P23) with pro-endothelialization and anti-thrombotic properties. However, the biological activity of the grafted peptide could be impact depending on its conformation related to linking arms (LA). For this study, Glutaric anhydride (GA), a short chain spacer and polyethylene glycol (PEG) with antifouling properties were used as LA. The direct covalent grafting of a CD31 agonist on L605 by using two different LA was confirmed by XPS and ToF-SIMS analyses. The biological performance of these functionalized surfaces showed that, compared to the bare alloy, grafting the P23 with both LA increases endothelial cells (ECs) adhesion and proliferation. Moreover, ECs formed a complete monolayer at the surface of the sample preventing clot formation (hemoglobin-free higher than 80%). Therefore, by using this novel plasma-based procedure, L605 was granted of properties desired in cardiovascular applications.

4.3 Introduction

Bare metal stents (BMS) are used to chirurgical treat atherosclerosis, a cardiovascular disease that narrows the artery by the formation of a plaque. These devices are implanted with a balloon catheter that is expanded on the obstructed area, pushing the plaque onto the arterial walls and deploying the device [133]. Nevertheless, complications after implantation exist and in-stent restenosis, the reformation of the plaque on the stent, might occur [134, 135]. These complications can be related to the damage on the endothelium whilst the deploying the device, the over proliferation of smooth muscle cells (SMC), and thrombus formation [136]. In order to lower complications, one strategy was to load the surface of cardiovascular stents with anti-proliferative drugs to avoid the undesired over proliferation leading to the development of drug eluting stents (DES) [137]. The mechanism of action of the drugs loaded on DES focus on the inhibition of SMCs proliferation, associated to in-stent restenosis (ISR) formation, nevertheless, these drugs also inhibit the proliferation of ECs, compromising the healing of the endothelium leading to long term complications [138]. Thus, one of the main problems for DES is late ISR, which seems to have shifted the time course of restenosis, from 6-8 months in BMS, to >3 years [139, 140]. This led to more than 200,000 number of patients developing restenosis each year only in the USA [141].

In recent years the research for other bioactive molecules with properties such as anti-thrombotic, anti-inflammatory and pro-endothelialization has been performed [142, 143, 144, 145]. A short peptide (P23) derived from the platelet endothelial cell adhesion molecule-1 (PECAM-1), also known as cluster of differentiation 31 (CD31), has shown promising results [146]. This protein is present on the surface of platelets, leukocytes and on the lateral junctions of endothelial cells. It promotes the adhesion and proliferation of endothelial cells whilst avoiding the activation of platelets, conferring properties desired for the stent application [147, 148].

The immobilization of this short peptide onto metallic surfaces can improve the integration of the cardiovascular device. Common strategies to perform this covalent grafting include the deposition of a polymeric coating that allows the further grafting of the molecule [149, 150]. Nevertheless, commonly used deposition techniques, principally wet-based, do not assure the stability of this polymeric layer [151]. However, a novel multi-step strategy to directly functionalize cobalt chromium alloys with amine groups that can be used as anchor points to graft molecules without the use of any polymeric coating has been developed [152]. These amine groups allow the use of different spacers (linking arms) to confer additional properties or to assure the biological activity of the grafted molecule [153]. Furthermore, by avoiding the use of polymeric layers onto the metallic devices, patients with hypersensitivity allergic reactions could potentially use these bioactive stents [154].

For this study, two different linking arms have been chosen in order to observe the impact of their structure on the biological activity of the peptide: Glutaric anhydride (GA), as a short chain linking arm [142, 153, 155, 156], and polyethylene glycol (PEG), as a long chain linking arm known for its anti-fouling properties [135, 157, 158,

159]. Characterization of these functionalized surfaces represents a challenge due to its nanometric range and the use of high-resolution techniques is necessary. The combination of techniques such as XPS and ToF-SIMS allow to obtain information regarding the chemical composition of the surface, the distribution and conformation of the peptide; which can be further correlated to the biological performance, in terms of endothelialization and hemocompatibility, of the functionalized surface. Moreover, the feasibility of transferring the functionalization from flat samples to cardiovascular devices is also studied by ToF-SIMS imaging.

4.4 Materials and Methods

4.4.1 Materials

L605 alloy sheets (wt %: Co 51%, Cr 20%, W 15%, Ni 10%, Fe ≤ 3%, C ≤ 0.15%) were purchased from Rolled alloys Inc. (Qc, Canada). ACS grade acetone and methanol were purchased from Fisher Scientific. From Sigma-Aldrich the following reagents were purchased: Glutaric anhydride (GA, 95%), MES (2-(N-morpholino)ethanesulfonic acid, ≥ 99%) and EDC (1-ethyl-3-(3-dimethylaminopropyl) carbodiimide hydrochloride, ≥ 98%). Phosphate buffered solution (PBS, 1 X powder) and Poly(ethylene glycol) bis(carboxymethyl) ether (PEG, average Mn 600) were purchased from Fisher Scientific. Stents were manufactured by Abbott Vascular, model Multi-Link 8 Coronary Stent.

4.4.2 Experimental procedure

4.4.2.1 Surface preparation

Round specimens of 13 mm diameter were punched from L605 sheets, cleaned in three successive ultrasonic baths of acetone, water and methanol for 10 minutes each. After the cleaning surfaces were electropolished as previously described [152]. Briefly, the process consists in three successive electropolishing in an acid solution in order to remove the native oxide layer and create a nano-smooth mirror like surface with an oxide layer rich in chromium oxides. After electropolishing, samples were exposed to three ultrasonic baths: nanopure water, NaOH 2 N and nanopure water, to remove any remnants of the electropolishing procedure.

4.4.2.2 Plasma amination

After sample preparation the direct plasma functionalization was carried out in a MW plasma reactor fed with nitrogen and hydrogen in a two-step process as described elsewhere [152]. Briefly, plasma amination was performed using a mixture of N_2 and H_2 as feeding gases for the first plasma, at 150 W during 10 min at 100 mTorr, 5/5 sccm of N_2/H_2, while the second was performed at 150 W during 30 s at 300 mTorr, 10 sccm of H_2. Primary amines obtained during this functionalization step were used as anchor points for the further grafting of the linking arms.

4.4.2.3 Linking arm grafting

L605 plasma treated disks were submerged in acetone and 0.3 g mL^{-1} of GA was added three times at 0, 20 and 40 minutes. For PEG, samples were immersed in 0.1 g mL^{-1} PEG solution, pH 4.75 in MES buffer, activated with 3 mg mL^{-1} EDAC added three times at 0, 10 and 20 minutes. Reaction was complete after 1 hour for both linking arms. Once the reaction was finished, samples were vortex washed three times with acetone or MES, for GA and PEG respectively, five times with deionized water, dried and stored under vacuum before use.

4.4.2.4 Peptide grafting

After the grafting of both linking arms, the activation of their respective terminal carboxylic group (-COOH) was performed in order to further graft the peptide. This activation was performed in 5ml of MES buffer with 3 mg mL^{-1} EDAC added three times at 0, 10 and 20 minutes. After 30 minutes of activation samples were removed from the tubes to immediately react with 500 µL of a $2.5x10^{-5}$ M peptide solution in PBS for 3 h. Once the reaction was finished, samples were vortex washed with five times with deionized water, dried and stored under vacuum before further characterization and tests were performed. The complete reaction schema is shown in Figure 27.

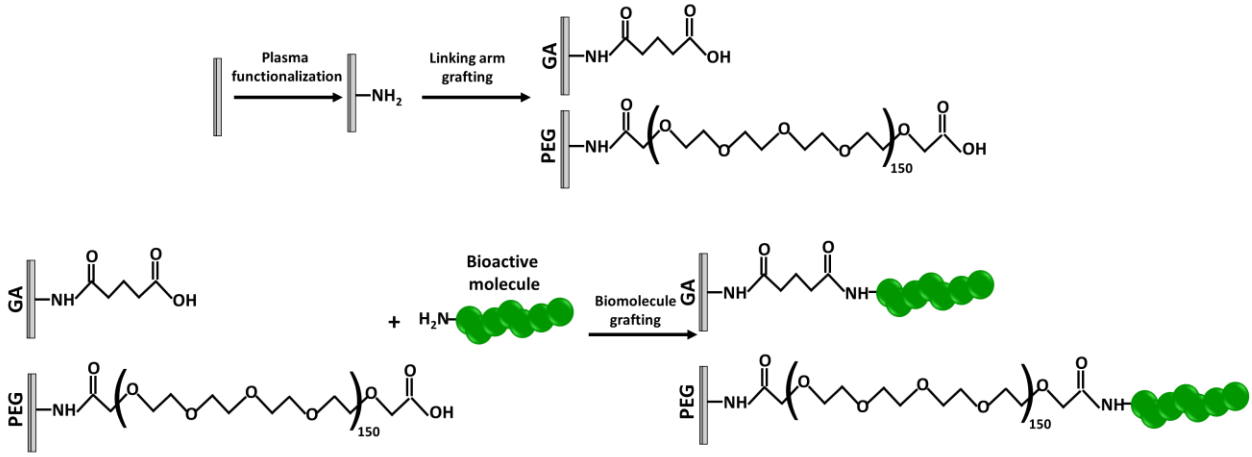

Figure 27 Reaction scheme of the surface modification of the cobalt chromium alloy, involving the plasma functionalization to create reactive amine groups used as anchor points for the linking arm grafting, followed by the biomolecule grafting.

4.4.2.5 Cell culture and cytotoxicity assays

Human umbilical vein ECs (HUVECs) were isolated as previously described [160] from human umbilical cord samples, obtained from normal term pregnancies. Written informed consent was obtained from all mother donors according to the Declaration of Helsinki. All experiments were performed in compliance with the Canadian Tri-Council Policy Statement: Ethical Conduct for Research Involving Humans and institutional CHU de Quebec – Laval University guidelines. The protocol was approved by the Ethics Committee of the CHU de Quebec Research Centre (CER #S11-03-168).

HUVECs were cultured in M199 (Life Technologies, 11995-065) supplemented with 1% PenStrep (G1146 Sigma), 5% Fetal Bovine Serum (Life Technologies, 12483-020), 2 ng/ml FGF (0.1%), 1 ng/ml EGF (0.2%), 1 ug/ml Acid ascorbic (0.1%), 1 ug/ml Hydrocortison (0.1%) and 90 ug/ml Heparin (1%).

Direct cytocompatibility tests were performed to evaluate cell adhesion and growth over samples. Samples were placed in 24-well plates and sterilized with 70% EtOH for 20 min. Then a culture-Insert 2 well (Ibidi) were transfert onto samples. Cells were seeded at a density of 5 x 10^4 cells/cm^2 in each culture-Insert well. After 24 h, inserts were carefully removed. Cell viability was evaluated 1, 3 days and 7 days after seeding, by AlamarBlue assay (Life Technologies, Burlington, ON, Canada), according to the manufacturer's guidelines. Briefly, culture medium was replaced with 400 µL of culture medium containing the resazurin dye. After 5 h incubation in standard culture conditions, the fluorescence of the medium was read (kex:560 nm; kem:590 nm). Viability was evaluated considering the fluorescence of the control cells as 100%.

4.4.2.6 Hemocompatibility assays

The coagulation of whole blood in contact with the surfaces of the developed models was evaluated using the hemoglobin free method. Briefly, 30 µL of human citrated blood were mixed with 6 µL of $CaCl_2$ 0.1 M (Sigma) were deposited onto the surfaces of the different samples and incubated thereafter at 37°C for 10, 20 and 60 min. Directly after, 2 mL of distilled water were added to each sample. The free hemoglobin molecules released in water following hemolysis were measured by reading the absorbance at a 540 nm wavelength by means of a SpectraMax i3x Multi-Mode Plate Reader (Molecular Devices, San Jose, CA, USA). Data where normalized towards the Max Hemoglobin value corresponding to the value obtained by immediate hemolysis after the citrate inhibition by $CaCl_2$. The experiments were performed in triplicate using blood from three different donors.

4.4.2.7 Stent functionalization and grafting

The feasibility of transferring the developed multi-step plasma procedure for the direct covalent grafting of molecules onto commercial stents have been studied. This was performed using the previously proposed strategy [152] with the following parameters: Plasma amination of the substrates was performed in the after-glow region (7 cm) of MW plasma (Plasmionique Inc., Varennes, Québec, Canada) by means of a two-step process using a mixture of N_2 and H_2 (grade 4.8 and 5.0, respectively, Linde, Québec, Canada) as the feeding gases. The first stage was carried out at 150 W during 10 min at 100 mTorr, 10/10 sccm of N_2/H_2, while the second was performed at 150 W during 30 s at 300 mTorr, 20 sccm of H_2. This plasma amination of stents was performed twice on the device, flipping the stent after the first treatment to create a homogeneous functionalization.

After plasma amination, the grafting of PEG as linking arm and the grafting of the peptide were performed as previously detailed for flat specimens.

4.4.3 Characterization techniques

4.4.3.1 X-Ray photoelectric spectroscopy (XPS)

The chemical composition of the different surfaces was assessed by XPS (XPS−PHI 5600-ci Spectrometer-Physical Electronics, USA), at a pressure under 10^{-8} Torr, survey analyses were performed with an achromatic Al X-ray source while high resolution spectra of C1s were obtained using an achromatic Mg X-ray source. The detection was performed at 45° with respect to the surface normal and the analysed area was 0.05 mm^2. The spectrometer work function was adjusted to give 285.0 eV for the main C1s peak.

4.4.3.2 Atomic force microscopy (AFM)

Surface texture investigations were performed using the tapping mode on a DimensionsTM 3100 Atomic Force Microscope (Digital Instruments/Veeco) with an etched silicon tip (model NCHV, tip radius = 10 nm, Bruker). Representative areas of 2×2 μm^2 were recorded and analyzed using the NanoScope Analysis software (Bruker). Average roughness (Ra) and root mean square roughness (Rq) were recorded for all surfaces. The measurements were performed in 3 different areas and on 3 different samples.

4.4.3.4 Immunofluorescence staining

After 1, 3, or 7 days of culture, samples were washed twice with PBS, fixed with 3.7% formaldehyde (Sigma) for 20 min, and treated with 0.5% Triton X-100 in PBS for 30 min at room temperature to permeabilize the cells. The constructs were incubated thereafter for 1 h at room temperature with mouse monoclonal antibody against VE-cadherin (Abcam, Ab7047, dilution 1/50), washed twice with 0.05% Tween 20 in PBS, and finally incubated at room temperature for 1 h with anti-mouse Alexa Fluor 488 antibody (Life Technologies). Rhodamine-phalloidin (Sigma) and DAPI were used to stain the F-actin and nuclei, respectively. Images were obtained under an Olympus BX51 fluorescence microscope.

4.4.3.5 Time of flight secondary ion mass spectroscopy (ToF-SIMS)

All ToF-SIMS analyses were performed using a ToF-SIMS IV spectrometer (ION-TOF GmbH, Munster Germany) with the following operating conditions: a pulsed 25 keV Bi_3^+ ion beam (current = 0.37 pA; pulse width = 20 ns; pulse width after bunching = 0.75 ns; repetition rate = 10 kHz) was rastered for an acquisition time of 120 s over areas of (250x250) μm^2 for flat specimens, (150x150) μm^2 and (500x500) μm^2 for stents. The total ion fluence was kept under 10^{12} ions per cm^2 in order to guarantee static conditions. In the meantime, a low-energy electron flood gun was used to ensure charge compensation. The secondary ions were extracted at a 2 kV acceleration voltage. By measuring the time of flight between the sample and the detector and after an appropriate calibration, one has access to the secondary ion mass distribution. In this case, positive and negative spectra were calibrated to the $Cr_2O_2^+$, $C_2H_6N^+$ and $C_4H_8N^+$ peaks and CN^-, CrO_2^- and I^- peaks, respectively. ToF-SIMS spectra were obtained from 0 to 880 m/z. Fragments of interest for this study are shown in Table 16.

Briefly, two kind of fragments were studied: a) fragments related to the peptide composition and b) fragments related to the surface and linking arm.

Table 16 ToF-SIMS fragments of interest, in positive mode, for the study of the conformation of the peptide. On top, single-letter code of the amino acids and bellow ToF-SIMS fragments for the linking arm (GA and PEG) and for the oxide layer (Chromium oxide) with their respective m/z.

Letter	Amino acid	ToF-SIMS fragment	m/z
V	Valine	$C_4H_{10}N^+$	72.082
P	Proline	$C_4H_8N^+$	70.069
K	Lysine	$C_5H_{10}N^+$	84.083
I	Isoleucine	$C_5H_{12}N^+$	86.097
L	Leucine	$C_5H_{12}N^+$	86.097
	Fragment	**ToF-SIMS fragment**	**m/z**
	GA/PEG	$C_2H_5O^+$	45.032
	Oxide layer	$Cr_2O_2^+$	135.871

4.4.3.6 Statistical analysis

Statistical analysis was carried out using GraphPad 6 (GraphPad software, La Jolla, CA, USA). Comparisons among groups were performed by unpaired t test or one-way ANOVA with post-hoc Tukey test for multiple comparisons. Significance was retained when $p<0.05$. Data are expressed as mean ± standard deviation (n=9).

4.5 Results

4.5.1 Surface characterization

Changes on the chemical composition of the surface after each grafting step was followed up by XPS survey analyses (Table 17). A general trend was observed on both GA and PEG: the percent of nitrogen and metals decreased compared to the aminated surface (NH_2), due to the grafting of the linking arm: from 11.2 ± 0.1 % on aminated surface to 5.9 ± 0.5 % and 5.1 ± 0.2 % for GA and PEG, respectively. Furthermore, the percentage of C increased on LA grafted surfaces when compared to NH_2 surfaces as the LA molecules are rich in carbon, this increase being more pronounced for PEG than for GA, as expected. Although the LA also contain O, a slight decrease of the O percentage was observed, due to the coverage of the O-rich metal oxide by the LA chains. The peptide grafting efficiency on the LA surfaces was evidenced by the nitrogen increase, 1 % for PEG and 2.4 % for GA, whilst the percentage of metals continued to decrease. Moreover, the percentage of carbon on the surface increased with the grafting of the peptide, as expected due to peptide chemical compositions. The C and N increase was higher for GA-P23 than PEG-P23, suggesting a more efficient grafting on GA than on PEG.

Table 17 Surface chemical composition of the L605 after each modification step, assessed by XPS survey analyses. Expressed as the mean ± standard deviation. Analyses performed on 3 different samples with 3 points per samples (n=9). Furthermore, the theoretic composition of the peptide is shown.

L605	%C	%O	%N	%Cr	%Co
NH_2	27.5 ± 1.8	49.9 ± 0.8	11.0 ± 0.1	9.2 ± 0.8	2.6 ± 0.2
GA	31.1 ± 1.3	46.5 ± 1.5	5.9 ± 0.5	9.1 ± 0.6	2.0 ± 0.2
GA-P23	39.5 ± 1.2	39.3 ± 0.5	8.3 ± 0.1	7.0 ± 0.4	1.3 ± 0.1
PEG	34.7 ± 1.3	44.3 ± 0.6	5.1 ± 0.2	8.6 ± 0.1	1.8 ± 0.5
PEG-P23	36.4 ± 2.1	42.6 ± 0.7	6.1 ± 0.7	8.3 ± 1.2	1.9 ± 0.5
P23 theoretical	64.7	15.8	19.6	-	-

Regarding changes on the roughness of the surface (Figure 28), it was found a significant increase after the grafting of the peptide with both linking arms compared to the aminated sample: from 1.3 ± 0.1 nm to 1.9 ± 0.2 nm and 2.5 ± 0.4 nm for GA-P23 and PEG-P23, respectively. Also, the fact that PEG-P23 surface presented a higher Rq than GA-P23 one could be associated to the longer chain in PEG than the one in GA.

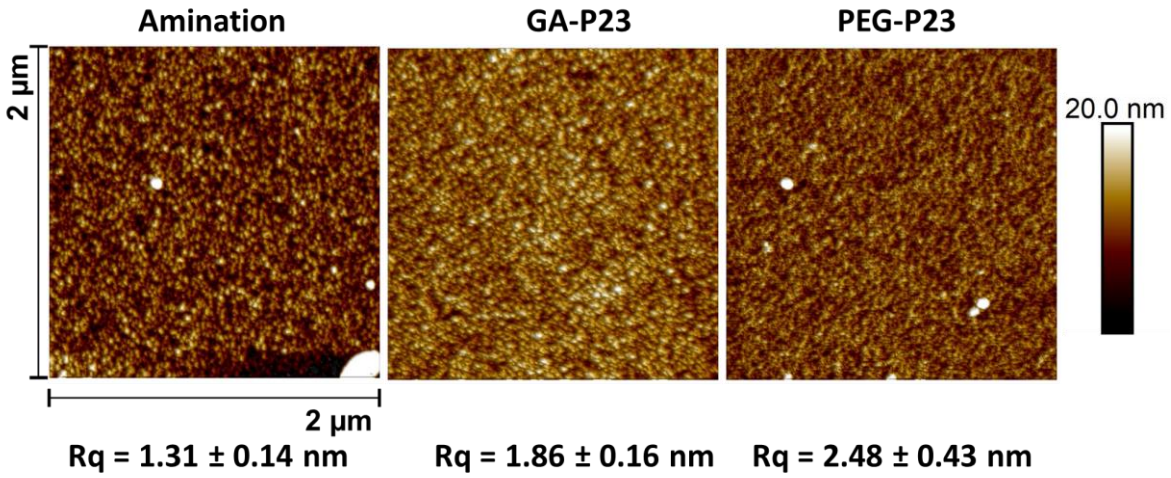

Figure 28 AFM images 2 µm × 2 µm of the L605 surface after the grafting of the peptide. (a) Amination sample, (b) GA-P23, (c) PEG-P23. After the grafting of the peptide there was a significant increase on the surface roughness compared to the plasma aminated L605 surface.

4.5.2 Biological performance

Two important properties for cardiovascular devices were studied: (1) interaction with endothelial cells by viability, proliferation and migration tests; and (2) hemocompatibility, with a hemoglobin-free test. Endothelial cell viability and proliferation were evaluated by direct seeding HUVECs on the different surfaces. As evidenced

in Figure 29, after 24 h the cell viability of the surfaces with the immobilized peptide was higher compared to EP: 68 ± 10 % vs GA-P23: 101 ± 7 % and PEG-P23: 106 ± 5 ($p < 0.05$). After 3 days, HUVEC viability was still higher on the functionalized surface than EP. Finally, after 7 days, only PEG-P23 surface showed a higher cell viability than EP surface: 243 % ± 12 vs 216 ± 10 %, respectively ($p < 0.05$).

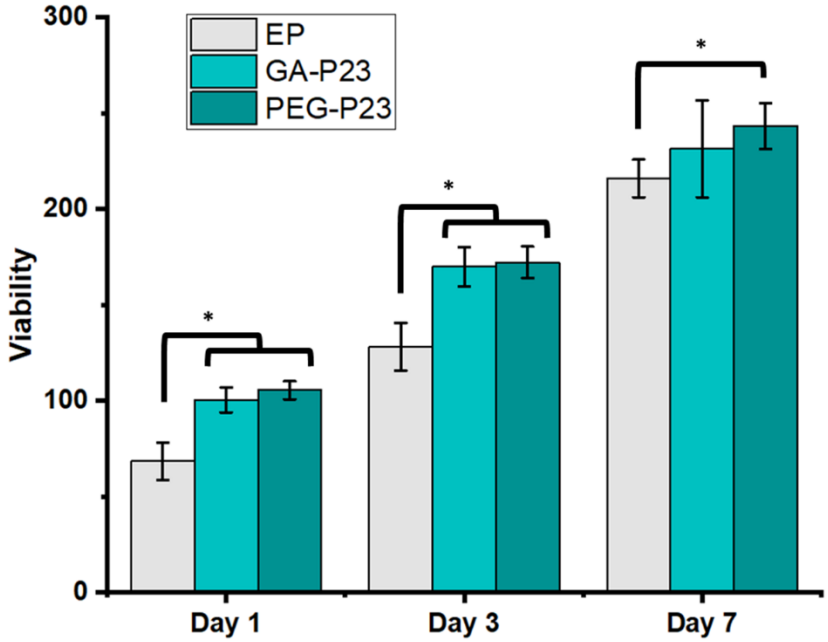

Figure 29 Endothelial cell viability up to seven days. It was found that grafting the peptide significantly increases the cell viability when compared to the electropolished surface. Only PEG-P23 presents a significant difference to EP at day 7. Samples normalized to control (well plate). Number of samples = 9, $p<0.05$.

After viability assays, endothelial cell proliferation and migration were studied up to seven days. HUVECs were seeded into a 2 well culture-insert which was removed after cell attachment. After the removal, at day 1, a cell-free gap was created in which the cell proliferation can be visualized as the time passed by, to simulate the re-endothelialization process. As observed in Figure 30, none of the surfaces presented any difference the first day of the test. After 3 and 7 days, cells started to proliferate on the surfaces of each samples until to fill the gap. At day 3, more ECs are detected in the gap for PEG-P23 surface compared to the GA-P23 and the EP surfaces, meaning that the cells migration appeared to be faster on PEG-P23. At day 7, the gap was completely filled by ECs on the P23 modified surfaces, both with PEG and GA. However, at this time, PEG-P23 showed a higher intensity on the coloration related to the cell junctions (green). This was due to a higher presence of endothelial cells with the best coverage compared to the other surfaces, thus, a complete monolayer was obtained on PEG-P23.

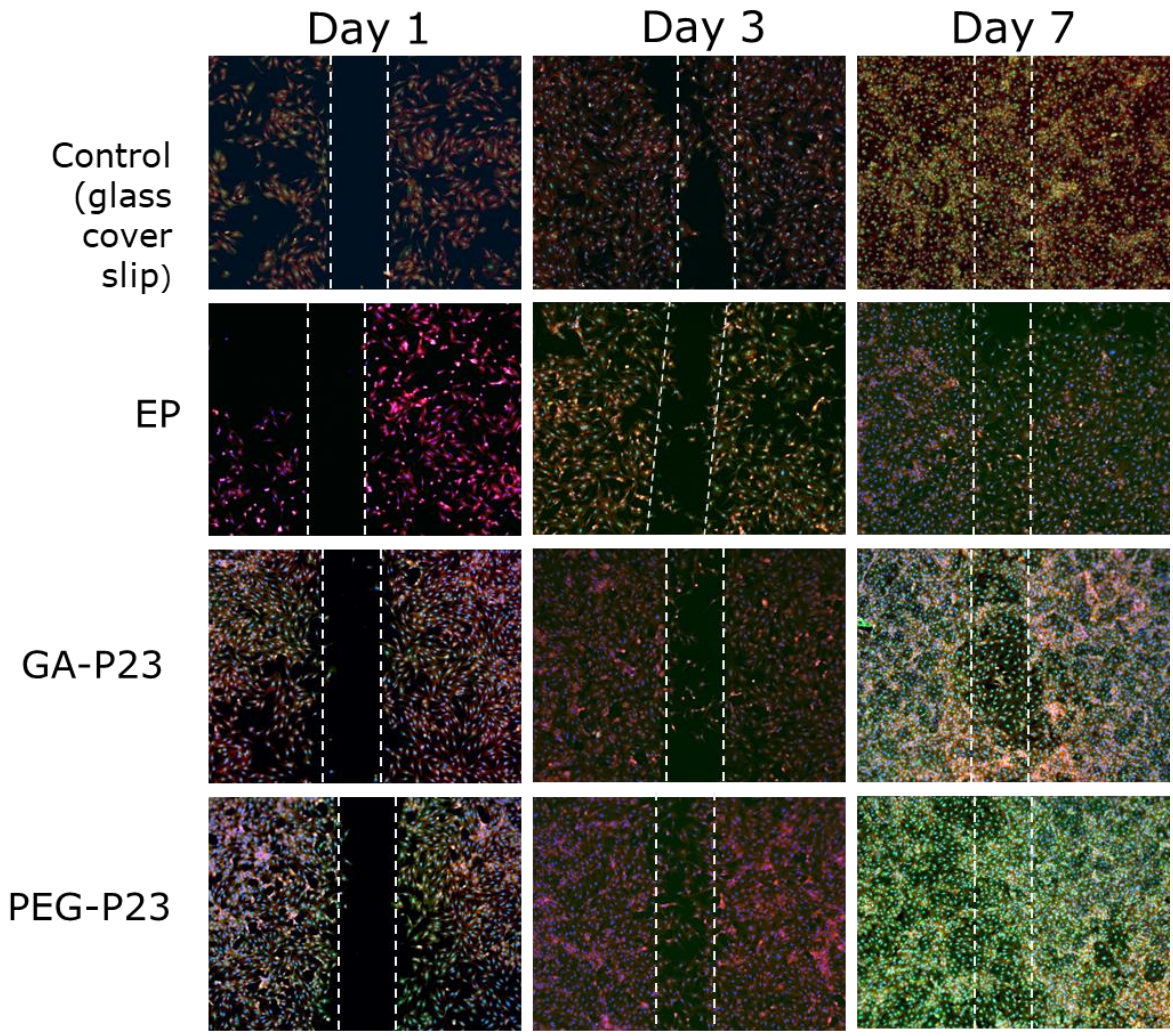

Figure 30 Endothelial cell migration essay up to seven days. It was found that grafting the peptide by any linking arm increases cell migration up to 7 days. Furthermore, PEG-P23 was the surface to promote a complete monolayer of endothelial cells after this period compared to the other surfaces.

Regarding the hemocompatibility of the surfaces it was found that surfaces with the P23 peptide can slightly slower the coagulation rate when compared to the EP surface during the first minutes of the coagulation cascade. As observed in Figure 31a, there is a significant difference after 10 min of contact on PEG-P23 and GA-P23 with EP ($p < 0.05$). Following the coagulation kinetic, after 20 min of incubation there were no significant differences between surfaces and at 30 min blood is completely coagulated (% of free hemoglobin < 20%). Furthermore, the blood coagulation was also evaluated on endothelialized surfaces. The selected time point for this experiment was 20 min. This time was chosen according the previous experiment were blood was nearly coagulated at the surface. The percentage of free hemoglobin free for these endothelialized surfaces prevented the formation of blood clots, since it was superior to 80%, as observed in Figure 31b. However, no difference was found between EP, GA-P23 and PEG-P23 probably because HUVECs can adhere and proliferate also on EP surface as shown in Figure 29 and Figure 30.

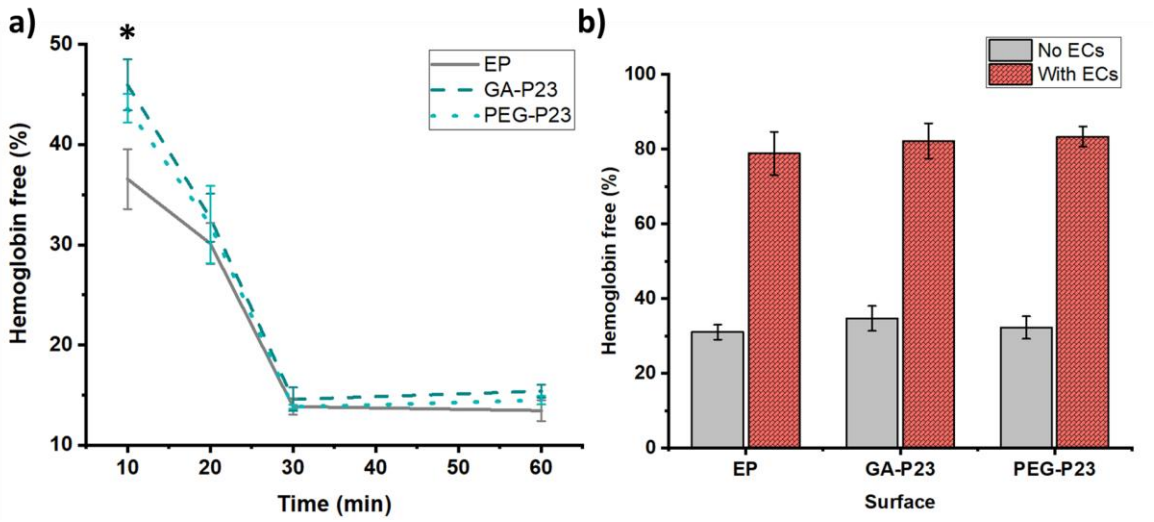

Figure 31 Hemoglobin free assays: a) kinetic of coagulation for the different surfaces, it can be observed that after 10 min there is a significant increase on the hemocompatibility on GA-P23 and PEG-P23 when compared to the bare metallic surface ($p < 0.05$).

4.5.3 Conformation of the peptide

After the biological performance and the composition of the surface, the study of the distribution and the conformation of the peptide by ToF-SIMS, both in imaging and static mode respectively, were assessed. Regarding imaging mode, as observed in Figure 32, three main fragments were studied: $C_4H_8N^+$ from proline, $C_2H_5O^+$ from the GA and PEG chain and $Cr_2O_2^+$ from the oxide layer. Furthermore, for the imaging mode, the sum of all the specific fragments related to the amino acids was selected as well. It was found that the fragment related to proline was more present in the GA-P23 surface compared to PEG-P23, with a total count (TC) of 5.998×10^5 to 4.876×10^5, respectively. The other fragments related to the presence of the linking arm and the oxide layer were higher on PEG-P23, with a TC of 2.011×10^5 and 1.309×10^5 compared to 1.122×10^5 and 9.926×10^4 on GA-P23. Both surfaces, GA-P23 and PEG-23, presented a homogeneous peptide distribution on the surface, as observed by the sum of all the specific fragments related to the composition of the peptide. However, GA-P23 presented a higher intensity of peptide fragments, with a TC of 2.204×10^6 to 1.779×10^6 when compared to PEG-P23.

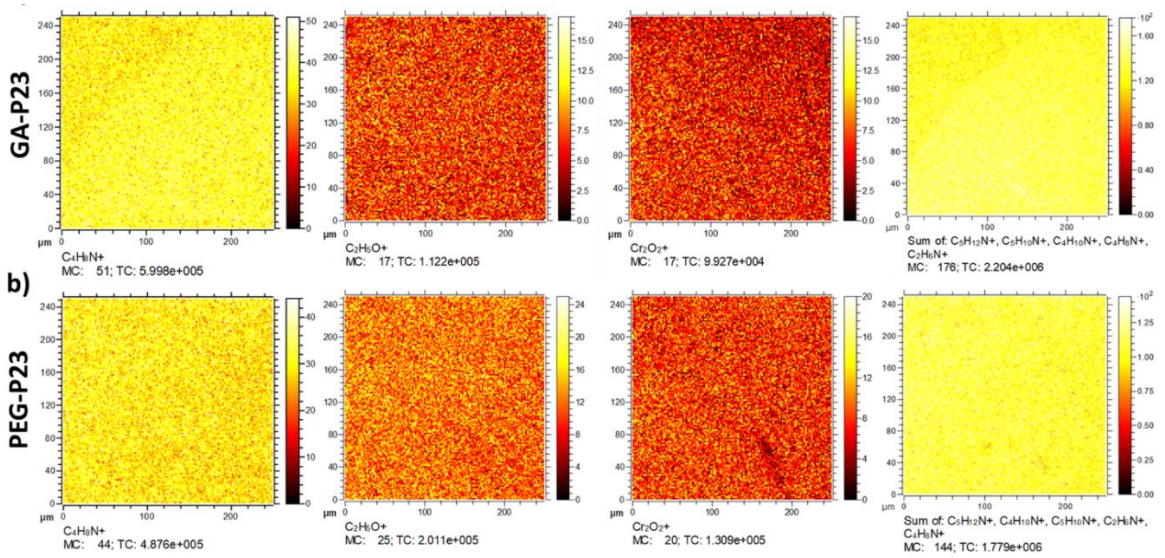

Figure 32 ToF-SIMS images 250 µm × 250 µm of fragment $C_4H_8N^+$, proline (m/z 70.069), $C_2H_5O^+$ (m/z 45.032), as a characteristic fragment from the linking arm, $Cr_2O_2^+$ (m/z 135.871), as a fragment related to the oxide layer of the alloy and the sum of all the fragments related to the peptide composition. (a) GA-P23 sample, and (b) PEG-P23. Both surfaces exhibited a homogeneous distribution of the peptide on the surface.

Furthermore, a comparison of the relative intensities (normalised to total counts) of the amino acids from the P23 grafted on the surface was performed in order to study the conformation of the peptide. As seen in Figure 33, an increase on the fragments related to the peptide composition was found. Furthermore, in the same figure it can be observed that the amino acid with the highest intensity for both GA-P23 and PEG-P23 surfaces was proline. Figure 33 shows that there are consistently less amino acid fragments on PEG-P23 compared to GA-P23, implying a lower P23 grafting density when using PEG as a linking arm. This observation was in line with the XPS data, showing higher C and N concentrations on GA-P23 surface. However, subtle differences were observed in the fragment's intensity drop from GA-P23 to PEG-P23, which can be related to conformation differences. In particular, the proline fragment intensity drop is more pronounced than for the other amino acids (valine, lysine and leucine). The proline to lysine ratio is 3.27 ± 0.04 on GA-P23 and 2.99 ± 0.01 on PEG-P23, which is a small but significant difference indicating different conformations.

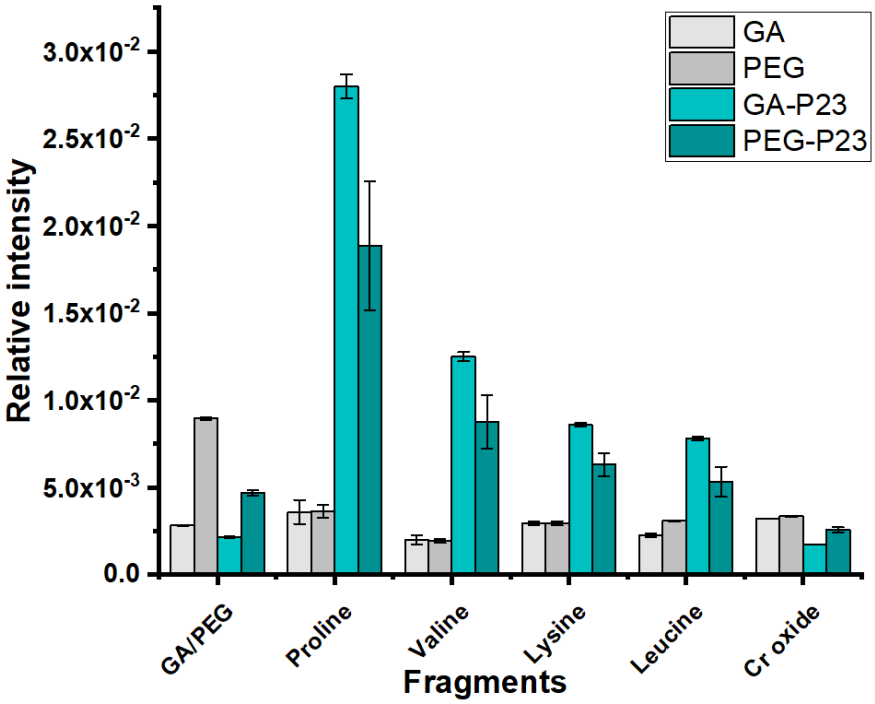

Figure 33 ToF-SIMS analyses in positive static mode, a comparison of the relative intensities of the specific fragments of the amino acids that compound the peptide to confirm its presence on the surface due to a significant increase on the peptide fragment after grafting.

4.5.4 Transfer to cardiovascular devices

The feasibility of commercial stents functionalization with bioactive molecules was studied by grafting a modified version of the peptide with iodine in its composition. ToF-SIMS images of the surface in the positive and the negative ion modes were performed to study specific fragments related to the oxide layer and the peptide. As observed in Figure 34, for positive ion mode the fragment related to the oxide layer is Cr^+ whilst for the peptide, $C_4H_8N^+$, from proline, was selected. Regarding negative ion mode the selected fragments for the oxide layer and the peptide were CrO_2^- and I^-, respectively. It was found that the fragments related to the peptide composition were present on the surface for both positive and negative mode. Furthermore, the metallic compounds were also present, confirming a functionalization but not a coating.

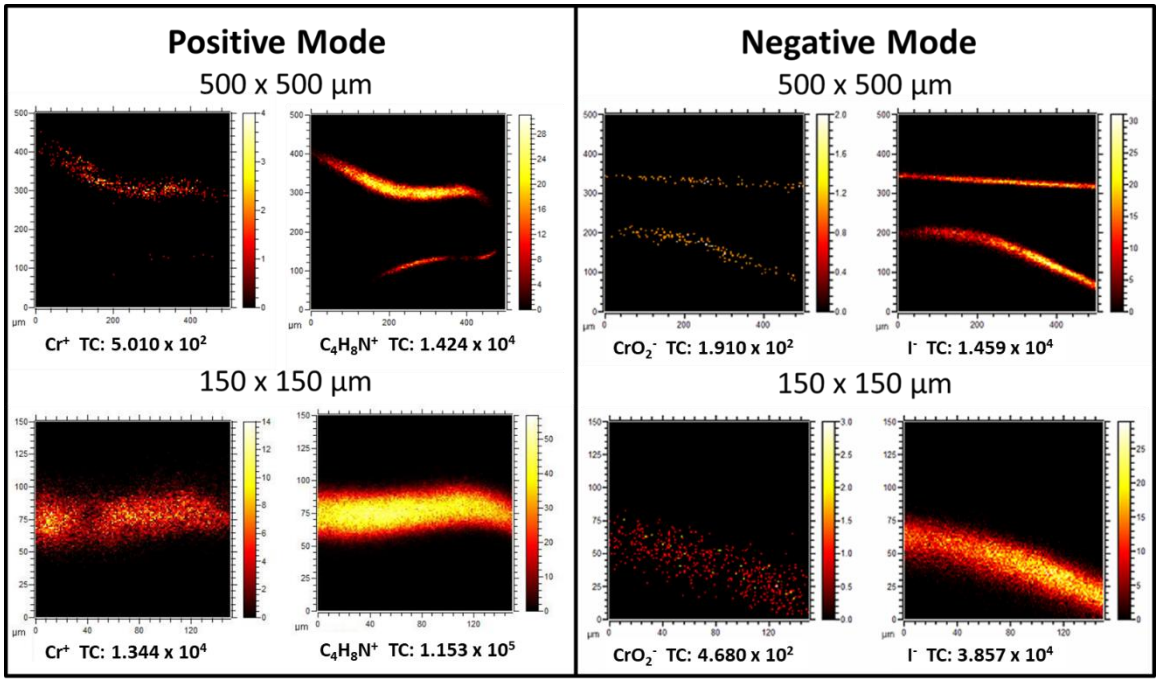

Figure 34 ToF-SIMS images 500 µm × 500 µm and 150 µm x 150 µm of a commercial stent modified by this plasma-based strategy. Positive mode: fragment $C_4H_8N^+$, proline (m/z 70.071) from the peptide and Cr^+, as a fragment related to the metallic surface of the alloy (m/z 51.939). Negative mode: fragment I^-, iodine (m/z 126.904) from the peptide and CrO_2^- (m/z 83.932), as a fragment related to the metallic surface of the alloy.

4.6 Discussion

4.6.1 Surface characterization

From Table 17, when comparing the surface chemical compositions after LA grafting, from the reference (the sample after plasma amination), a decrease of the percentage of nitrogen and metals can be observed. Furthermore, when grafting any of the linking arms an increase in the percentage of carbon related to the chemical composition of both GA and PEG is observed. As the grafting procedure continues, with the addition of the P23 peptide, the percentage of nitrogen and carbon increases whilst the percentage related to the oxide layer continues to decrease. These observations suggest that this plasma-based strategy, shown in Figure 27, allows the direct functionalization with bioactive molecules, but it does not create a coating as the metallic percentage remains large, as seen on XPS analyses. Moreover, the changes of the %C, %O and %N for both GA-P23 and PEG-P23 were similar to what was expected from the theoretical peptide composition (%C = 64.7, %O = 15.8 and %N = 19.6). As regards GA to GA-P23, there was a large increase in %C of ~8% and in %N of ~2%, which was expected from the addition of the peptide. Nevertheless, the percentage of oxygen decreased by ~ 5%, which is related to the partial coverage of the metallic surface by the grafted peptide with a short linking arm (5 atoms of carbon) leading to a decrease of the oxygen from the oxide layer. A similar trend was observed on PEG-P23, nevertheless, the increases were smaller when compared to GA-P23. As regards %C, only an increase of ~2% was observed whilst the %N increased only ~1%. The N increase is due to the presence of the

peptide at the surface. It was about twice less than in the GA case, which probably means that fewer peptide molecules were grafted. This was also confirmed by the lower intensity of amino acids fragments in ToF-SIMS (Figure 33). As for the carbon, the relatively small increase was due to the small contribution of the peptide (119 atoms of carbon), which represents only a weak contribution compared to the long chain of PEG (Mn = 600, ~1200 atoms of carbon). This effect was quite different when the peptide was grafted on the small GA linking arm, where the carbon added by the peptide now represented a major contribution.

Furthermore, the distribution of the grafted molecules on the first layer of the surface was assessed by ToF-SIMS imaging mode, shown in Figure 32. It was found that both linking arms presented a homogeneous distribution on the fragments related to the peptide. Nevertheless, GA-P23, Figure 32a, presented higher intensities for fragments related to proline and for the sum of the peptide fragments, which suggested that the bioactive molecule was more exposed to the surface when compared to PEG-P23 (Figure 32b). The signal from the metal oxide, ($Cr_2O_2^+$), was higher on PEG-P23 compared to GA-P23. Again, this suggested that less peptide was grafted in PEG-P23, so that the metallic substrate was less covered, giving rise to a higher secondary ion signal from the oxide compared to GA-P23.

4.6.2 Biological performance

After studying the chemical composition of both GA-P23 and PEG-P23 and the physical distribution of the biomolecule on the flat samples, biological tests were performed to evaluate the toxicity of the surface, endothelialization and hemocompatibility. Regarding the toxicity of the surface, a cell viability test with endothelial cells was performed (Figure 29). It was found that since day 1 GA-P23 and PEG-P23 presented significantly higher cell viability compared to the bare metal surface (electropolished control), this higher cell viability continued up to 7 days where only PEG-P23 continued to be significantly different. These results were completed with a migration essay, to simulate the wound healing after the implantation of the cardiovascular device where a fast formation of a monolayer of endothelial cells is desired [161]. Results for this migration test, Figure 30, were according to what was previously found in the cell viability essay: PEG-P23 was the surface that presented a faster migration of endothelial cells, which can be clearly observed after 3 days of migration. Furthermore, after 7 days of migration, PEG-P23 presented a complete monolayer of endothelial cells on the surface, confirmed by showing the highest intensity on the staining related to the intercellular junctions (VE-cadherin) [162]. This behaviour could be related to two properties related to PEG as linking arm: a) The potential synergic effect of the antifouling properties of PEG, and the bioactivity of the peptide. Even if a PEG of Mn= 600 is considered a small chain PEG, it had already been previously confirmed that can present this antifouling behaviour when grafted onto a surface [163]. This synergic effect could have promoted the specific interaction between the endothelial cells and the peptide, leading to their faster migration. b) due to a higher degree of freedom conferred by the long chain of PEG the peptide can expose its active site to the cells faster than GA

which could be restricted by its small chain. Similar observations have already been found for other proteins when grafted by PEG [164].

Hemocompatibility was studied due to the potential properties of the peptide and for its importance to decrease complications after a stent implantation. It was found that the presence of the peptide significantly increased blood compatibility during the first minutes of contact (10 minutes) for both GA-P23 and PEG-P23 when compared to the bare metallic surface, as shown in Figure 31a. However, no difference was found between the linking arms. Following the blood coagulation kinetic it was found that after this time, no significant difference was found among the surfaces and after 30 minutes a clot was completely formed. Furthermore, blood compatibility studies were performed also on endothelialized surfaces, Figure 31b, where it was found that the presence of ECs on the surface prevented clot formation at 20 minutes. No significant difference was observed between any surfaces since ECs can attach and proliferate also on the bare metallic surface, as previously confirmed on the cell viability studies (Figure 29).

These findings suggested that the mechanism of action of the P23 peptide to enhance the biocompatibility of the L605 metallic surface is first to promote a fast endothelialization by the active site of the peptide, by a signal/receptor interaction between the surface and the endothelial cells which lead to an increase in the blood compatibility caused by the attachment and coverage of the metallic surface by endothelial cells.

4.6.3 Conformation of the peptide

To further understand why the biological performance on both surfaces was similar and how the peptide was arranged on the surface, the conformation of the immobilized bioactive molecule was studied using ToF-SIMS in static positive mode. Relative intensities, shown in Figure 33, indicated that the most intense fragment for both GA-P23 and PEG-P23 was from proline, $C_4H_8N^+$, which as observed in Figure 35a, is present twice in the composition of the peptide. Proline fragments, as well as the other fragments from the peptide are always more intense on GA-P23 than on PEG-P23, again confirming a higher peptide surface density on GA-P23. However, the biological activity appears better on PEG-P23 even if less peptide is available. This could be due to a different conformation of the peptide. Indeed, when looking carefully at the intensity changes from GA-P23 to PEG-P23, the valine, lysine, leucine relative drops are similar while the proline drop is significantly stronger. The proline to valine ratio is 3.27 ± 0.04 on GA-P23 while it is 2.99 ± 0.01 on PEG-P23, a small but statistically relevant difference. If the peptide chains had random orientations for both LA, there should be no observable differences between the amino-acid fragments relative intensities. If a preferential conformation exists on one of the LA, subtle variations of the relative intensities should be observed, as is the case in this study. The slightly higher proline intensity on GA-P23 suggests that the peptide conforms in such a way that proline is more exposed on the surface. On the other hand, the polymeric PEG chains, long compared to the short GA molecule, will tend to

fold at the surface so that the grafted peptides will have random orientations. Taking under consideration these results and the fact that ToF-SIMS analyses are performed under high vacuum, Figure 35b and c presents the potential conformation for GA-P23 and PEG-P23, respectively. This conformation was proposed considering that for this immobilization strategy free amine groups are needed, as observed in the reaction schematics (Figure 27), and based on the high intensity of proline on both linking arms, the most probable zone where the peptide is grafted is either by the arginine or the middle lysine (located in the bottom of the 3D model shown Figure 35a). Thus, Figure 35b shows a potential conformation for GA-P23 which under vacuum exposes the peptide and that once in contact with the cells, due to a low degree of freedom conferred by the small linking arm, the peptide could not expose the bioactive site so easily, leading to a slower biological response, especially in terms of endothelial cell migration, as seen in Figure 30. On the other hand, PEG-P23, Figure 35c, under vacuum was in a folded state caused by the shrinking of the PEG chains, partially hiding the peptide. However, once this surface was in contact with the endothelial cells, due to the longer chain and higher degree of freedom, a faster biological response was obtained, thus, a faster cell migration that could lead to promote re-endothelialization and avoid thrombus formation on cardiovascular devices, as suggested by hemocompatibility studies (Figure 31).

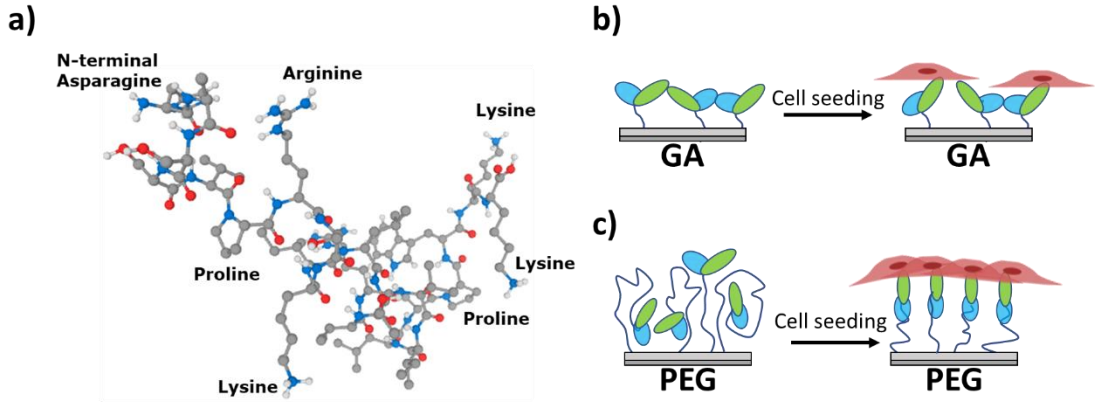

Figure 35 Schematics of: a) P23 Peptide 3D model, b) proposed conformation of GA-P23 before (under vacuum) and after cell seeding, with a potential steric impediment that does not allow the peptide to expose the bioactive site for ECs and c) proposed conformation for PEG-P23, which under vacuum it shrinks and exposes the linking arm onto the surface hiding the peptide but when in contact with the cell medium it allows the bioactive peptide to obtain the optimal conformation which promotes cell adhesion.

4.6.4 Transfer to cardiovascular devices

Finally, the feasibility to transfer this technology onto bare metal stents was assessed by ToF-SIMS imaging both in positive and negative mode. Similar studies had already been performed on flat samples to confirm the immobilization of a peptide modified with iodine [152]. As shown in Figure 34, fragments studied in positive mode were Cr^+, from the metallic surface and proline from the immobilized peptide. In negative mode the fragment related the metallic surface was CrO_2^- and I^- for the peptide. The presence of fragments these fragments confirmed the direct immobilization of the peptide onto the metallic cardiovascular device. Moreover, the

presence of the fragments related to the alloy confirmed a functionalization and not a coating. This confirmation opens a new alternative to what can be currently found in the market: bare metallic stents or drug eluting stents, that use polymeric coatings to elute drugs.

4.7 Conclusion

It was possible to graft a CD31 derived peptide onto the surface of L605 cobalt chromium without the use of any polymeric matrix, by using a plasma-based multi-step treatment. This technique allowed to graft the peptide by different linking arms, GA and PEG, confirmed by following the chemical composition changes of the surface by XPS and ToF-SIMS. It was found that both LA increased the biological performance of the surface, on endothelialization and hemocompatibility, when compared to the bare metallic one. However, PEG-P23 demonstrated the most promising properties to be used for stent application due to its fast-endothelialization that could lead to anti-thrombotic activity. The advantage of PEG over GA is its long and mobile chain, allowing the peptide to better reach out to the endothelial cells. Furthermore, by ToF-SIMS analyses it was possible to confirm the grafting of a peptide onto the surface of a commercial stent, proving that this novel procedure may be used not only on flat structures but also onto complex 3D structures. By using this technique combined with newly developed drugs that can promote the biological properties desired for stent application a new generation of commercial devices can be developed.

4.8 Acknowledgements

Sergio Diaz-Rodriguez is a recipient of a PhD scholarship from the NCPRM (www.ncprm.ulaval.ca). This work was supported by the Natural Sciences and Engineering Research Council of Canada (NSERC), the CHU de Québec Research Center, The Ministry of Economy, Science and Innovation of Quebec, and the Linkage Grants Québec/Wallonie-Brussels of the Ministery of International Relations and “La francophonie” of Quebec.

Chapter 5 Direct immobilization of a CD31 agonist improves *in vitro* and *in vivo* biological performance of CoCr coronary stents

Authors: Sergio Diaz-Rodriguez[1], Pascale Chevallier[1], Jules Mesnier[2], Diego Mantovani[1] and Giuseppina Caligiuri[2]

[1] Laboratory for Biomaterials and Bioengineering (CRC-I) Department of Min-Met-Mat Engineering and the CHU de Québec Research Center, Laval University, PLT-1745G, Québec, QC Canada G1V 0A6

[2] Institut National de la Santé et de la Recherche Médicale U1148, Department of Cardiology, Bichat Hospital, Paris, France.

Keywords: biomimetic coating, stent, plasma amination, biomolecule grafting, biocompatibility, preclinical evaluation

Chapter to be submitted to Biomaterials.

5.1 Résumé

L'une des principales complications des endoprothèses suite à une intervention coronarienne percutanée est la resténose, qui se caractérise par la réduction du diamètre luminal de l'artère, semblable à une plaque d'athérosclérose. Ce rétrécissement est essentiellement provoqué par une prolifération excessive des cellules musculaires lisses, qui a été induite suite à une lésion de l'endothélium lors de l'implantation de l'endoprothèse. Malgré les progrès obtenus par différentes générations d'endoprothèses, de nouvelles stratégies ciblant spécifiquement l'endothélialisation tout en réduisant la formation de thrombus et les réactions inflammatoires demeurent nécessaires. La nouvelle approche développée au sein du laboratoire est l'immobilisation directe de molécules bioactives à la surface de stents métalliques en chrome-cobalt (L605), sans aucun recouvrement préliminaire. Dans le cadre de ce travail, un peptide court (8 acides aminés, P8RI), dérivé de la molécule d'adhésion des cellules endothéliales des plaquettes (PECAM-1), a été choisi pour ses propriétés pro-endothélialisation, anti-inflammatoire et anti-thrombotique, puis greffé sur des substrats de L605. La performance biologique de ces surfaces biomimétiques a été évaluée d'abord en effectuant des tests in vitro, puis des tests in vivo. Pour cela, des implantations de 7 jours et 28 jours dans un modèle porcin ont été effectués. Les résultats in vitro ont démontré que l'adhésion de cellules endothéliales de l'artère coronaire humaine (HCAEC) était significativement augmentée lorsque le substrat était greffé avec le peptide versus le métal nu. De plus, ces cellules présentent un phénotype anti-thrombotique et anti-inflammatoire et sont fortement liées à la surface modifiée. Les tests in vivo ont corroboré les résultats précédents. En effet, les endoprothèses fonctionnalisées avec P8RI (Plasma-P8RI) présentaient une meilleure ré-endothélialisation après 7 jours par rapport au DES commercial, et une faible adhésion des leucocytes et des plaquettes par rapport au BMS. De plus, après 28 jours d'implantation, sur les stents greffés Plasma-P8RI, il n'y a pas eu de diminution significative du diamètre luminal des artères, ce qui signifie que les stents modifiés ne présentaient pas de signe de resténose alors que les BMS en présentaient. Ces premiers essais sont très prometteurs et les stents Plasma-P8RI ouvrent un nouvel horizon vers de nouveaux dispositifs cardiovasculaires.

5.2 Abstract

In-stent restenosis remains one of the main complications after a percutaneous coronary intervention. This complication is characterized by the reduction of the lumen diameter, similar to an atherosclerotic plaque, and it is related to the wound caused on the endothelium by the stent implantation followed by the over-proliferation of smooth muscle cells. Despite the advances obtained by different generations of stents, there is still the need for new strategies that can specifically target endothelialisation whilst reducing thrombus formation and inflammation responses. A novel approach that allows the direct immobilization of bioactive molecules onto the surface of cobalt chromium bare metal stents has been developed. For this work a short peptide (8 amino acids, P8RI) derived from the platelet endothelial cell adhesion molecule (PECAM-1) has been grafted due to its potential pro-endothelialization, anti-inflammatory and anti-thrombotic behaviour. A combination of in vitro and in vivo tests was performed to study the biological performance of these biomimetic surfaces. As regards in vitro tests, it was found that using this peptide increased the presence of human coronary artery endothelial cells (HCAEC) which exhibited an anti-thrombotic and anti-inflammatory phenotype and were strongly attached to the surface, in comparison with the crude metallic surface. Furthermore, in vivo tests in porcine model confirmed that stents functionalized with P8RI (Plasma-P8RI) presented a better re-endothelialization after 7 days when compared to commercial DES, with further, a low adhesion of leukocytes and platelets when compared to BMS. Moreover, after 28 days of implantation, Plasma-P8RI did not present a significant decrease on the lumen diameter, which was not the case for BMS that presented in-stent restenosis after this period. Overall, these initial trials demonstrated a promising panorama for Plasma-P8RI stents.

5.3 Introduction

Atherosclerosis is one of the main causes of death in the western world [165]. This cardiovascular disease takes years to develop and is characterized by the formation of a plaque on the arterial walls that narrow the lumen. The presence of this plaque, depending of the level of progression, may result in blood flow disturbances and thrombosis which could lead to myocardial infarction [166]. Nowadays there are different programs developed to prevent atherosclerosis which mainly consist on a list of recommendations, such as having a healthy diet, being physically active and avoiding smoking, as a preventive measure [167]. Nevertheless, once the atherosclerotic plaque has been developed, clinical intervention in the form of percutaneous coronary intervention (PCI) procedure is performed. Percutaneous coronary intervention (PCI), formerly known as angioplasty completed by the implantation of a stent, has become a keystone in the management of patients with coronary artery disease [168]. The coronary stents are mounted onto an angioplasty balloon connected to a catheter to allow its pressure-driven deployment and stable implantation in the target vessel segment. The balloon and the catheter are retrieved at the end of the procedure whereas the metallic scaffold, is left in place to avoid the collapse of the recanalized artery. The first stents, bare metal stents (BMS), introduced in the middle 80s [166], focused on reopening and supporting the stenotic arteries, nonetheless, damage on the arterial wall (endothelium) lead to excessive inflammatory damage and further complications such as in-stent restenosis. This complication characterizes by the reduction of the lumen diameter, similar to atherosclerosis, related to wound caused by the deployment of the device and the over proliferation of smooth muscle cells where the endothelium is not present [165,169]. As a strategy to lower in-stent restenosis and to avoid a second intervention, drug eluting stents (DES) were developed. These devices consist of a metallic stent, as support, coated with a polymer that allow the elution of anti-proliferative drugs, such as paclitaxel and sirolimus, thus, decreasing in-stent restenosis. Nevertheless, complications persist due to the low specificity of the eluted drugs that inhibit the proliferation of both smooth muscle cells and endothelial cells, there is a compromise in the endothelium recovery, and to potential inflammation response due to hypersensitivity allergic reactions [170, 171]. Despite the advances obtained by DES, there is still a need for new strategies that can specifically promote endothelial cell proliferation whilst avoiding the over proliferation of smooth muscle cells, thus, aiming to decrease in-stent restenosis. In parallel to DES development, the trend to decrease the wall thickness of these medical devices, the demands for materials with a higher strength, rigidity and radiopacity have led to the development of a new alloys, including cobalt-chromium ones [172, 173]. Indeed, CoCr alloy has a higher strength and better radiopacity than SS316, and also has good corrosion resistance, fatigue resistance, nonmagnetic and has been demonstrated that devices with thinner struts made of this alloy lead to a decrease on the in-stent restenosis rate [168, 174].

Therefore, a different approach that allows the direct immobilization of bioactive molecules onto the surfaces of cobalt chromium BMS have been developed [175]. Briefly, this multi-step plasma-based procedure focuses on the direct functionalization of the metallic surface with reactive amine groups that act as anchor points for the covalent grafting peptide. This procedure foregoes the previously mandatory coating deposition step, thus, potentially decreasing inflammation response caused by the allergic reactions to the polymeric layer [176]. This plasma procedure has been confirmed to immobilize peptides derived from CD31, also known as platelet endothelial cell adhesion molecule (PECAM-1), a transmembrane protein found in endothelial cells, platelets and leukocytes [177, 178, 179]. These molecules have exhibited anti-inflammatory, pro-endothelialization and-stenotic behaviour, which are key properties for stent applications [180]. Thereby, these functional surfaces are expected to improve the performance of BMS by promoting the endothelialization of the device whilst decreasing in-stent restenosis.

A combination of in vitro and in vivo tests was performed in order to study the performance of these functionalized surfaces. In vitro tests involved the incubation of human coronary artery endothelial cells (HCAEC) onto flat surfaces to study their distribution, by immunocytochemistry, and their phenotype, by studying the soluble factors released in the supernatant of cultured cells. Three molecules have been selected to study EC phenotype: a) Vascular cell adhesion molecule-1 (VCAM-1), a protein that mediates the adhesion and interaction of leukocytes onto the endothelium; its expression an cleavage reflects the extent of endothelial activation [181]; b) Interleukin-6 (IL-6), an inflammatory cytokine released in the initial states of endothelial inflammation [182]; and c) Tissue factor pathway inhibitor (TFPI), a primary inhibitor of the initiation of the blood coagulation cascade, produced by a healthy, non-activated endothelium [183]. The study of these soluble factors can be used as a surrogate marker of the potential biological response in vivo. Furthermore, static immersion stability tests up to one month were performed on flat samples [184], where the complete chemical characterization was assessed by XPS. Regarding in vivo studies, the implantation of BMS, DES and the functionalized stent with the CD31 peptide, Plasma-P8RI were implanted in porcine coronary arteries, due to their similarities to human arteries [185], to obtain insights about the tissue response. Short term studies, 7 days of implantation, were performed to study the re-endothelialization, characterized by SEM and histology [186]. Furthermore, in-stent restenosis was studied after 28 days of implantation by angiography and immunohistochemistry of the coronary arteries after euthanasia [187]. Thus, by combining both in vitro and in vivo tests it is expected to obtain an insight about how these surfaces can perform in a human trial.

5.4 Materials and methods

5.4.1 Materials

L605 alloy sheets (wt %: Co 51%, Cr 20%, W 15%, Ni 10%, Fe ≤ 3%, C ≤ 0.15%) were purchased from Rolled alloys Inc. (Qc, Canada). ACS grade acetone and methanol were purchased from Fisher Scientific. From Sigma-Aldrich the following reagents were purchased: MES (2-(N-morpholino)ethanesulfonic acid, ≥ 99%) and EDC (1-ethyl-3-(3-dimethylaminopropyl) carbodiimide hydrochloride, ≥ 98%). Phosphate buffered solution (PBS, 1 X powder) and Poly(ethylene glycol) bis(carboxymethyl) ether (PEG, average Mn 600) were purchased from Fisher Scientific. From Bio-rad laboratories, inc (PA, USA) the following reagents were purchased: bio-plex staining buffer, Bio-plex Pro human cytokine IL-6, V-CAM1 and TFPI beads and their respective detection antibody, streptavidin-PE. Stents were manufactured by Abbott Vascular, model Multi-Link 8 Coronary Stent. Custom peptide, P8RI, derived from CD31, was purchased from Proteogenix (Strasbourg, France). Fluorescence microscopy analysis was performed after fixation in PFA 4% and overnight incubation of cultured cells onto the experimental alloy samples with Rhodamine Phalloidin and Hoechst 33342 (from Thermo Fisher Scientific) and mouse monoclonal antibodies directed against human CD31 (clone JC70/A from DAKO), revealed by a goat anti-mouse IgG coupled to Alexafluor® 488 (Jackson immunoresearch).

5.4.2 Flat sample preparation

5.4.2.1 Electropolishing

Flat round 12.7 mm diameter specimens were cut from L605 alloy sheets and cleaned in three successive 10 min ultrasonic baths of acetone, nanopure water (18.2 MΩ·cm at 25 °C), and methanol, air-dried after each cleaning and stored under vacuum until electropolishing (EP). EP was performed as described in [175], briefly, samples underwent a three-cycle electropolishing procedure; each cycle was performed for 2 minutes with a fixed current density of 2.4 A/cm^2 in a 67 vol.% phosphoric acid, 20 vol.% sulfuric acid, 10 vol.% nanopure water and 3 vol.% hydrofluoric acid a solution at 10 °C with a round L605 specimen as cathode. After electropolishing samples were cleaned in three ultrasonic baths for 10 min each using nanopure water, sodium hydroxide 2 N and nanopure water, respectively.

5.4.2.2 Plasma amination

After electropolishing, samples were functionalized with reactive amine groups (-NH_2) in a MW plasma reactor using nitrogen and hydrogen as feeding gases in a two-step procedure, as detailed in [175]. These functional groups were used as anchor points for the further grafting of the linking arm and the peptide.

5.4.2.3 Linking arm and peptide grafting

L605 plasma treated disks were submerged in a 0.1 g mL^{-1} PEG solution, pH 4.75 in MES buffer, activated with 3 mg mL^{-1} EDAC added three times at 0, 10 and 20 minutes. Reaction was complete after 1 hour. Once the

reaction was finished, samples were vortex washed three times with MES five times with deionized water, dried and stored under vacuum before the covalent grafting of the peptide [175].

After the grafting of the linking arm, the activation of its terminal carboxylic group (-COOH) was performed in order to graft the peptide. This activation was performed in 5ml of MES buffer with 3 mg mL^{-1} EDAC added three times at 0, 10 and 20 minutes. After 30 minutes of activation samples were removed from the tubes to immediately react with 500 µL of a $2.5x10^{-5}$ M peptide solution in PBS for 3 h. Once the reaction was finished, samples were vortex washed with five times with deionized water, dried and stored under vacuum before further characterization and tests were performed.

5.4.3 Stent functionalization

5.4.3.1 Stent preparation

Multi-Link 8® (Abbott) commercial stents were deployed from their catheter and were immersed in three 10 minutes ultrasonic baths of nanopure water, NaOH 1N and nanopure water respectively. After this step, the plasma amination of the substrates was performed in the after-glow region (7 cm) of MW plasma (Plasmionique Inc., Varennes, Québec, Canada) by means of a two-step process using a mixture of N_2 and H_2 (grade 4.8 and 5.0, respectively, Linde, Québec, Canada) as the feeding gases. The first stage was carried out at 150 W during 10 min at 100 mTorr, 10/10 sccm of N_2/H_2, while the second was performed at 150 W during 30 s at 300 mTorr, 20 sccm of H_2. The plasma amination of stents was performed twice on the device, flipping the device after the first treatment to create a homogeneous functionalization. After plasma amination, the grafting of PEG as linking arm and the grafting of the peptide were performed as previously detailed in section 6.4.2.3. After the immobilization of the peptide, stents were cramped back onto the catheter using tweezers and sterilized by beta radiations (25 kGγ) by Ionisos (Chaumesnil, France).

5.4.4 In vitro stability and biological tests (flat samples)

5.4.4.1 Static immersion test

Static immersion tests were conducted on flat samples placed in polyethylene vessels filled with PBS and incubated at 37 ± 1 °C for 28 days under sterile conditions. After this period, samples were rinsed with nanopure water, air-dried and stored under vacuum until further characterization [184].

5.4.4.2 Cell seeding and distribution analysis

Human coronary artery ECs (HCAECs, from Promocell) were cultured in Endothelial cells growth medium MV2 (Promocell) supplemented with nutrients and growth factors needed by ECs. These cells were used at passages 3-5. Flat samples (EP, PEG and PEG-P8RI) were placed in 24-well plates and sterilized in ethanol. After sterilization, 200,000 ECs, suspended in their growth medium, were seeded on the surface of each of the previously mentioned samples and incubated for 48h at 37 ± 1 °C and 5 % of CO_2. After this time, supernatants

were collected to study the endothelial cell phenotype by multiplex assay analysis whilst the cells attached on the surface were stained for immunocytofluorescence.

Immunostaining of CD31, ECs actin filaments and the nuclei by Hoechst was performed as follows: after the incubation samples were washed with PBS to remove the medium and not attached cells, then were incubated for during night in a solution containing 1 % of bovine serum albumin (BSA) and 0.02 % of fish gelatin in PBS with mouse anti-human CD31 (10 µl/ml, Dako M0823). Samples were rinsed in PBS and a second incubation for 1h with the BSA and fish gelatin solution containing the secondary antibody for CD31 (goat anti-mouse IgG, A488, 5 µl/ml) and phalloidin (5 µl/ml) was performed. After this, samples were rinsed in PBS and the nuclei staining was performed by the addition of Hoechst (10 µg/ml) in PBS for 5 minutes.

After staining, samples were rinsed in PBS, and placed down in imaging dishes and covered with Prolong Gold mounting medium. Images were obtained under an Axio Observer inverted fluorescence microscope (Zeiss), equipped with the Zen software (Zeiss). Analysis of the intensity and nuclei counting was performed using the LEICA QWIN® software and custom macro written in QUIPS language program guide and imaging principles available at their website [188].

5.4.4.3 Endothelial cell phenotype analysis

The measure of pro-inflammatory and anti-coagulant endothelial cell biomarkers in the supernatants was achieved using a custom multiplexed cytometric bead assay (Luminex technology). ECs culture supernatant were centrifuged to remove any dead cells, transferred to Eppendorf tubes and frozen before the assay. Supernatants were diluted 1:2 in order to avoid over saturation and transferred to a 96-well plate containing a mixture of the capture beads. Standard solutions were used to perform a calibration curve containing a known concentration of each antigen. The plate was rinsed using an automated washing station that holds the magnetic beads at the bottom of the well plate. Detection antibodies were diluted and incubated with the beads for 30 minutes. Another rinsing was performed to remove the antibodies that did not react with the beads was performed. Streptavidin-PE was added to the wells and incubated for 10 minutes to bind to the detection antibody's biotin. Finally, after the last rinsing step, the beads were suspended in assay buffer and analysed in a Bio-Plex 200 (Bio-rad inc.).

5.4.5 In vivo implantation

The protocol for the study of the coronary stents in farm pigs was in accordance with the Guide for the Care and Use of Laboratory Animals (National Institutes of Health 1985) and the European Directive 2010/63/EU, and was approved by the local ethic committee (Agence nationale de sécurité sanitaire de l'alimentation, de l'environnement et du travail, 14 rue Pierre et Marie Curie, 94701 Maisons-Alfort Cedex, n° APAFiS:

2017032116276884). The pigs were housed at the Centre de Recherche Biomédicale (CRBM) at the veterinary school of Alfort, where all the in vivo experiments were conducted.

5.4.5.1 Stenting

Three groups of Multi-Link (Abbott) stents, with different coatings were implanted in the coronary arteries of 8 female farm pigs: BMS unmodified, everolimus-eluting stents (Xience, Abbott) and Plasma-P8RI. First, a preload of ticagrelor (180 mg) and aspirin (75 mg) was administered and after an overnight fast the animals were sedated, intubated and connected to a ventilator. Anesthesia was maintained with gas anesthetics throughout the procedure. After administering heparin (intravenous bolus, 5000 UI) and antibiotic prophylaxis, the arterial access was obtained under sterile conditions by femoral or carotid artery cutdown. Coronary angiography was performed to locate the three epicardial coronary arteries (interventricular, left circumflex and right coronary arteries) to deploy the devices. The balloon was inflated to a maximal pressure of 8 atm for 30 seconds, deflated and withdrawn deploying the stent in the artery. After the stent deployment, the arteriotomy was repaired, skin closed, and the animals recovered from anesthesia. Finally, aspirin (75 mg/day) and ticagrelor (90 mg, twice a day) were administered until the euthanasia of the specimens. A total of 8 stents per group were implanted in 4 animals per group for both studies (7 and 28 days).

5.4.5.2 Endothelialization studies

After 7 days of implantations, the animals were euthanized under anesthesia. Stented arteries were explanted and rinsed with PBS and fixed in formaldehyde for 48h. For SEM characterization, arteries were cut longitudinally in halves to expose the luminal side. Further dehydration was performed in ethanol baths. Finally, arteries were coated by gold sputtering in order to be suitable for SEM imaging. The degree of stent strut endothelialization and platelet adherence was evaluated by imaging mode. Furthermore, histological analyses were performed by staining transversal cuts of the arteries embedded in polymethyl methacrylate/polybutyl methacrylate (PMMA/PBMA) with Masson's trichrome. Fluorescent microscopy analysis was performed after staining of alpha smooth cell actin using the mouse monoclonal antibody clone 1A4 from Sigma Aldrich, revealed by a goat anti-mouse IgG coupled to rhodamine (from Jackson immunoresearch) and nuclear counterstaining by Hoechst 33342 (Thermo Fischer).

5.4.5.3 In stent restenosis studies

After 28 days of implantation, angiographies of the stented coronary arteries were taken to observe a potential reduction in the lumen due to in-stent restenosis whilst the animal was still alive. Followed after, animals were euthanized, arteries were explanted, rinsed and fixed as previously described. For in-stent restenosis analyses, arteries were embedded in PMMA/PBMA, sectioned transversally in a microtome and stained with Sirius red for immunohistochemical studies in a confocal microscope.

5.5 Results

5.5.1 In vitro tests

Chemical composition changes were followed by XPS survey analyses. As shown in Table 18, the chemical composition of the functionalized surfaces since the plasma amination part (NH_2) to the immobilized peptide (PEG-P8RI) is shown. It can be observed that the percentage of nitrogen decreases after the reaction of with the linking arm (PEG), from a 11.0 ± 0.1 % to 2.9 ± 0.3 % of N, nonetheless, once the peptide is covalently grafted onto the linking arm (PEG-P8RI) this percentage increases due to the composition of the peptide to 4.5 ± 0.7 %. Furthermore, after the static immersion test in PBS for four weeks, it can be observed that no significant change in the percent of nitrogen was found when compared to the non-aged surface. Another important thing to notice is the fact that the percent of metal decreased as the functionalization of the surface is performed, however, it is always present on the surface analyses.

Table 18 Chemical composition of the functionalized surfaces obtained by XPS survey analyses. It can be observed that after one month of static immersion, no significant loss on the elements related to the peptide composition was found.

L605	%C	%O	%N	%Metal
NH_2	27.5 ± 1.8	49.9 ± 0.8	11.0 ± 0.1	11.8 ± 1
PEG	31.8 ± 1.1	48.0 ± 1.1	2.9 ± 0.3	10.5 ± 0.6
PEG-P8RI	34.9 ± 1.7	45.0 ± 2.2	4.5 ± 0.7	10.9 ± 1.8
PEG-P8RI 4 weeks	30.7 ± 1.3	44.6 ± 3.1	4.1 ± 0.6	8.4 ± 1.2

After the study of the composition and the stability of the functionalized surfaces, in vitro biological essays were performed to study the endothelial cell distribution and to analyse the supernatant of these cells, thus, their phenotype. HCAECs were seeded and incubated for 48 h onto EP, as a bare metallic control, PEG, to study the influence of the linking arm and finally in PEG-P8RI, to study the effect of immobilizing the bioactive peptide. Surfaces were stained for immunofluorescence analysis of the ECs nuclei, CD31 to study their junction and finally their actin filaments in order to observe their attachment to the surface. It was found, as observed in Figure 36, that the addition of both PEG and PEG-P8RI significantly increased the cell viability (number of nuclei, intensity of CD31 staining) onto the surface when compared to EP. Furthermore, the immobilization of the peptide increased the formation of stress fiber (presence of acting filaments, in red), reflecting a stronger cell attachment onto the surface, when compared to the control surfaces.

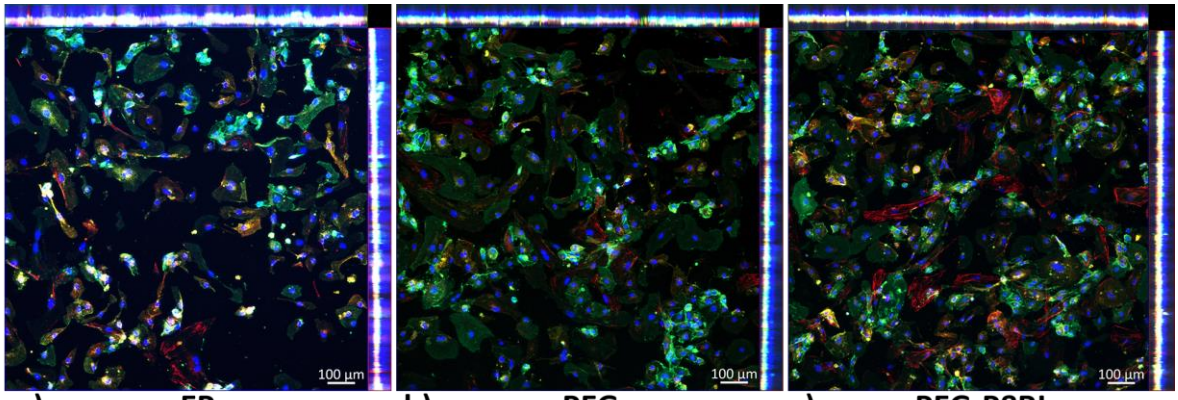

d)

Sample	Nuclei	CD31 Area (µm2)	CD31 intensity
EP	133 ± 35	6731.5 ± 3974	40108 ± 21164
PEG	219 ± 17.4	26366 ± 10777	173000 ± 75434
PEG-P8RI	292 ± 29	27873 ± 5909	179000 ± 46189

Figure 36 Fluorescent images after cell viability studies of HCAEC incubated for 48h onto a) electropolished surface, b) PEG and c) PEG with the bioactive peptide (P8RI). It can be observed that functionalizing the bare metallic surface with the linking arm and furthermore with the peptide increases quantity (number of nuclei) and viability (intensity of CD31 staining) of cells; quantitative data are reported in d). Furthermore, as compared to control surfaces, the cells growing ont PEG-P8RI surfaces exhibited an increase intensity on phalloidin, in red, reflecting an increased polymerization of the actin filaments, reflecting an improved attachment of the cells onto the surface.

To study the EC phenotype, the analysis of released soluble factors by a multiplex assay was performed. Regarding the inflammatory properties, IL-6 and VCAM-1 were selected as molecules of interest whilst the release of TFPI was measured to reflect the anti-thrombotic activity. Several experiments were performed, using different donors and multiple replicate. In order to compare the results of different donors and experiments, the results were analyzed after normalization of the data compared to the internal results obtained with the EP surface. As observed in Figure 37, inflammation markers were significantly lower when the cells were cultured onto peptide-immobilized surfaces. Furthermore, regarding the anti-thrombotic activity, a significant difference was observed when both PEG ± peptide were immobilized onto the surface, as compared to the bare metallic substrate, EP. Altogether, our data suggest that the phenotype of coronary endothelial cells growing onto the alloy is anti-thrombotic and anti-inflammatory when the bare metallic surface is functionalized with PEG as linking arm and P8RI as the bioactive molecule.

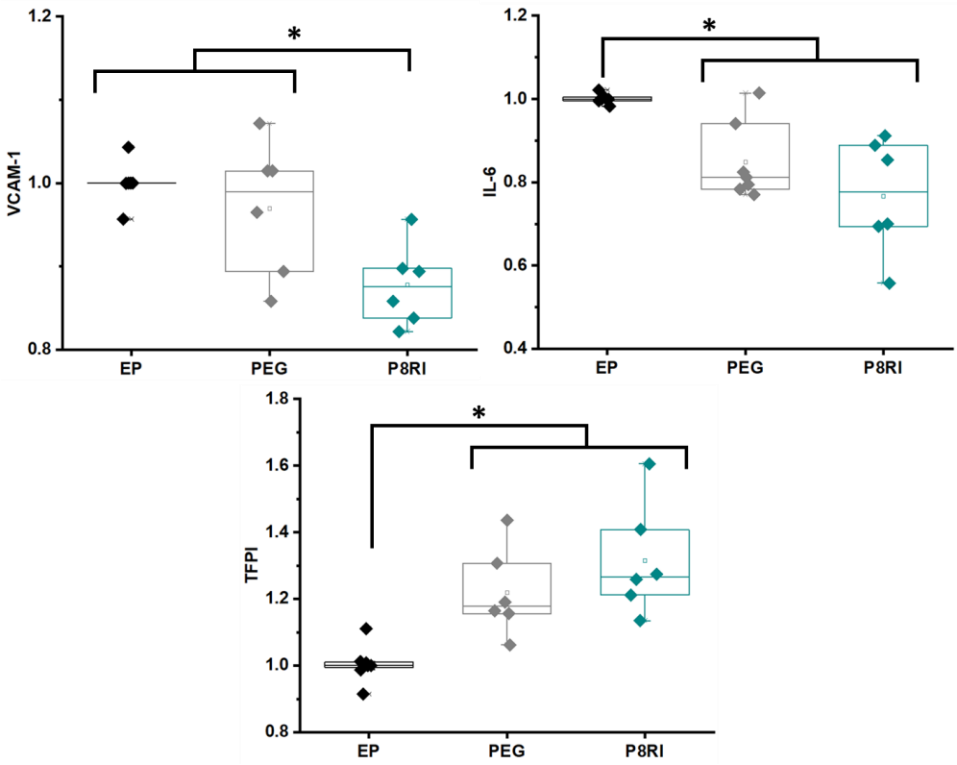

Figure 37 Quantification of the soluble factors of HCAEC after 48h of incubation with the surfaces, normalized to EP. It can be observed that both inflammation markers, VCAM-1 and IL-6, decrease with the presence of the peptide on the surface, when compared to the metallic substrate. Furthermore, functionalizing the surface by the proposed strategy increases its anti-thrombotic activity when compared to electropolished, as evidenced by TFPI marker.

5.5.2 In vivo tests

After seven days of implantation stented arteries were explanted from the euthanized animals to study the degree of stent strut endothelialization, evaluated by SEM images. As observed in Figure 38, both BMS and Plasma-P8RI present a complete strut covering by the endothelium, which was not the case of DES that presented a weakly coverage on the device. As regards leukocytes and platelets adhered to the endothelium, which was observed on higher magnification (x2500), on the case of BMS, it was found a high quantity of platelet/fibrin deposition whilst compared to the other two surfaces. In the case of DES, the shape of adhered leukocytes was spherical, thus, not activated but the presence of platelets and fibrin was already noticeable on the surface of the endothelium. Finally, on Plasma-P8RI, the density of the adhered leukocytes is significantly low when compared to the other surfaces and in a non-activated state, furthermore, no platelet/fibrin deposition was observed after 7 days of implantation for these stents.

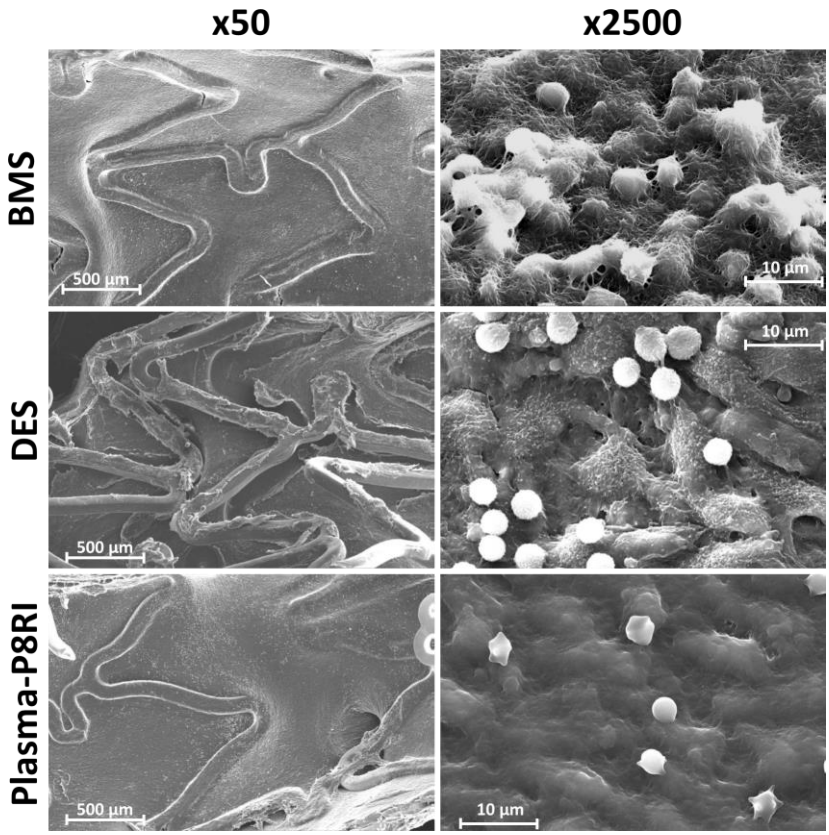

Figure 38 SEM images of extracted porcine coronary arteries after one week of implantation. It can be observed that both BMS and Plasma-P8RI have a better re-endothelialization when compared to DES, whose endothelium was found out to be damaged and not healed after 7 days. Furthermore, BMS presented adsorption of platelets and in early state of fibrillar conformation when compared to the other surfaces. Plasma-P8RI presented the less quantity of platelets adhered to the surface when compared to the other devices.

Regarding histological analyses, similar trend to what was found by SEM imaging was observed after the Masson's trichrome staining. As seen in Figure 39, transversal sections of porcine coronary arteries stented with BMS, DES and Plasma-P8RI were stained and studied. At short term implantation, it was found that both BMS and Plasma-P8RI present a complete endothelialization of the struts of the cardiovascular devices, whilst on the case of DES, this was not yet achieved.

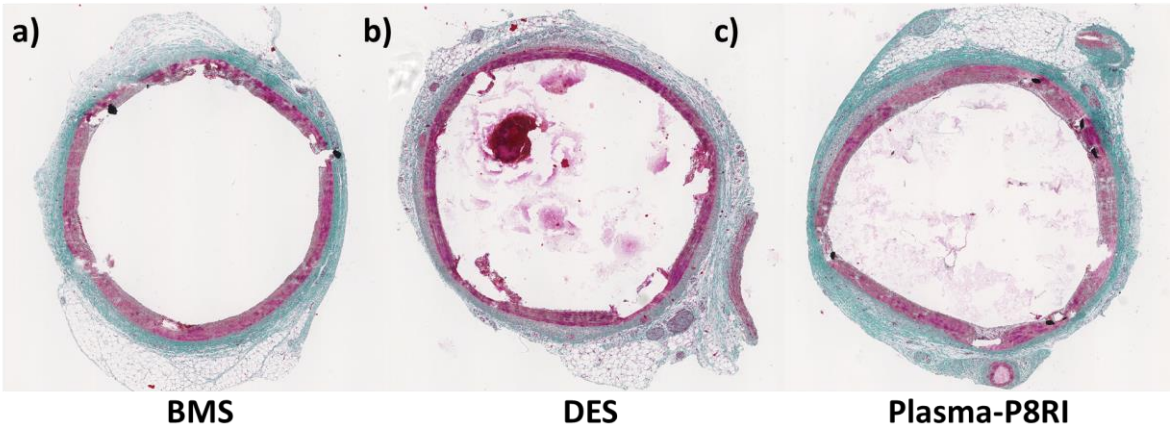

Figure 39 Optical microscope images of a transversal section of a porcine coronary artery after 7 days of implantation. Histological analyses performed by trichrome staining. It can be observed that BMS and Plasma-P8RI present a better re-endothelialization after 7 days of implantation, whilst on the case of DES the regeneration of the endothelium is not achieved.

Angiographic monitoring after 28 days of implantation was performed to follow up the evolution of the implanted devices and to observe the presence in-stent restenosis before the euthanasia of the animals. As seen in Figure 40, representative angiographies are shown to observe the reduction of the arterial diameter. As a general trend, it was observed a reduction on the arterial diameter on the case of BMS, whilst on the case of DES and Plasma-P8RI was not so evident. Moreover, a quick calculation of this reduction allowed to obtain an estimation on the restenosis percentage, shown in Figure 41. This calculation was performed by the inverse of the ratio (Lumen/stent), it was found a reduction on the in-stent restenosis on DES and Plasma-P8RI when compared to what was observed in BMS.

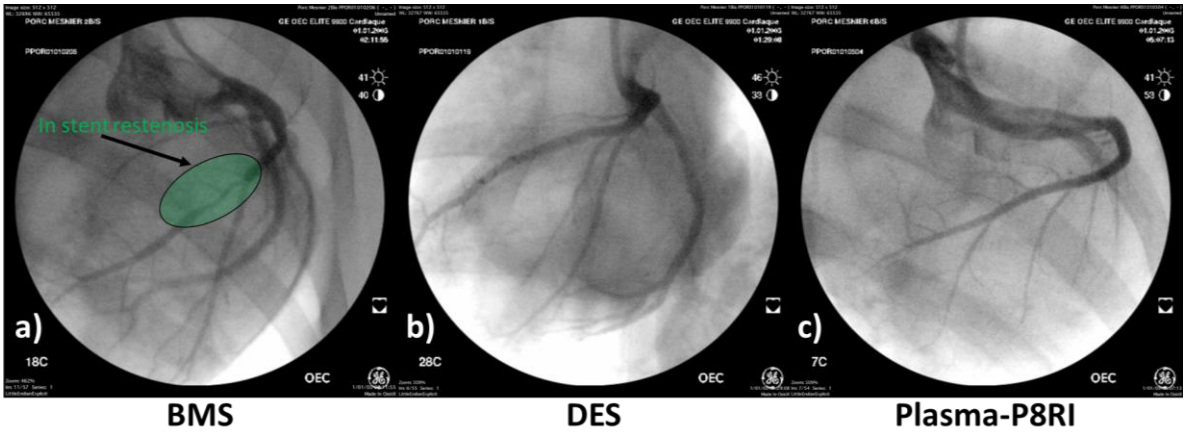

Figure 40 Representative angiography images of the left anterior descending artery of a) bare metal stent, b) drug eluting stent and c) plasma-P8RI modified cobalt chromium stent. Angiographies obtained before the euthanasia of the animals at day 28 to study in-stent restenosis whilst in vivo. It was observed a decrease in the lumen diameter of coronary arteries on the pigs with an implanted BMS.

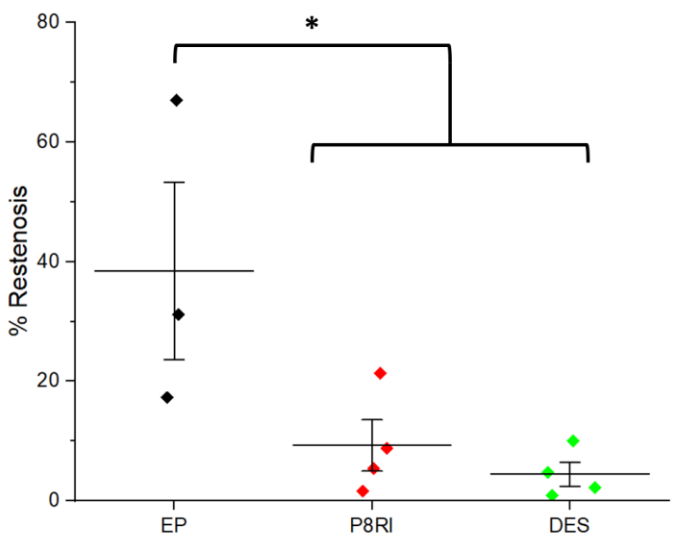

Figure 41 Estimation of the in-stent restenosis based on angiographies. It was found that both Plasma-P8RI and DES significantly decrease the in-stent restenosis in vivo in animal model after 28 days of implantation.

Finally, immunohistochemistry staining with Sirius red was performed to stain the collagen of the arteries, which in combination with the autofluorescence of the cells, allowed to study the in-stent restenosis post-euthanasia. It was found, that similar to what was previously observed in the angiographies, BMS presents a bigger reduction when compared to the other surfaces. Plasma-P8RI followed BMS with a reduction of the arterial lumen. Finally, DES presented no visible reduction on the diameter of the artery.

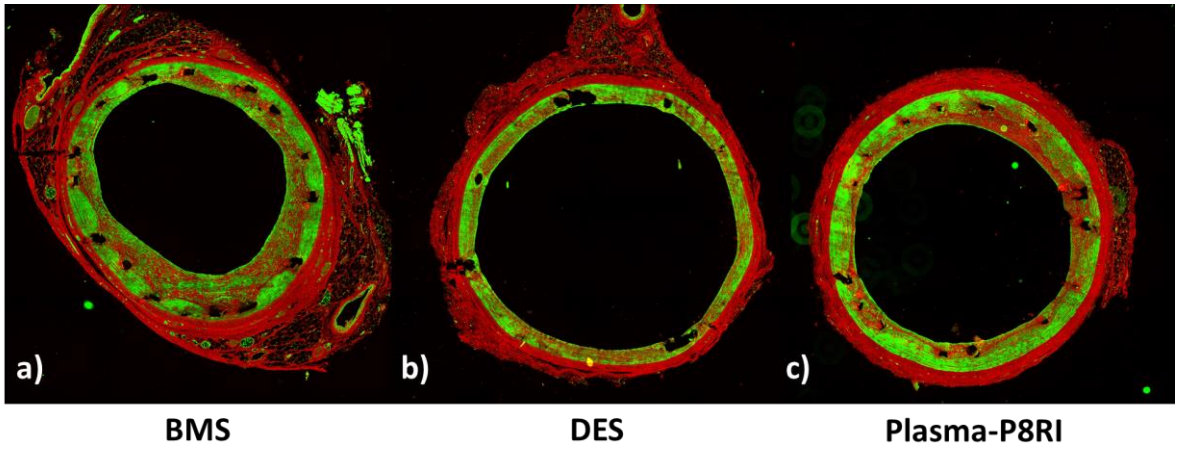

Figure 42 Immunohistochemical staining of the explanted porcine coronary arteries after 28 days of implantation. Similar to what was observed on the angiographies before the euthanasia, Plasma-P8RI and DES decrease the potential risk of in-stent restenosis when compared to BMS which presents a reduction on the lumen. On red = Sirius red to observe the collagen and in green the autofluorescence of the arteries.

5.6 Discussion

A novel strategy to directly functionalize metallic surfaces with bioactive molecules was studied as a potential alternative to bare metal stents and drug eluting stents was herein studied. A combination of in vitro and in vivo

tests was performed in order to study the potential for this novel strategy. Flat samples were used for in vitro tests, whilst for in vivo tests, functionalized commercial stents were used. One of the first things to characterize, regarding flat samples, was the composition and the stability of the functionalized surfaces. It was found by XPS survey analyses, as observed in Table 18, that after the grafting of the linking arm, PEG, there was a decrease on the percentage of nitrogen, related to the attachment of this molecule onto the surface of the alloy. After the grafting of the peptide, it was found an increase on nitrogen and carbon, related to the chemical composition of the peptide. Finally, static immersion tests, performed as a stability test for the functionalized surface, demonstrated that this strategy allows the covalent immobilization of a bioactive principle, by not presenting a significative lost on the percent of nitrogen, oxygen and carbon, related to presence of the peptide. Furthermore, throughout the functionalization procedure, atoms related to the metallic surface (mainly cobalt and chromium) were always detectable, demonstrating that this is in fact a functionalization and not a coating of the metallic surface. As regards the decrease on the metallic percentage after immersion test, the deposition of salts from the solution could have covered the detection of these atoms.

After the characterization of the surface, the in vitro performance of the functionalized surfaces was studied. Initial tests involved the seeding of HCAEC onto EP, PEG and PEG-P8RI, in order to study their distribution and attachment by immunofluorescent staining. It was found out, as observed in Figure 36, that functionalizing the metallic surface with the linking arm (PEG) and with the peptide (PEG-P8RI) improves the presence of HCAECs. This result was observed qualitatively, in the images (a, b and c) and quantitatively (d). Furthermore, it was also observed (d) that the functionalization significantly increases the cellular junction of endothelial cells, suggesting the potential formation of a monolayer onto the surface. Finally, the covalent immobilization of the peptide increased the presence of actin filaments, in red, thus increasing the cellular attachment onto the metallic surface. As regards the study of the supernatant after incubation, it was found that grafting the peptide decreases the presence of inflammation related molecules, VCAM-1 and IL-6, when compared to the electropolished sample. For the anti-thrombotic molecule, TFPI, it was found out that attaching both PEG and PEG-P8RI increase the anti-thrombotic activity of the surface, when compared to EP. The general trend after grafting the peptide is that the produced surface is more anti-inflammatory and anti-thrombotic than the EP surface, thus, this suggests a potential decrease on complications in vivo. This behaviour can be related to a potential synergic effect of PEG, an anti-fouling molecule with the specific signalization of the peptide for ECs. This synergic effect between PEG and P8RI could create bioactive surfaces suitable for the cardiovascular application, thus, in vivo tests in animal model were performed to study its performance.

In vivo tests were performed for two times of implantation: 7 days, to study the re-endothelialization; and 28 days, to study in-stent restenosis. The comparison of commercial stents (BMS and DES) to the functionalized stent proposed in this work was performed. As regards re-endothelialization, results demonstrated (Figure 38)

that BMS did not present a problem on the re-endothelialization of the device, as seen in lower magnifications, but on the deposition of leukocytes, fibrin and platelets, suggesting a potential thrombogenic reaction. DES's struts were not covered by the endothelium and the adhered leukocytes and platelets were not in an active state, this can be related to the effectiveness of the eluted drugs that avoid the thrombus formation and the over proliferation of cells, thus compromising the endothelium healing. Finally, Plasma-P8RI showed promising results due to the complete coverage of the stent's struts by the endothelium whilst also significantly decreasing the presence of adhered leukocytes and platelets onto the arterial walls. These observations were complemented by histological analyses of the cross section of the stented porcine arteries, Figure 39, which showed a similar trend: BMS and Plasma-P8RI with an advanced re-endothelialization, whilst DES presented a compromised endothelium. Furthermore, the analyses of the supernatant of HCAEC demonstrated to be a suitable technique to obtain a prediction for the in vivo response: the immobilization of the P8RI peptide (as Plasma-P8RI) presents an increased anti-inflammatory and anti-thrombotic activity when compared to the EP surface or BMS.

Further in vivo studies were performed to analyse the in-stent restenosis. First, angiographies were performed whilst the animal was still alive to observe the potential stenotic arteries on the pigs. It was observed, in Figure 40, a decrease on the lumen diameter on the stented arteries with a BMS. No significant difference was observed for DES and Plasma-P8RI. To complement these observations, the percentage of reduction was calculated from the angiographies, Figure 41, where it was found that both DES and Plasma-P8RI does not present a significant difference among them in terms of in-stent restenosis, but a significant difference when compared to BMS, which presented a stenotic arteries. Finally, after the euthanasia of the animals, immunohistochemical studies were performed on the stented arteries, Figure 42, where the same observed trend was observed, BMS presented a decrease on the arterial lumen, followed by Plasma-P8RI and then by DES.

5.7 Conclusion

A novel strategy allowed the direct functionalization of commercial cardiovascular devices with a bioactive peptide, derived from CD31. This peptide had previously been studied by its anti-thrombotic, anti-inflammatory and pro-endothelialization bioactivity, thus the interest of using it on stents. Furthermore, the immobilization of this molecule using PEG as a linking arm or spacer conferred a synergic effect that improved the biological properties of the metallic surfaces. This was first confirmed by in vitro, where the stability and biological properties of flat samples were assessed. XPS survey analyses confirmed the covalent grafting of the peptide, which after a 4-weeks immersion test, no significant change regarding surface composition was found. Furthermore, in vitro biological tests demonstrated that the grafting of PEG-P8RI onto the metallic surface of L605 increased the presence of endothelial cells which exhibited an anti-thrombotic and anti-inflammatory phenotype and were strongly attached to the surface, in comparison with the crude metallic surface. In vitro

results were used as a prediction of what was found on in vivo tests in porcine model. Functionalized stents by this proposed strategy, Plasma-P8RI, presented a better re-endothelialization at 7 days when compared to commercial DES with a low adhesion of leukocytes and platelets when compared to BMS. Moreover, at 28 days of implantation, Plasma-P8RI did not present a significant decrease on the lumen diameter, which was not the case for BMS that presented in-stent restenosis after this period. Overall, this small trial gave a promising panorama for Plasma-P8RI stents. Further trials at longer term, with an increased number of specimens, must be performed in order to understand if these devices are suitable for human trials.

Chapter 6 General discussion

This research was focused on the development of an alternative strategy for the immobilization of bioactive molecules onto metallic surfaces and its application in cardiovascular devices. This strategy combines different surface modification processes, that allow the creation of reactive functional groups directly on the surface that can be used as anchor points to immobilize molecules of interest. This idea is known and have been used since decades on other substrates such as polymers, but it has never been explored and reported in metals. The process includes several steps, and this multi-step strategy was applied to generate functionalities to improve the clinical performances of commercially available cardiovascular devices. The overall originality of the research was to design and develop easier and effective plasma-based processes to grafting bioactive molecules to promote the re-endothelialization with anti-thrombotic activity whilst decreasing in-stent restenosis. These processes were designed, and their effect was assessed to represent a potential alternative to Drug Eluting Stents. In fact, after more than 10 years of clinical experiences with few commercially available molecules (paclitaxel, sirolimus and a few derivatives) eluted from stents, clinicians agreed in concluding that a part few patients typology (poor vascular bed, several complications already experienced and fragile general health), drug eluting stents did not fulfill the expectations As presented in Figure 9, the core of this strategy is divided in three big steps:

a) Surface optimization

b) Direct plasma amination

c) Bioactive molecule grafting

Each of these steps have a critical impact on the development of the functional device. This chapter focuses on the discussion of the published results from Chapters 2, 3, 4, and 5, as well as unpublished results. They will be presented transversally, i.e. following the structure presented above. Finally, some perspectives and future works will be detailed to transfer this multi-step procedure to other alloys.

6.1 Optimization of the surface properties for stent application

The interaction between the surface of the device and the biological medium (*in vitro* or *in vivo*) will dictate the success or failure of the implant. Thus, the complete characterization and understanding of the surface is critic. The fact that the metallic surface of the device will be directly aminated in plasma, and therefore will not be coated with a molecule-rich polymeric layer, certainly represents a main difference. In fact, the metallic substrate is always exposed to the biological medium. From this point of view, bioactive molecule-rich surfaces by direct amination will interface blood and the surrounding tissue in a manner much more similar to the one that bare

metal stents do. Thus, the composition, texture, morphology and energy of the surface must be carefully considered.

Once identifying the properties required for an effective use of a biomaterial, both a) the mechanical properties and b) the biological properties must be compromised. The selection of a material is based on the *in vivo* application of the device. Mechanical and biological properties are not the same for a hip implant than for a skin substitute, for example. Something that needs to be taken into consideration is the fact that there is no ideal material that possess both mechanical and biological properties, *there is always a compromise* on one side. Generally, the compromise is on the biological properties, thus the need for strategies to enhance them.

In the case of stents, due to the nature of the implantation of the device, they must present [13]:

- ✓ Ability to be cramped to the balloon catheter supported on the guide wire:
- ✓ Proper expandability to stay on the deployed area after implantation: high elastic modulus
- ✓ Low recoil after implantation, thus avoiding the collapse: high yield strength
- ✓ Flexibility to travel through small and rigid atherosclerotic arteries
- ✓ Radiopacity for the clinician's characterization by magnetic resonance imaging, and therefore, high density
- ✓ Corrosion resistance
- ✓ Good biocompatibility

L605's mechanical properties, reported in Table 2, make it a suitable material for this application, thus, the interest for using this alloy on this project. Nevertheless, the biological properties of this material require to be modified to be suitable for a stent application, where the reendothelialization process is critic and presenting anti-thrombotic behaviour can lead to lower in-stent restenosis.

6.1.1 Modulation of the surface properties and their impact in the performance of the alloy

The comparison of the different surface treatments was performed as a function of their stability and their biological performance. On the metallic surface, the desired properties related to stability are corrosion and deformation resistance. Regarding biological performance, the cytotoxicity of the surface and the hemocompatibility were mainly studied. For the optimization of the surface, as discussed in Chapter 3, three different surface treatments were proposed to modify the oxide layer of the alloy: electropolishing, followed by thermal treatment or PIII of oxygen. These treatments are intrinsically different and modify the surface thanks to different mechanisms:

- ✓ **Electropolishing (EP):** An electrochemical procedure employed to remove impurities and to smoothen the surface. Therefore, the surface is composed of a thin layer of chromium oxides (depth profile sputtering time= ~50 s, Figure 21a).

- ✓ **Thermal treatment (TT):** Used to modify the chemical composition of the oxide layer by diffusion of atoms from the alloy to the surface. This treatment produced a thick oxide layer composed of a mixture of chromium and cobalt oxides (depth profile sputtering time= ~600 s, Figure 21b). The main investigated conditions were: 400, 500 and 600 °C for 1 h and 2 h.

- ✓ **PIII of oxygen (PIII):** to create a new amorphous oxide layer after the implantation of oxygen ions. This surface modification produced a bilayer oxide layer of first cobalt oxides followed by a layer of chromium oxide. Fixed conditions: 10 sccm of O_2, pulse of 50 µs with a frequency of 100 Hz at 5 mTorr, 300 W of power. Variable conditions: time of implantation 15, 30 and 60 mins; bias -0.1, -1 and -10 kV.

The different chemical compositions had an impact on both the stability and the biological performance of the surface.

- **Stability of the oxide layer:** *Deformation resistance* of the different surface treatments was evaluated using the small punch test. This test, which simulates stent deformation, demonstrated that the only conditions suitable for the desired application exhibiting no cracks nor delamination were EP, TT at 400 °C for 1 h and PIII at lowest bias, -0.1 kV for 1 h of implantation. It was also determined that TT at higher temperatures created a brittle surface with internal micro-cracks that caused the failure of these surfaces [123]. PIII led to a different arrangement of the oxide layer, an amorphous configuration, that induced delamination instead of cracks [42]. Regarding *corrosion resistance*, it is known that L605 is resistant to marine environments, acids and body fluids thanks to the presence of a passive oxide layer composed of chromium oxides [23, 87]. Thus, modifying the chemical composition of the oxide layer influenced the corrosion resistance of the material. In fact, the corrosion resistance of the surfaces was: EP > PIII > TT (Figure 23). This finding correlated with the different chemical composition of the surfaces: EP's passive oxide layer was composed by a thin layer of chromium (Figure 21a); PIII presented an oxide layer with a "bilayer" composition of cobalt oxide followed by chromium oxide, which could have initially increased the dissolution of cobalt ions followed by a decrease on the corrosion rate due to the presence of chromium oxide (Figure 21c); And finally, TT was composed by a mixture of both cobalt and chromium oxides on the surface which could have led to an increase on the corrosion rate (Figure 21b). Therefore, after deformation and corrosion tests, the surface treatment which presented the best stability regarding corrosion and deformation resistance was EP.

- **Biological performance of the oxide layer:** Regarding the *cytotoxicity* studies, or short-term cellular response, it was found that the viability of endothelial cells was higher on the EP surface, followed by TT and finally PIII, with a significant difference to EP (Figure 26a). This was similar to what was previously observed by Maffi et al. [131]: Higher endothelial cell viability was found on chromium rich surfaces. However, after one day of incubation, all the surfaces demonstrated a cell viability of >60%, thus, no negative short-term cellular response, even under the presence of cobalt known for possessing a negative effect on cells [127]. Nonetheless, as observed in Figure 26b, the *hemocompatibility* of the surfaces needs to be improved due to a low percentage of hemoglobin free, thus a potential thrombogenic behaviour.

Hence, based on the observations from this part of the work, the most suitable surface treatment, for this application is EP. Regarding stability of the oxide layer it possesses both stability to deformation and corrosion resistant. Nevertheless, it is on the biological performance that this alloy needs to be improved. Therefore, the interest of using this surface modification technique as base pre-treatment on the development of the direct functionalization strategy with bioactive molecules. After the optimization of the surface, the plasma functionalization with reactive amine groups needs to be performed and optimized. Next subsection discusses the feasibility, optimization of the surface and parameters, and the transfer from flat samples to commercial stents.

6.2 Direct plasma amination: influence of surface pre-treatments on the efficiency of the plasma functionalization

As observed in Figure 9, plasma functionalization with reactive amine groups is performed, after surface optimization. Amine groups are crucial to fulfill the planned strategy. In fact, the generation of these functional groups have been comprehensively studied on polymers and have been often used as anchor points for the immobilization of molecules. Nevertheless, to the best of our knowledge, plasma-based strategies have never been reported to effectively functionalize metals through primary amine groups. Thus, there is a need to study the role of the surface in this functionalization. This has a great potential to eventually lead to the understanding mechanisms of plasma-based functionalization of metals, including L605.

The research deployed in this Thesis was focused on using plasma to create amine groups, hereafter called plasma amination. This strategy was focused on: a) the feasibility to create reactive amine groups on flat metallic surfaces, b) optimization of the functionalization procedure and c) feasibility to transfer the developed procedure to commercial stents. Moreover, another objective was the establishment of a characterization strategy due to the complexity of the surfaces. In fact, conventional surface-based techniques (such as FT-IR), generally used on polymeric matrixes, do not represent suitable characterization methods due to the depth of analyses and their

characterization principle, thus, the use of a combination of techniques with high sensitivity such as XPS and ToF-SIMS were proposed.

6.2.1 Feasibility to functionalize a metallic surface with reactive amine groups by plasma treatments

One of the initial objectives was the feasibility to create reactive amine groups onto metallic surfaces. The core of the developed doctoral strategy was centered on this feature. Thus, the feasibility was studied on the previously proposed surface treatments for the optimization on the surface. These treatments were selected initially to be studied for their different surface chemical composition, but all shared the same bulk composition, the L605 alloy.

- **Direct plasma functionalization of the oxide layer:** As observed in Figure 24, nitrogen was confirmed by *XPS survey analyses* on the three surfaces (EP, TT and PIII) after plasma treatments. The surface with highest percent of nitrogen was PIII (~15 %), followed by TT and then EP, showing the lowest percentage (~10 %). Chemical derivatization of the functionalized surface with a specific reagent for primary amine groups (5-bromosalycylaldehyde) lead to the quantification of primary amine groups on the surface in which no significant difference was found on the three surfaces, ~1.5 % of NH_2 groups. A calculation of the efficiency based on XPS results %(NH_2/N) demonstrated that EP was the most efficient surface with ~ 15% of efficiency, followed by PIII and TT with ~9.5 efficiency. Furthermore, *ToF-SIMS analyses* in positive mode of the specific fragment (NH_2^+) confirmed the same trend on the results. It was found a significant quantity of the fragment on the EP surface compared to the other oxide layers.

Based on the observations obtained after the study of the feasibility to directly functionalize with reactive amine groups metallic surfaces, EP surface was clearly showing the highest efficiency (NH_2/N), when compared to the others. EP presented around 1.5 % of reactive amine groups on the surface with an efficiency of around 15%. These values are significantly lower when compared to polymeric matrixes. In polymers, such as polyethylene [189], polypropylene [190] and polystyrene [84], plasma amination efficiency goes from 20 to 75% and percent of primary amine groups goes up to 3.5 - 4%. Thus, one of the perspectives of this works is optimize the direct plasma amination on metallic alloys to promote the promote the quantity of reactive amine groups on the surface.

6.2.2 Efficiency of plasma functionalization: Influence of surface pre-treatments and plasma parameters

Initial efforts to improve the quantity of reactive amine groups and to increase the efficiency of the plasma functionalization were performed. These are non-published preliminary results that aimed to understand which parameters can influence the amination process. Amination efficiency can be influenced by the material, thus

the surface and the pre-treatments and by the plasma treatment by themselves. These preliminary studies were performed on EP surfaces due to their previously discussed properties and by its selection as base surface pre-treatment for the developed strategy to directly immobilize bioactive molecules onto metallic surfaces.

- **Influence of the pre-treatment on the direct plasma amination:** One of the first efforts to understand the importance of the surface pre-treatment was to directly functionalize *clean L605 samples without electropolishing*. Samples were cleaned using solvents to remove any impurity on the surface and further functionalized as mentioned in section 2.4.2. The quantity of reactive amine groups on the surface was reduced almost by half when compared to electropolished samples: ~0.8 % of NH_2.

- **Impact of hydrogen plasma post-treatment on amination efficiency:** Preliminary studies on the optimization of the plasma treatment were focused on the use or not of a hydrogen post-treatment. As can be observed in section 2.4.2 the direct plasma functionalization is performed in a two-step treatment: for 5 minutes in a mixture of H_2 and N_2, followed by a short treatment of 30 s in hydrogen. This second step seems to promote the amination by reducing the other nitrogen species that were produced by the plasma, as Fabia et al. proposed previously on polymeric surfaces [56]. As regards L605 it was found a significant difference on the percentage of amine groups on the surface from a 0.3 ± 0.2 %NH_2, without the post-treatment, to 1.5 ± 0.3 %NH_2, with the short hydrogen post-treatment. In terms of efficiency from a 2.3% of efficiency to 15%.

Furthermore, one of the hypotheses for the formation of amine groups by plasma on metallic surfaces is that the presence of hydroxyl groups (-OH) on the surface, obtained in the sodium hydroxide bath after the electropolishing, promoted the presence of amine groups. If this is true, then, why EP compared to TT and PIII present a higher percentage of reactive amine groups? On the case of TT, a re-oxidation of these hydroxyl groups could happen after the thermal treatment, whilst on the case of PIII, the bombardment with oxygen radicals could detach them from the surface. As a *perspective* for further studies, a complete characterization of the percentage of hydroxyl groups on the surface of the alloy obtained by different surface treatments such as plasma oxidation or acid dipping must be performed.

6.2.3 From flat samples to commercial stents: Optimization

After the confirmation that direct functionalization was effectively performed and that primary amine groups were present on flat surfaces of L605 alloys, the feasibility to transfer the process onto commercial stents was investigated. Preliminary tests were first performed on flat samples in a vertical arrangement, as observed in Figure 43. Three flat electropolished samples, labeled as 1, 2 and 3 were used to optimize the conditions of the plasma amination. Plasma functionalization was then performed in a series of two plasmas, the first one labeled

as Plasma 1, and the second one with the sample 1 and 3 inverted, labeled as Plasma 2. The rationale to inverse these samples was to simulate a plasma functionalization that was equal for both extremes due to the distance to the glow area of the plasma. Furthermore, the plasma conditions were modified as follows: The first step was carried out at 150 W during 10 min at 100 mTorr, *10/10 sccm of N_2/H_2*, followed by a second step at 150 W during 30 s at 300 mTorr, *20 sccm* of H_2.

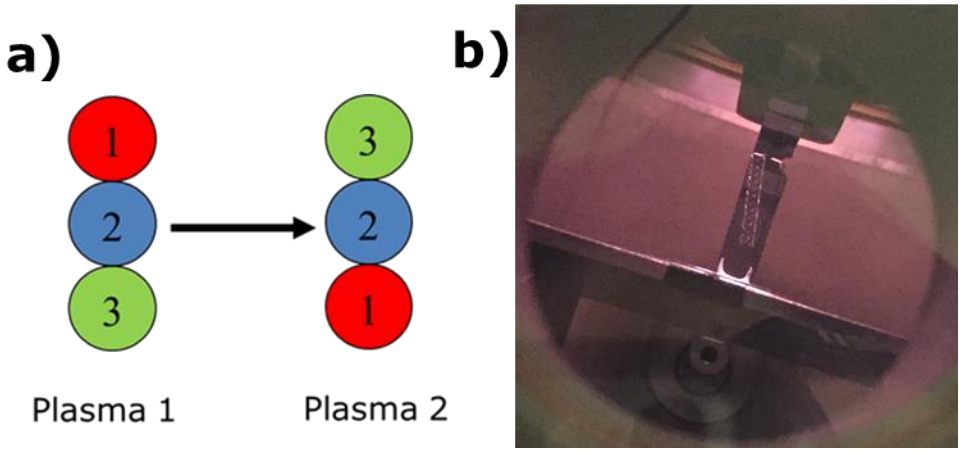

Figure 43 Schematic of the sample arrangement for optimizing the plasma functionalization of cardiovascular devices (a). The numbers 1, 2 and 3 represent an electropolished sample of L605. Briefly, for the second plasma the samples 1 and 3 were inverted to simulate an homogeneous plasma treatment due to the distance with the afterglow of the extremes of the cardiovascular device. Image of the plasma amination treatment of a stent (b).

It was found that, after this proposed methodology for the functionalization of vertical samples the presence of ~1.3 % of amine groups on the three samples with no significant difference among them. Thus, these conditions were used for the functionalization of the cardiovascular devices which were placed on a support made of tungsten, as observed in Figure 43b. Nonetheless, the big challenge that was present on this part of the project was the characterization of the functionalized stents. XPS was not a suitable technique due to the complex geometry of the device. Thus, a different methodology to characterize it needed to be developed. Two different characterization methods were proposed: Fluorescent microscopy and ToF-SIMS imaging mode.

- **Fluorescent microscopy:** One of the first efforts to confirm the presence of a molecule on the surface was to use fluorescent microscopy as a qualitative study. As shown in Annex 1, stents were functionalized using the developed multi-step plasma procedure, to create amine groups then the use of GA and PEG as linking arm for fluorescent peptides, which one contained a TAMRA fluorophore and the other a FTIC fluorophore in their composition, were performed. Nevertheless, the characterization of the surface by fluorescent microscopy was not suitable for this device. Some of the challenges to overcome and general observations for the use of fluorescent microscopy are: a) due to the complex geometry of the device, a confocal microscope is recommended to create a "z-stack" of images and thus avoiding blurred images, b) concentration of the fluorescent peptide must be optimized to avoid

the adsorption of fluorescent grains of salt, c) high magnification analyses to be able to observe the fluorescent peptide.

- **ToF-SIMS imaging mode:** As an alternative to fluorescent microscopy, ToF-SIMS imaging mode was proposed. The main advantage of technique was the possibility to study specific fragments located on the surface of the functionalized device. As observed in Figure 34, ToF-SIMS imaging characterization confirmed the presence of a peptide both in positive and negative mode. The study of specific fragments related to the peptide, $C_4H_8N^+$ and I^-, confirmed the presence of the peptide on the surface of the stent. Furthermore, observing Cr^+ and CrO_2^- fragments, related to the oxide layer, confirmed that the result of this multi-step strategy was a functionalization and not a coating.

The characterization of the plasma functionalized surfaces represents a challenge that needs to be overcome if this strategy is aimed to be used at industrial scale. The combination of XPS and ToF-SIMS both in static and imaging mode have shown promising results as the solution to this challenge at laboratory scale. Nevertheless, for the industrial application, the development of characterization methods that lead to the quality control of the functionalized surfaces is critical. Thus, further studies of other characterization methodologies aiming towards the industrial scale and application must be performed as a continuation of this research work.

6.3 Optimization of the direct immobilization of bioactive molecules

Reactive amine groups generated after plasma treatments were used as anchor points for the immobilization of different molecules. In the search of the most suitable bioactive surface, different linking arms as spacers between the surface and the bioactive molecule were studied, furthermore, the bioactivity and the distribution of different peptides were studied. The optimization for the immobilization strategy mainly focused on two objectives: a) the selection of the most suitable linking arm and peptide for the cardiovascular application based on the stability and b) the biological performance of the bioactive surfaces. Besides the optimization of the grafting strategy, settling the characterization techniques for the bioactive surface was another objective for this section of the research project. Following the characterization methodology proposed for the plasma amination block, ToF-SIMS and XPS play a major role in the characterization for the study of the immobilized molecules.

6.3.1 Optimization of the biomolecule grafting: Linking arm selection

One of the first studies performed was the feasibility to immobilize molecules onto the reactive amine groups. Followed by these studies, the comparison of the linking arms was performed in order to obtain the most suitable spacer for its application in cardiovascular devices. This comparison focused on the study of the homogeneity of the functionalization and the stability of the grafting.

- **Feasibility of the direct immobilization on metallic surfaces:** As showed in Figure 17, the combination of XPS high resolution of carbon (HR C1s) and ToF-SIMS in static mode confirmed the presence of a peptide grafted onto the surface. For the feasibility studies, the first linking arm to be used due to the simplicity of the reaction was GA. The combination of the previously mentioned techniques allowed the follow up of the grafting procedure: by XPS HR C1s the increase in bonds related to the linking arm (C-C, C-O and C=O) compared to the plasma aminated sample with a further increase mainly on (C-O/C-N and C=O) for the peptide due to its chemical composition. Furthermore, regarding ToF-SIMS static mode, the selected fragments to study the grafting procedure were three, one related to the peptide ($C_5H_{10}N^+$, from lysine), one related to the linking arm ($C_2H_5O^+$) and finally one related to the metallic surface ($Cr_2O_2^+$). The same trend was confirmed by analysing the surface by ToF-SIMS: an increase on the fragments related to GA after the linking arm when compared to the aminated surface and finally a significant increase after the peptide grafting. The advantage of ToF-SIMS offer to this kind of functional surfaces is the possibility to observe that after the grafting of the peptide the fragments related to the GA and the oxide layer decreased but were still present, thus, confirming the immobilization reaction. Regarding the characterization of PEG as linking arm by the same methods, it was not as direct compared to GA at least on high resolution analyses. XPS HR C1s of PEG (not published results), presented no significant difference between the PEG sample and after the peptide grafting. This could be related to the fact that the linking arm molecule is significantly big compared to GA and the peptide (PEG Mn = 600), thus the addition of these molecules did not modify the high-resolution spectrum. However, ToF-SIMS allowed the characterization of the surface, as observed in Figure 32, with the study of the specific fragments from the grafted peptide.

- **Homogeneity of the grafting:** As an alternative to fluorescent microscopy, ToF-SIMS imaging mode was proposed as characterization technique to study the homogeneity of the grafting. The main advantage of technique was the possibility to study specific fragments from the molecules of interest and how they are distributed on the functionalized surface. Two peptides were used for the study of the distribution of the bioactive molecule on the surface: a peptide with a modified amino acid with three iodine in its chain, and the P23 peptide, derived from CD31. For GA, regarding the first peptide, it can be observed in Figure 18 that the I^- fragment is present on the surface with a homogeneous distribution, whilst on the case of PEG (not published data, Annex 5) there are some areas where the fragment is more present. Two hypothesis might explain this: a) the effect of the linking arm could have influenced the way the peptide arranged onto the surface under the high vacuum required for ToF-SIMS analyses, GA as a small chain spacer could have promoted an arrangement that exposed the iodine of the peptide onto the surface, due to a steric impediment, whilst PEG, a long chain spacer allowed the folding of the peptide to a minimum energy state conformation where the iodine fragments were located in specific

zones of the surface; b) PEG and GA are grafted to the peptide from different parts of the molecule, thus, the orientation of the iodine fragments would be different for both spacers. However, regardless of the distribution, it is important to remind that the metallic surface was always exposed. This was confirmed in Figure 32 and Figure 33, where fragments of the peptide, GA/PEG and the oxide layer are shown in order to compare the distribution of the surface. In fact, the grafting of this peptide by the means of any of the linking arms did not affect the distribution on the surface, compared to the peptide with the iodine in its structure.

- **Stability of the grafting:** Besides the characterization of the feasibility to directly graft molecules onto metallic surfaces, their stability was studied. Non-published results, Annex 2, about static immersion tests in PBS at 37 °C for up to one month showed that no significant loss of the peptide was found for GA nor PEG with P23. This can be related to the nature of the functionalization and the grafting procedure that creates a covalent bond between the surface of the alloy and the linking arms: |-NH-CO-$(CH_2)_n$-COOH, where n is the length of the linking arm. Nevertheless, as a perspective, further studies need to be performed using different solutions for the stability test and as well under dynamic conditions.

6.3.2 Biological performance of the bioactive surfaces: Does the linking arm limits the biological activity of the peptide?

It is known that denaturation and potential loss on the biological properties of bioactive molecules during their immobilization onto surfaces might happen. Thus, the comparison of the molecule effectiveness after both processes leading to linking arms on the biological activity of a peptide (P23) known for its anti-thrombotic, anti-inflammatory and pro-endothelialization behaviour was performed. These studies were performed with the main objective to investigate the impact of the linking arm on the bioactivity of the peptide. Furthermore, these results were used as a starting point to confirm if the multi-step plasma-based strategy to immobilize bioactive molecules could in fact, enhance the biological properties of bare metallic surfaces. The tests used to study these properties were: cell viability and migration of endothelial cells, related to the promotion of re-endothelialization; hemocompatibility tests to understand the anti-thrombotic activity; and finally, the quantification of soluble factors of endothelial cells after incubation with the surface to study the phenotype of the cells, thus, anti-inflammatory behaviour.

- **Pro-endothelialization behaviour:** Cell viability essays were carried out on EP, GA-P23 and PEG-P23 to observe the proliferation of endothelial cells on the functionalized surfaces up to 7 days. As observed in Figure *29*, it was found that both linking arms present a higher viability compared to the metallic surface since day 1, nevertheless, it was found out that only PEG-P23 was the surface with a

significant higher viability to the EP surface after day 7. Furthermore, as observed in Figure 30, a migration essay was performed for the same time period to study the feasibility of the surfaces to produce a monolayer of endothelial cells, simulating the re-endothelialization process. It was found that PEG-P23 was the fastest surface to promote the formation of the monolayer compared to EP and GA-P23. Even if GA-P23 was able to form a monolayer at day 7, fast re-endothelialization is crucial for the wound healing in vivo after the stent implantation.

- **Anti-thrombus formation:** Hemoglobin free tests were performed to study the cloth formation onto the previously mentioned surfaces. As observed in Figure 31, it was found at short times in contact with blood a significant difference between EP and both GA-P23 and PEG-23, where the later two samples demonstrated a more hemocompatible behaviour compared to EP. Nevertheless, after 20 minutes in contact with blood no significant difference was present among them and after 30 minutes all surfaces presented cloth formation. Thus, at short times the addition of the peptide increases the hemocompatibility of the metallic surface.

- **Anti-inflammatory surface:** Non-published results of the quantification of soluble molecules in the supernatant of endothelial cells after being in contact for 48 h with the functionalized studies allowed to study the inflammatory response of the cells with the surfaces, Annex 3. For this part of the project, two factors were of interest: IL-6, an inflammatory interleukin, and VCAM-1, an adhesion molecule that is plays a role in the development of atherosclerosis. These molecules were quantified by flow cytometry, as explained in section 5.4. It was found that for both inflammation markers (VCAM-1 and IL-6) molecules only PEG-P23 presented a significant decrease when compared to EP, thus the grafting of the peptide by this linking arm lowers the probability of a secondary reaction while in vivo.

It can be observed from the evaluation of the biological properties of the peptide after immobilization, PEG-P23 presented a better performance in comparison with the grafting by GA. One of the hypotheses is that, as previously mentioned, the use of different linking arms can affect the conformation of a molecule after immobilization, thus, conformation studies were performed using ToF-SIMS static mode. In Figure 33 a comparison of both GA-P23 and PEG-P23 on the fragments from the peptide are present. It can be observed that by any linking arm there is a similar trend on both surfaces, nevertheless it is on alanine and proline fragments where there is a difference. This suggests that there can be a small change on the conformation of the small peptide which could decrease the biological activity of the grafted surface. One of the hypotheses is that both linking arms graft the P23 peptide by its terminal amine group located in the asparagine amino acid (N), and for GA due to a steric impediment one of the alanine present on the peptide is close to the surface, thus less intense than on PEG where all the peptide presents a high degree of freedom to fold. Moreover, the anti-

fouling properties of PEG can also create a synergic effect which could promote the biological performance of the molecule grafted by this linking arm than with GA. Further studies regarding the conformation need to be performed.

6.4 In vitro and in vivo performance of the functionalized surfaces with a short chain peptide derived from CD31: P8RI.

Thanks to the collaboration between the Laboratory of Biomaterials and Bioengineering of Laval University in Quebec City, and the Laboratory for Vascular Translational Science of INSERM in Paris, in vivo testing of stents functionalized by strategy developed within this Thesis framework was carried out. Before performing in vivo testing, the selection of the peptide with the best biological performance, regarding endothelial cell adhesion, viability and phenotype, assessed by in vitro tests on flat samples was performed. These peptides were grafted using the strategy developed in this research project: Electropolishing as surface pre-treatment, followed by direct plasma amination with PEG as linking arm. This part of the project focused on the confirmation of one of the main hypotheses of the project: Plasma functionalization can create reactive amine groups directly onto metallic surfaces that can be used to graft biomolecules to improve the biological performance of bare metal stents. After the optimization and selection of the bioactive peptide on flat samples, the functionalization of commercial cardiovascular stents was performed. The *in vivo* performance, in terms of re-endothelialization and in-stent restenosis, of these functionalized stents was compared to commercial stents both BMS and DES.

6.4.1 In vitro performance: Selection of the peptide for in vivo test

Initially, three peptides were pre-selected to study for this part of the project. All the peptides were derived from the same protein, CD31: P23, which has been discussed in previous sections of this work, P8FI and P8RI. These two last peptides were a smaller chain composed of only 8 amino acids, with one being a retroversion of the other (F= forward, R= retro). The main analysis performed was the study of the phenotype of endothelial cells after their contact with the flat samples, to observe if a potential secondary reaction could occur whilst in vivo. As shown in Annex 4, this study demonstrated that by grafting any of the peptides derived from CD31 significant decreased both inflammation markers, IL-6 and VCAM-1, when compared to the electropolished surface, thus, suggesting an increase on the anti-inflammatory activity of the surface. Furthermore, it was P8RI that demonstrated a significant difference with the other peptides, thus the selected for a deeper in vitro testing. These studies were focused mainly on the stability of grafted peptide and its biological performance.

- **In vitro stability evaluation:** Chemical composition of the functionalized surface was assessed by XPS survey analyses. Regarding nitrogen a significant decrease on this element was found out after grafting PEG as linking arm when compared to the aminated sample, from 11.0 ± 0.1% to 2.9 ± 0.3%. Nevertheless, the percentage of nitrogen increased from 2.9 ± 0.3% to 4.5 ± 0.7% after the grafting of

the peptide. Furthermore, static immersion tests in PBS at 37 °C were performed to study the stability of the functionalized surface. It was found that after 4 weeks of immersion less than 10% loss on the percentage of nitrogen when compared to the control, from 4.5 ± 0.7% to 4.1 ± 0.6%. Which could be related a loss on peptide that was adsorbed and not immobilized covalently onto the metallic surface.

- **In vitro biological performance:** Human coronary artery endothelial cells were incubated for 48 h onto EP, PEG and PEG-P8RI surfaces, then the supernatant was used to study the phenotype of the cells and the cells attached to the surfaces were stained to study their distribution. As observed in Figure *36*, endothelial cells were significantly more present on PEG-P8RI and PEG compared to the EP surface, with a mean of nuclei 292 ± 29 and 219 ± 17 to 133 ± 35, respectively. Moreover, besides the significant difference on the quantity of cells present on the surface after the direct immobilization of the peptide onto the surface when compared to only PEG, the study of endothelial cells after immunofluorescence staining demonstrated a higher intensity on the actin filaments on the PEG-P8RI surface. This was caused due to a stronger attachment of the cells to the surface due to the presence of the immobilized peptide. Followed by these analyses the study of the phenotype of endothelial cells demonstrated a significant decrease on the concentration of molecules related to an inflammatory response, VCAM-1 and IL-6, and an increase on molecules with anti-thrombotic activity, TFPI, on the PEG-P8RI surface when compared to the other surfaces.

After these studies it was found out that the combination of this multi-step plasma-based strategy for the direct grafting of P8RI onto the EP surface improved the biological performance. As a general trend, it was observed that the grafting of the peptide increased the anti-inflammatory and anti-thrombotic activity of the alloy. Moreover, the presence of P8RI also increased the endothelial cell viability and the interaction between them and the surface. The information obtained from of these in vitro studies supported the selection of P8RI as the bioactive molecule to be immobilized onto cardiovascular stents. Based on the in vitro performance, the presence of this molecule could lead to a potential decrease on complication in vivo, when compared to BMS.

6.4.2 In vivo performance of Plasma-P8RI stents

The implantation of functionalized stents was performed in the coronary arteries of female pigs, as described in 5.4. The implantation period were 7 days to study the reendothelialization of the devices and 28 days for in-stent restenosis. Well stablished characterization methodologies were used for the study of the explanted arteries. SEM and histology stained with trichrome were selected for the study of re-endothelialization, and angiography combined with immunohistochemical staining for in-stent restenosis. For the sake of simplicity, from now own the functionalized stents by the developed strategy with this peptide are labeled as Plasma-P8RI.

- **In vivo re-endothelialization:** After 7 days of in vivo implantation, using SEM imaging demonstrated the formation of a complete monolayer of endothelial cells onto the Plasma-P8RI stent, similar to what was observed on the BMS. Nevertheless, Plasma-P8RI exhibited a surface with less platelets adhered and without activation, which represented a promising surface with a higher hemocompatibility when compared to BMS that presented a surface full of platelets activated with an early dendritic phenotype. Regarding DES, in term of endothelium it was found that no monolayer was formed after 7 days of implantation, which was expected due to the release of anti-proliferative drugs. Furthermore, on DES a higher quantity of platelets were adhered, but not activated, when compared to Plasma-P8RI but less when compared to BMS. Similar trend was observed by histology, where it was observed that on both BMS and Plasma-P8RI the endothelium had recovered after the deployment of the device, whereas on the case of DES the damage was noticeable (Figure *38*). Furthermore, the observations on Plasma-P8RI were similar to what was obtained in in vitro studies for the soluble molecules after their contact with endothelial cells. It was found that the presence of the P8RI grafted by PEG would decrease the inflammation response and the thrombus formation (Figure *37*).

- **In-stent restenosis:** Initial studies of in vivo in-stent restenosis was performed using angiographies obtained before the extraction of the devices. It was observed, as seen in Figure *40*, that both Plasma-P8RI and DES exhibited a significant less percent of restenosis when compared to BMS, even though no significant different between them. Furthermore, once the arteries were extracted and stained with Sirius red, to it was found out that BMS significantly reduced the lumen of the artery when compared to the other two stents. Followed by BMS it was Plasma-P8RI that exhibited some reduction of the lumen and finally DES. Nevertheless, further information is needed to compare the proliferation of smooth muscle cells and to observe the inflammation after the stent implantation.

After the in vivo studies regarding in-stent re-stenosis and re-endothelialization, it can be observed that functionalizing the metallic surfaces with the P8RI peptide by this plasma-based strategy improves the performance of bare metal stents. Nevertheless, studies at longer times, with a higher number of samples, need to be performed in order to obtain more statistical information that could lead to a potential human clinical trial.

6.5 Limitations and perspectives of this work

6.5.1 Limitations on the developed platform: The challenge of characterizing cardiovascular devices

The main limitations for this research project rely on the characterization of the surface on complex structures, specifically on stents. As previously discussed in section 6.2.3, fluorescent microscopy and ToF-SIMS were initially proposed to characterize the functionalized stents. However, due to the nature of the functional surfaces

obtained by the developed platform, only the latest technique was used since it allows the study of the first layer of atoms of a surface. Nonetheless, several aspects must be taken into consideration regarding the limitations of this characterization technique:

- **Geometrical limitation:** ToF-SIMS was used to study the surface of the functionalized stent, as shown in Figure *34*. However, even if the technique allowed the observation of the relative intensities of fragments in positive and negative modes, it is only possible to characterize the external part of the stent. However, for this application both internal and external sides of the device are important since both are exposed to biological medium once deployed in the artery.

- **Qualitative analysis limitation:** As a consequence of the geometrical limitation, the quantitative analysis of fragments on the internal, external and the strut side is another challenge to overcome. In order to use this technique for quantitative analyses, normalizations must be performed to either the total counts of the immobilized molecule or to the total counts of all the fragments. However, even if images taken can be of a specific area, for example 200 µm x 200 µm, in the case of a stent it does not necessarily represents the same area taken for two different images due to the angle of the image acquisition and to the stent structure. Thus, at this early stage on the characterization of the functionalized surfaces by this novel multi-step strategy, ToF-SIMS remains a powerful qualitative characterization technique.

Due to the current impossibility to quantify how much peptide is immobilized on the stent, the development of stability tests suitable for these devices represents another challenge to overcome. The use of techniques that allow the study the density of the peptide grafted onto the surface, such as a micro-imager using radiolabeled peptides with ^{3}H-Lys [191]. The pertinence to overcome this limitation arrives when aiming to produce this biomimetic device in the industry, where different quality controls must be guaranteed.

6.5.2 Perspectives

The main perspectives of this research project can be divided in two: those related with the developed platform for the direct immobilization of molecules and those related with the cardiovascular application:

- Perspectives related to the ***developed platform***:

    - *Feasibility to directly functionalize with reactive amine groups other alloys*, such as SS316L, titanium alloys and nitinol for example. Opening the door for other applications such as orthopedics and dentals implants.

- Further optimization and understanding of the direct plasma amination, is it possible to *increase the density of reactive amine groups* on the surface of L605? What is the mechanism behind the direct plasma amination on L605 alloy?

➢ Perspectives of the ***cardiovascular application***:

- *Stability under dynamic tests combined with endothelial cell culture* to observe if the bioactivity of the peptide is conserved after the stability test.

- *What happens with smooth muscle cells?* Migration essays on co-cultured cellular models with ECs and SMCs to observe if there is a higher specificity on the response of endothelial cells.

- Further in vivo tests, at longer times for *studying late in-stent restenosis* and *increased number of samples*.

- Study on the *shelf life* of the functionalized surfaces and metallic stents by this multi-step plasma-based strategy.

- Study of the *peptide density* present on the surface of the cardiovascular device.

- Exploring other strategies to graft the peptide onto the functionalized surface. Is "click chemistry" a suitable approach for the industry?

- Further study of spacers/linking arms. Would a peptide *grafted by a natural linking arm* perform better than when it is grafted by a synthetic linking arm (PEG)?

Conclusion

A multi-step plasma-based strategy that allowed the direct immobilization of bioactive molecules onto L605 alloy was developed. This strategy consisted of three blocks: a) surface optimization, b) direct plasma amination and c) molecule grafting. Among the different surface treatments, studied in the surface optimization block, electropolishing was selected as the most suitable surface pre-treatment for the developed strategy. Furthermore, the direct plasma functionalization, using a two-step procedure with nitrogen and hydrogen treatments in a microwave reactor, allowed to achieve ~1.5% of reactive amine groups on a metallic surface, without the use of any polymeric intermediate, for the first time reported in literature. These amine groups were used as anchor points for the immobilization of two linking arms, glutaric anhydride and PEG, with different peptides with properties desired for cardiovascular applications. Overall, regarding stability properties and biological activity, peptides grafted by PEG shown a better performance than those grafted by GA. Peptides grafted using PEG as linking arm showed faster re-endothelialization, and an endothelial cell phenotype that predicted a potential decrease on complications in vivo due to its anti-inflammatory and anti-thrombotic activity. Moreover, in vivo tests were performed in porcine model for 7 days to study the re-endothelialization and for 28 days to study in-stent restenosis. These tests demonstrated that the cardiovascular stents functionalized using the strategy developed in this project, Plasma-P8RI, had a faster re-endothelialization compared to commercial drug eluting stents and without the adhesion and activation platelets compared to bare metal stents. Furthermore, a better in-stent restenosis when compared at day 28 when compared to bare metal stents. Besides the promising results of the developed surfaces using the multi-step plasma-based strategy to directly immobilize bioactive molecules on metallic surfaces, the relevance of combining multiple characterization techniques that allow the comprehension between the physicochemical properties of the surfaces and the biological activity was assessed. Moreover, the importance of in vitro tests as a prediction for in vivo performance was proved.

Furthermore, the development and application of this multi-step plasma-based strategy directly on cardiovascular devices for the immobilization of bioactive peptides derived from CD31 allowed the fabrication of a “biomimetic” stent. Contrary to the mechanism of action of drug eluting stents, which by eluting anti-proliferative drugs to delay the complications post-implantation end up damaging the endothelium, this “biomimetic” stent aimed for a more “peaceful” mechanism of action: to promote the adhesion, proliferation and migration of endothelial cells to hide the metallic stent from the biological medium as fast as possible. This strategy, that can be considered as a “Trojan horse” strategy, might represent a new alternative to avoid the use of DES with their antiplatelet therapy for patients whose medical condition can be compromised (diabetic patients for example). Thus, it has the potential to be used as a “personalized therapy”. Nonetheless, an exhaustive study regarding

the functionalization process reproducibility, scalability and cost is mandatory and crucial for this highly competitive industry.

Finally, the answer of the 4 questions that this research project, based on the previously discussed results throughout this thesis are:

- ✓ **Feasibility:** MW plasma treatments allow the functionalization with reactive amine groups directly onto the surface of L605, without the use of any polymeric coating.
- ✓ **Surface optimization:** Electropolishing, among the proposed surface modifications is the most suitable surface pre-treatment for stent application.
- ✓ **Grafting optimization:** PEG demonstrated to be the most suitable linking arm to be used as spacer with the P23 peptide and P8RI.
- ✓ **Biological performance:** The use of peptides derived from CD31 significantly increases the endothelialization rate and the anti-thrombotic activity of the surface in vitro and in vivo, compared to metallic surfaces.

Annexes

1 Characterization of stents by fluorescent microscopy

One of the first efforts to characterize the direct functionalization of bioactive molecules directly grafted onto bare metal stents involved the grafting of a fluorescent peptide followed by the analysis of the surface by fluorescent microscopy. Figure X presents the images obtained after the characterization of these devices of a) a peptide with a TAMRA fluorophore and b) a peptide with a FTIC fluorophore on the surface. Both peptides were grafted using previously discussed immobilization protocols with PEG as linking arm.

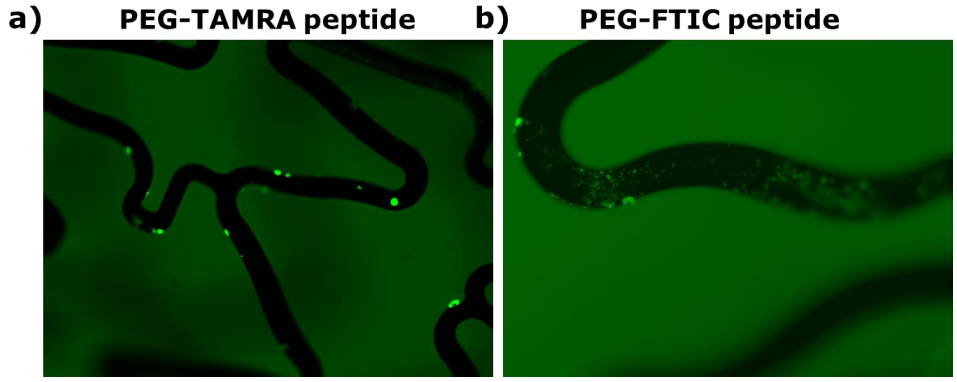

Figure 44 Cardiovascular devices functionalized with a fluorescent peptide: a) TAMRA fluorophore and b) FTIC fluorophore.

2 Static immersion tests of the grafted P23

Preliminary studies regarding the stability of the grafting of P23 was assessed by static immersion test using PBS at 37 °C for one week. No significant difference was found after the ageing test.

Table 19 Surface chemical composition of the L605 functionalized with the peptide before and after one week of static immersion test in PBS at 37 °C. n=9

L605	%C	%O	%N	%Cr	%Co
GA-P23	39.5 ± 1.2	39.3 ± 0.5	8.3 ± 0.1	7.0 ± 0.4	1.3 ± 0.1
GA-P23 1 week	48.5 ± 1.3	36.3 ± 1.1	7.9 ± 1.0	5.3 ± 1.0	0.9 ± 0.2
PEG-P23	36.4 ± 2.1	42.6 ± 0.7	6.1 ± 0.7	8.3 ± 1.2	1.9 ± 0.5
PEG-P23 1 week	36.8 ± 3.4	49.9 ± 2.9	5.2 ± 1.2	8.1 ± 1.1	2.1 ± 0.7

3 Comparison of linking arms for the immobilization of P23 based on HCAEC phenotype

Table 20 Comparison of inflammation markers of HCAEC after 48 h of incubation with the functionalized surfaces. It can be observed that only by grafting the peptide with PEG significantly decreases the presence of both VCAM-1 and IL-6. Thus, a potential inflammatory response after implantation, when compared to EP.

Surface	VCAM-1	IL-6
EP	617.5 ± 127.1	819.1 ± 112.7
GA-P23	655.6 ± 68.1	670.6 ± 101.1
PEG-P23	558.8 ± 12.4	675.5 ± 59.1

4 Comparison of CD31 peptides grafted by PEG based on HCAEC phenotype.

Table 21 Comparison of inflammation markers of HCAEC after 48 h of incubation with the surfaces. It can be observed that for VCAM-1 only PEG-P8RI is significantly different to EP, whilst on IL-6 both P8RI and P8FI are significantly different to EP.

Surface	VCAM-1	IL-6
EP	617.5 ± 127.1	819.1 ± 112.7
PEG-P23	558.8 ± 12.4	675.5 ± 59.1
PEG-P8RI	482.4 ± 20.7	555.8 ± 53.8
PEG-P8FI	558.8 ± 37.2	548.1 ± 56.9

5 Comparison of Peptide-I grafted by GA and PEG

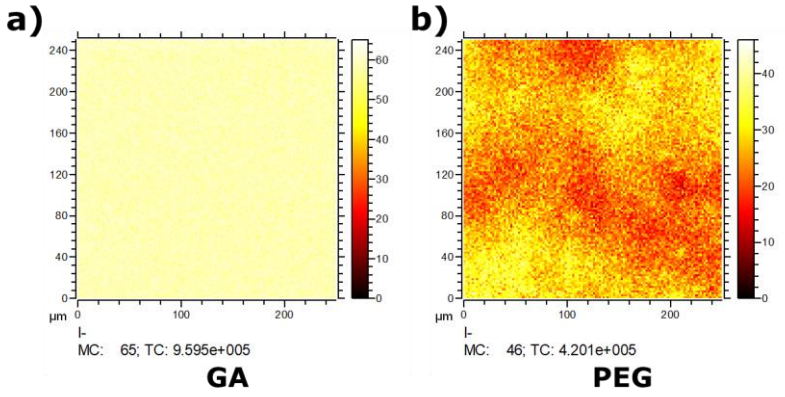

Figure 45 ToF-SIMS images 250 µm x 250 µm of fragment I^-, m/z 126.904. a) GA with the iodine peptide, and b) PEG with the iodine peptide. It can be observed that the distribution for both peptides changes depending on the linking arm used for the grafting of the peptide.

Bibliography

[1] Day, W. H. World Health Day 2013. *A Glob. Br. Hypertens.* **2013**, 9.

[2] Heron, M.; Hoyert, D. L.; Murphy, S. L.; Xu, J.; Kochanek, K. D.; Tejada-Vera, B. National Vital Statistics Reports. *Natl. Vital Stat. Reports* **2009**, *57* (14).

[3] Kavey, R. E. W.; Daniels, S. R.; Lauer, R. M.; Atkins, D. L.; Hayman, L. L.; Taubert, K. American Heart Association Guidelines for Primary Prevention of Atherosclerotic Cardiovascular Disease Beginning in Childhood. *Circulation* **2003**, *107* (11), 1562–1566.

[4] Lloyd-Jones, D. M.; Larson, M. G.; Beiser, A.; Levy, D. Lifetime Risk of Developing Coronary Heart Disease. *Lancet* **1999**, *353* (9147), 89–92.

[5] Adams, M. R.; Kinlay, S.; Blake, G. J.; Orford, J. L.; Ganz, P.; Selwyn, a P. Pathophysiology of Atherosclerosis: Development, Regression, Restenosis. *Curr. Atheroscler. Rep.* **2000**, *2* (3), 251–258.

[6] Atherosclerosis | Stroke and Heart Attack | High Blood Pressure - Heart Research Institute https://www.hri.org.au/about-heart-disease/what-is-atherosclerosis (accessed Nov 17, 2018).

[7] Granada, J. F.; Kaluza, G. L.; Raizner, A. Drug-Eluting Stents for Cardiovascular Disorders. *Curr. Atheroscler. Rep.* **2003**, *5* (4), 308–316.

[8] What You Need To Know About A Heart Stent - Central Georgia Heart Center https://centralgaheart.com/need-know-heart-stent/ (accessed Nov 17, 2018).

[9] Arrigan, D. W. M.; Caplice, N.; Benvenuto, P.; Nazneen, F.; Galvin, P.; Thompson, M. Surface Chemical and Physical Modification in Stent Technology for the Treatment of Coronary Artery Disease. *J. Biomed. Mater. Res. B Appl. Biomater.* **2012**, *100B* (7), 2006–2013.

[10] Roach, P.; Eglin, Æ. D.; Rohde, Æ. K.; Perry, C. C. Modern Biomaterials : A Review — Bulk Properties and Implications of Surface Modifications. **2007**, 1263–1277.

[11] Kipshidze, N.; Dangas, G.; Tsapenko, M.; Moses, J.; Leon, M. B.; Kutryk, M.; Serruys, P. Role of the Endothelium in Modulating Neointimal Formation: Vasculoprotective Approaches to Attenuate Restenosis after Percutaneous Coronary Interventions. *J. Am. Coll. Cardiol.* **2004**, *44* (4), 733–739.

[12] Yin, R. X.; Yang, D. Z.; Wu, J. Z. Nanoparticle Drug- and Gene-Eluting Stents for the Prevention and Treatment of Coronary Restenosis. *Theranostics* **2014**, *4* (2), 175–200.

[13] Mani, G.; Feldman, M. D.; Patel, D.; Agrawal, C. M. Coronary Stents: A Materials Perspective. *Biomaterials* **2007**, *28* (9), 1689–1710.

[14] Mani, G.; Feldman, M. D.; Patel, D.; Agrawal, C. M. Coronary Stents: A Materials Perspective. *Biomaterials* **2007**, *28* (9), 1689–1710.

[15] Riepe, G.; Heintz, C.; Kaiser, E.; Chakf, N.; Morlock, M.; Delling, M.; Imig, H. What Can We Learn from Explanted Endovascular Devices? *Eur. J. Vasc. Endovasc. Surg.* **2002**, *24* (2), 117–122.

[16] Pache, J.; Kastrati, A.; Mehilli, J.; Schühlen, H.; Dotzer, F.; Hausleiter, J.; Fleckenstein, M.; Neuman, F. J.; Sattelberger, U.; Schmitt, C.; et al. Intracoronary Stenting and Angiographic Results: Strut Thickness Effect on Restenosis Outcome (ISAR-STEREO-2) Trial. *J. Am. Coll. Cardiol.* **2003**, *41* (8), 1283–1288.

[17] Schiavone, A.; Zhao, L. G. Effects of Material , Coating , Design and Plaque Composition on Stent Deployment inside a Stenotic Artery — Finite Element Simulation. *Mater. Sci. Eng. C* **2014**, *42*, 479–488.

[18] Foin, N.; Lee, R. D.; Torii, R.; Guitierrez-Chico, J. L.; Mattesini, A.; Nijjer, S.; Sen, S.; Petraco, R.; Davies, J. E.; Di Mario, C.; et al. Impact of Stent Strut Design in Metallic Stents and Biodegradable Scaffolds. *Int. J. Cardiol.* **2014**, *177* (3), 800–808.

[19] Levine, G. N.; Bates, E. R.; Bittl, J. A.; Brindis, R. G.; Fihn, S. D.; Fleisher, L. A.; Granger, C. B.; Lange, R. A.; Mack, M. J.; Mauri, L.; et al. 2016 ACC/AHA Guideline Focused Update on Duration of Dual Antiplatelet Therapy in Patients With Coronary Artery Disease. *J. Am. Coll. Cardiol.* **2016**, *68* (10), 1082–1115.

[20] Road, M. METAL CARCINOGENESIS: MECHANISTIC IMPLICATIONS. *Pharmac. Ther.* **1992**, *53*, 31–65.

[21] Sydow-Plum, G.; Tabrizian, M. Review of Stent Coating Strategies: Clinical Insights. *Mater. Sci. Technol.* **2008**, *24* (9), 1127–1143.

[22] Rosales-leal, J. I.; Rodríguez-valverde, M. A.; Mazzaglia, G.; Ramón-torregrosa, P. J. Colloids and Surfaces A : Physicochemical and Engineering Aspects Effect of Roughness , Wettability and Morphology of Engineered Titanium Surfaces on Osteoblast-like Cell Adhesion. **2010**, *365*, 222–229.
[23] Milleret, V.; Buzzi, S.; Gehrig, P.; Ziogas, A.; Grossmann, J.; Schilcher, K.; Zinkernagel, A. S.; Zucker, A.; Ehrbar, M. Acta Biomaterialia Protein Adsorption Steers Blood Contact Activation on Engineered Cobalt Chromium Alloy Oxide Layers. *Acta Biomater.* **2015**, *24*, 343–351.
[24] John, A. A.; Subramanian, A. P.; Vellayappan, M. V.; Balaji, A.; Jaganathan, S. K.; Mohandas, H.; Paramalinggam, T.; Supriyanto, E.; Yusof, M. Review: Physico-Chemical Modification as a Versatile Strategy for the Biocompatibility Enhancement of Biomaterials. *RSC Adv.* **2015**, *5* (49), 39232–39244.
[25] Ratner, B. D.; Bryant, S. J. Biomaterials: Where We Have Been and Where We Are Going. *Annu. Rev. Biomed. Eng.* **2004**, *6* (1), 41–75.
[26] Montaño-Machado, V.; Sikora-Jasinska, M.; Bortolan, C. C.; Chevallier, P.; Mantovani, D. Medical Devices: Coronary Stents. In *Reference Module in Biomedical Sciences*; Elsevier, 2017; pp 386–398.
[27] Love, M. P.; Chb, M. B.; Schampaert, E.; Cohen, E. A.; Webb, J. G.; Anderson, T. J.; Labinaz, M.; Tanguay, J.; Džavík, V. The Canadian Association of Interventional Cardiology and the Canadian Cardiovascular Society Joint Statement on Drug-Eluting Stents. **2007**, *23* (2), 121–123.
[28] Kim, J. M.; Bae, I.-H.; Lim, K. S.; Park, J.-K.; Park, D. S.; Lee, S.-Y.; Jang, E.-J.; Ji, M. S.; Sim, D. S.; Hong, Y. J.; et al. A Method for Coating Fucoidan onto Bare Metal Stent and in Vivo Evaluation. *Prog. Org. Coatings* **2015**, *78*, 348–356.
[29] Cheruthazhekatt, S.; Černák, M.; Slavíček, P.; Havel, J. Gas Plasmas and Plasma Modified Materials in Medicine. *J. Appl. Biomed.* **2010**, *8* (2), 55–66.
[30] Chu, P. K.; Chen, J. Y.; Wang, L. P.; Huang, N. Plasma-Surface Modification of Biomaterials. **2002**, *36*, 143–206.
[31] Bogaerts, A.; Neyts, E.; Gijbels, R.; Mullen, J. Van Der. Gas Discharge Plasmas and Their Applications. **2002**, *57*, 609–658.
[32] Perucca, M. *Introduction to Plasma and Plasma Technology*; 2010.
[33] Schr, K.; Finke, B.; Ohl, A. Current Trends in Biomaterial Surface Functionalization — Nitrogen-Containing Plasma Assisted Processes with Enhanced Selectivity. *Vacuum* **2003**, *71*, 391–406.
[34] Siow, K. S.; Britcher, L.; Kumar, S.; Griesser, H. J. Plasma Methods for the Generation of Chemically Reactive Surfaces for Biomolecule Immobilization and Cell Colonization - A Review. **2006**, 392–418.
[35] Almeida, E. Surface Treatments and Coatings for Metals. A General Overview. 1. Surface Treatments, Surface Preparation, and the Nature of Coatings. *Ind. Eng. Chem. Res.* **2001**, *40* (1), 3–14.
[36] Santos, M.; Wise, S. G.; Santos, M.; Bilek, M. M. M.; Wise, S. G. Plasma-Synthesised Carbon-Based Coatings For Cardiovascular Applications. *Biosurface Biotribology I* **2015**, 146–160.
[37] Inagaki, N. *Plasma Surface Modification and Plasma Polymerization*; Technomic Pub. Co, 1996.
[38] Mangindaan, D.; Kuo, W. H.; Chang, C. C.; Wang, S. L.; Liu, H. C.; Wang, M. J. Plasma Polymerization of Amine-Containing Thin Films and the Studies on the Deposition Kinetics. *Surf. Coatings Technol.* **2011**, *206* (6), 1299–1306.
[39] Manakhov, A.; Kedroňová, E.; Medalová, J.; Černochová, P.; Obrusník, A.; Michlíček, M.; Shtansky, D. V.; Zajíčková, L. Carboxyl-Anhydride and Amine Plasma Coating of PCL Nanofibers to Improve Their Bioactivity. *Mater. Des.* **2017**, *132*, 257–265.
[40] MUCHA, J. A.; HESS, D. W. Plasma Etching; 1983; pp 215–285.
[41] Conrads, H.; Schmidt, M. Plasma Generation and Plasma Sources. *Plasma Sources Sci. Technol.* **2000**, *9* (4), 441–454.
[42] Dorri, M.; Turgeon, S.; Brodusch, N.; Cloutier, M.; Chevallier, P.; Gauvin, R.; Mantovani, D. Characterization of Amorphous Oxide Nano-Thick Layers on 316L Stainless Steel by Electron Channeling Contrast Imaging and Electron Backscatter Diffraction. *Microsc. Microanal.* **2016**, *22* (05), 997–1006.
[43] Kasemo, B. Biological Surface Science. *Curr. Opin. Solid State Mater. Sci.* **1998**, *3* (5), 451–459.
[44] Keselowsky, B. G.; Collard, D. M.; Garcia, A. J. Integrin Binding Specificity Regulates Biomaterial Surface Chemistry Effects on Cell Differentiation. *Proc. Natl. Acad. Sci.* **2005**, *102* (17), 5953–5957.
[45] Kasemo, B.; Gold, J. Implant Surfaces and Interface Processes. *Adv. Dent. Res.* **1999**, *13* (1), 8–20.

[46] Griesser, H. J.; Chatelier, R. C.; Gengenbach, T. R.; Johnson, G.; Steele, J. G. Growth of Human Cells on Plasma Polymers: Putative Role of Amine and Amide Groups. *J. Biomater. Sci. Polym. Ed.* **1994**, *5* (6), 531–554.
[47] Friedrich, J.; Kühn, G.; Mix, R.; Hoffmann, K.; Resch-Genger, U. Tailoring of Polymer Surfaces with Monotype Functional Groups of Variable Density Using Chemical and Plasma Chemical Processes. In *Characterization of Polymer Surfaces and Thin Films*; Springer-Verlag: Berlin/Heidelberg; pp 62–71.
[48] Inagaki, N.; Tasaka, S.; Hibi, K. Surface Modification of Kapton Film by Plasma Treatments. *J. Polym. Sci. Part A Polym. Chem.* **1992**, *30* (7), 1425–1431.
[49] Cueff, R.; Baud, G.; Benmalek, M.; Besse, J. .; Butruille, J. .; Jacquet, M. X-Ray Photoelectron Spectroscopy Studies of Plasma-Modified PET Surface and Alumina/PET Interface. *Appl. Surf. Sci.* **1997**, *115* (3), 292–298.
[50] Vesel, A.; Mozetic, M.; Jaganjac, M.; Milkovic, L.; Cipak, A.; Zarkovic, N. Biocompatibility of Oxygen-Plasma-Treated Polystyrene Substrates. *Eur. Phys. J. Appl. Phys.* **2011**, *56* (2), 24024.
[51] Gancarz, I.; Bryjak, J.; Poźniak, G.; Tylus, W. Plasma Modified Polymers as a Support for Enzyme Immobilization II. Amines Plasma. *European Polymer Journal*. 2003, pp 2217–2224.
[52] Meyer-Plath, A. A.; Schröder, K.; Finke, B.; Ohl, A. Current Trends in Biomaterial Surface Functionalization—nitrogen-Containing Plasma Assisted Processes with Enhanced Selectivity. *Vacuum* **2003**, *71* (3), 391–406.
[53] Steele, J. G.; Johnson, G.; McFarland, C.; Dalton, B. A.; Gengenbach, T. R.; Chatelier, R. C.; Underwood, P. A.; Griesser, H. J. Roles of Serum Vitronectin and Fibronectin in Initial Attachment of Human Vein Endothelial Cells and Dermal Fibroblasts on Oxygen- and Nitrogen-Containing Surfaces Made by Radiofrequency Plasmas. *J. Biomater. Sci. Polym. Ed.* **1995**, *6* (6), 511–532.
[54] Ertel, S. I.; Ratner, B. D.; Horbett, T. A. Radiofrequency Plasma Deposition of Oxygen-Containing Films on Polystyrene and Poly(Ethylene Terephthalate) Substrates Improves Endothelial Cell Growth. *J. Biomed. Mater. Res.* **1990**, *24* (12), 1637–1659.
[55] Swaraj, S.; Oran, U.; Lippitz, A.; Friedrich, J. F.; Unger, W. E. S. Study of Influence of External Plasma Parameters on Plasma Polymerised Films Prepared from Organic Molecules (Acrylic Acid, Allyl Alcohol, Allyl Amine) Using XPS and NEXAFS. *Surf. Coatings Technol.* **2005**, *200* (1–4), 494–497.
[56] Favia, P.; Palumbo, F.; d'Agostino, R.; Lamponi, S.; Magnani, A.; Barbucci, R. Immobilization of Heparin and Highly-Sulphated Hyaluronic Acid onto Plasma-Treated Polyethylene. *Plasmas Polym.* **1998**, *3* (2), 77–96.
[57] Ko, T.-M.; Cooper, S. L. Surface Properties and Platelet Adhesion Characteristics of Acrylic Acid and Allylamine Plasma-Treated Polyethylene. *J. Appl. Polym. Sci.* **1993**, *47* (9), 1601–1619.
[58] O'Toole, L.; Beck, A. J.; Short, R. D. Characterization of Plasma Polymers of Acrylic Acid and Propanoic Acid. *Macromolecules* **1996**, *29* (15), 5172–5177.
[59] Gancarz, I.; Bryjak, J.; Bryjak, M.; Poźniak, G.; Tylus, W. Plasma Modified Polymers as a Support for Enzyme Immobilization 1. *Eur. Polym. J.* **2003**, *39* (8), 1615–1622.
[60] Gengenbach, T. R.; Vasic, Z. R.; Li, S.; Chatelier, R. C.; Griesser, H. J. Contributions of Restructuring and Oxidation to the Aging of the Surface of Plasma Polymers Containing Heteroatoms. *Plasmas Polym.* **1997**, *2* (2), 91–114.
[61] Zhang, Z.; Knoll, W.; Förch, R. Amino-Functionalized Plasma Polymer Films for DNA Immobilization and Hybridization. *Surf. Coatings Technol.* **2005**, *200* (1–4), 993–995.
[62] Zhang, Z.; Chen, Q.; Knoll, W.; Foerch, R.; Holcomb, R.; Roitman, D. Plasma Polymer Film Structure and DNA Probe Immobilization. *Macromolecules* **2003**, *36* (20), 7689–7694.
[63] Steffen, H. J.; Schmidt, J.; Gonzalez-Elipe, A. Biocompatible Surfaces by Immobilization of Heparin on Diamond-like Carbon Films Deposited on Various Substrates. *Surf. Interface Anal.* **2000**, *29* (6), 386–391.
[64] Mason, M.; Vercruysse, K. P.; Kirker, K. R.; Frisch, R.; Marecak, D. M.; Prestwich, G. D.; Pitt, W. G. Attachment of Hyaluronic Acid to Polypropylene, Polystyrene, and Polytetrafluoroethylene. *Biomaterials* **2000**, *21* (1), 31–36.
[65] Siow, K. S.; Britcher, L.; Kumar, S.; Griesser, H. J. Plasma Methods for the Generation of Chemically Reactive Surfaces for Biomolecule Immobilization and Cell Colonization - A Review. **2006**, 392–418.
[66] Hayat, U.; Tinsley, A. M.; Calder, M. R.; Clarke, D. J. ESCA Investigation of Low-Temperature Ammonia Plasma-Treated Polyethylene Substrate for Immobilization of Protein. *Biomaterials* **1992**, *13* (11), 801–806.

[67] Ben Rejeb, S.; Tatoulian, M.; Arefi Khonsari, F.; Fischer Durand, N.; Martel, A.; Lawrence, J. F.; Amouroux, J.; Le Goffic, F. Functionalization of Nitrocellulose Membranes Using Ammonia Plasma for the Covalent Attachment of Antibodies for Use in Membrane-Based Immunoassays. *Anal. Chim. Acta* **1998**, *376* (1), 133–138.
[68] Puleo, D. A.; Kissling, R. A.; Sheu, M. S. A Technique to Immobilize Bioactive Proteins, Including Bone Morphogenetic Protein-4 (BMP-4), on Titanium Alloy. *Biomaterials* **2002**, *23* (9), 2079–2087.
[69] Michel, E. C.; Montaño-Machado, V.; Chevallier, P.; Labbé-Barrère, A.; Letourneur, D.; Mantovani, D. Dextran Grafting on PTFE Surface for Cardiovascular Applications. *Biomatter* **2014**, *4* (1), F28805.
[70] Carbodiimide Crosslinker Chemistry - CA. https://www.thermofisher.com/ca/en/home/life-science/protein-biology/protein-biology-learning-center/protein-biology-resource-library/pierce-protein-methods/carbodiimide-crosslinker-chemistry.html
[71] Holmes, C.; Tabrizian, M. Surface Functionalization of Biomaterials. In *Stem Cell Biology and Tissue Engineering in Dental Sciences*; Elsevier, 2015; pp 187–206.
[72] Roach, P.; Eglin, Æ. D.; Rohde, Æ. K.; Perry, C. C. Modern Biomaterials: A Review — Bulk Properties and Implications of Surface Modifications. **2007**, 1263–1277.
[73] Vaz, J. M.; Taketa, T. B.; Hernandez-Montelongo, J.; Chevallier, P.; Cotta, M. A.; Mantovani, D.; Beppu, M. M. Antibacterial Properties of Chitosan-Based Coatings Are Affected by Spacer-Length and Molecular Weight. *Appl. Surf. Sci.* **2018**, *445*, 478–487.
[74] Campelo, C. S.; Chevallier, P.; Vaz, J. M.; Vieira, R. S.; Mantovani, D. Sulfonated Chitosan and Dopamine Based Coatings for Metallic Implants in Contact with Blood. *Mater. Sci. Eng. C* **2017**, *72*, 682–691.
[75] Hu, Y.; Winn, S. R.; Krajbich, I.; Hollinger, J. O. Porous Polymer Scaffolds Surface-Modified with Arginine-Glycine-Aspartic Acid Enhance Bone Cell Attachment and Differentiation in Vitro. *J. Biomed. Mater. Res.* **2003**, *64A* (3), 583–590.
[76] Montaño-Machado, V.; Hugoni, L.; Díaz-rodríguez, S.; Tolouei, R.; Pauthe, E.; Mantovani, D. A Comparison of Adsorbed and Grafted Fibronectin Coatings under Static and Dynamic Conditions. *Phys. Chem. Chem. Phys.* **2016**, *18* (35), 1–29.
[77] Vallières, K.; Petitclerc, É.; Laroche, G. Covalent Grafting of Fibronectin onto Plasma-Treated PTFE: Influence of the Conjugation Strategy on Fibronectin Biological Activity. *Macromol. Biosci.* **2007**, *7* (5), 738–745.
[78] Lutz, J.; Díaz, C.; García, J. A.; Blawert, C.; Mändl, S. Surface & Coatings Technology Corrosion Behaviour of Medical CoCr Alloy after Nitrogen Plasma Immersion Ion Implantation. *Surf. Coat. Technol.* **2011**, *205* (8–9), 3043–3049.
[79] Lutz, J.; Lehmann, A.; Mändl, S. Nitrogen Diffusion in Medical CoCrNiW Alloys after Plasma Immersion Ion Implantation. **2008**, *202*, 3747–3753.
[80] Cao, G.; O'Brien, C. D.; Zhou, Z.; Sanders, S. M.; Greenbaum, J. N.; Makrigiannakis, A.; DeLisser, H. M. Involvement of Human PECAM-1 in Angiogenesis and in Vitro Endothelial Cell Migration. *Am.J.Physiol Cell Physiol* **2002**, *282* (5), C1181–C1190.
[81] Jones, C. I.; Garner, S. F.; Moraes, L. A.; Kaiser, W. J.; Rankin, A.; Ouwehand, W. H.; Goodall, A. H.; Gibbins, J. M. PECAM-1 Expression and Activity Negatively Regulate Multiple Platelet Signaling Pathways. *FEBS Lett.* **2009**, *583* (22), 3618–3624.
[82] Jackson, D. E. The Unfolding Tale of PECAM-1. *FEBS Lett.* **2003**, *540* (1–3), 7–14.
[83] Caligiuri, G.; Nicoletti, A. Patent: Use of CD31 Peptides in the Treatment of Atherothrombosis and Autoimmune Disorders. *WO 2010/000741 A1* **2009**.
[84] Meyer-Plath, A. A.; Schröder, K.; Finke, B.; Ohl, A. Current Trends in Biomaterial Surface Functionalization—nitrogen-Containing Plasma Assisted Processes with Enhanced Selectivity. *Vacuum* **2003**, *71* (3), 391–406.
[85] Takahashi, H.; Letourneur, D.; Grainger, D. W. Delivery of Large Biopharmaceuticals from Cardiovascular Stents: A Review. *Biomacromolecules* **2007**, *8* (11), 3281–3293.
[86] Milleret, V.; Ziogas, A.; Buzzi, S.; Heuberger, R.; Zucker, A.; Ehrbar, M. Effect of Oxide Layer Modification of CoCr Stent Alloys on Blood Activation and Endothelial Behavior. *J. Biomed. Mater. Res. Part B Appl. Biomater.* **2015**, *103* (3), 629–640.
[87] Hodgson, A. W. E.; Kurz, S.; Virtanen, S.; Fervel, V.; Olsson, C.-O. A.; Mischler, S. Passive and Transpassive Behaviour of CoCrMo in Simulated Biological Solutions. *Electrochim. Acta* **2004**, *49* (13), 2167–2178.

[88] Chevallier, P.; Castonguay, M.; Turgeon, S.; Dubrulle, N.; Mantovani, D.; McBreen, P. H.; Wittmann, J.-C.; Laroche, G. Ammonia RF−Plasma on PTFE Surfaces: Chemical Characterization of the Species Created on the Surface by Vapor−Phase Chemical Derivatization. *J. Phys. Chem. B* **2001**, *105* (50), 12490–12497.
[89] Cheruthazhekatt, S.; Černák, M.; Slavíček, P.; Havel, J. Gas Plasmas and Plasma Modified Materials in Medicine. *J. Appl. Biomed.* **2010**, *8* (2), 55–66.
[90] Schr, K.; Finke, B.; Ohl, A. Current Trends in Biomaterial Surface Functionalization — Nitrogen-Containing Plasma Assisted Processes with Enhanced Selectivity. *Vacuum* **2003**, *71*, 391–406.
[91] Siow, K. S.; Britcher, L.; Kumar, S.; Griesser, H. J. Plasma Methods for the Generation of Chemically Reactive Surfaces for Biomolecule Immobilization and Cell Colonization - A Review. **2006**, 392–418.
[92] Almeida, E. Surface Treatments and Coatings for Metals. A General Overview. 1. Surface Treatments, Surface Preparation, and the Nature of Coatings. *Ind. Eng. Chem. Res.* **2001**, *40* (1), 3–14.
[93] Sojitra, P.; Engineer, C.; Kothwala, D.; Raval, A.; Kotadia, H.; Mehta, G. Electropolishing of 316LVM Stainless Steel Cardiovascular Stents: An Investigation of Material Removal, Surface Roughness and Corrosion Behaviour. *Trends Biomater. Artif. Organs* **2010**, *23* (3), 115–121.
[94] Dorri, M. M.; Turgeon, S.; Cloutier, M.; Chevallier, P.; Mantovani, D. Nano-Thick Amorphous Oxide Layer Produced by Plasma on Stainless Steel 316L for Improved Corrosion Resistance under Plastic Deformation. *CORROSION* **2018**, 2674.
[95] Wu, G.; Li, P.; Feng, H.; Zhang, X.; Chu, P. K. Engineering and Functionalization of Biomaterials via Surface Modification. *J. Mater. Chem. B* **2015**, *3* (10), 2024–2042.
[96] Jackson, D. E. The Unfolding Tale of PECAM-1. *FEBS Lett.* **2003**, *540* (1–3), 7–14.
[97] Jones, C. I.; Garner, S. F.; Moraes, L. A.; Kaiser, W. J.; Rankin, A.; Ouwehand, W. H.; Goodall, A. H.; Gibbins, J. M. PECAM-1 Expression and Activity Negatively Regulate Multiple Platelet Signaling Pathways. *FEBS Lett.* **2009**, *583* (22), 3618–3624.
[98] Newman, P. J.; Newman, D. K. Signal Transduction Pathways Mediated by PECAM-1 New Roles for an Old Molecule in Platelet and Vascular Cell Biology. *Arterioscler. Thromb. Vasc. Biol.* **2003**, *23* (6), 953–964.
[99] Ming, Z.; Hu, Y.; Xiang, J.; Polewski, P.; Newman, P. J.; Newman, D. K. Lyn and PECAM-1 Function as Interdependent Inhibitors of Platelet Aggregation. *Blood* **2011**, *117* (14), 3903–3906.
[100] Privratsky, J. R.; Newman, D. K.; Newman, P. J. PECAM-1 : Con Fl Icts of Interest in Inflammation. *Life Sci.* **2010**, *87*, 69–82.
[101] Lhoest, J.-B.; Wagner, M. S.; Tidwell, C. D.; Castner, D. G. Characterization of Adsorbed Protein Films by Time of Flight Secondary Ion Mass Spectrometry. *J. Biomed. Mater. Res.* **2001**, *57* (3), 432–440.
[102] Galon, M. Z.; Takimura, C. K.; Figueira Chaves, M. J.; de Campos, J. C.; Eduardo Krieger, J.; Gutierrez, P. S.; Laurindo, F. R. M.; Filho, R. K.; Neto, P. A. L. Porcine Model for the Evaluation and Development of Catheter-Based Coronary Devices: An Essential Preclinical Tool. *Rev. Bras. Cardiol. Invasiva (English Ed.* **2013**, *21* (4), 378–383.
[103] Brunski, J. B. Metals: Basic Principles. In *Biomaterials Science: An Introduction to Materials: Third Edition*; Elsevier, 2013; Vol. 69, pp 111–119.
[104] Lewis, F.; Horny, P.; Hale, P.; Turgeon, S.; Tatoulian, M.; Mantovani, D. Study of the Adhesion of Thin Plasma Fluorocarbon Coatings Resisting Plastic Deformation for Stent Applications. *J. Phys. D. Appl. Phys.* **2008**, *41* (4), 045310.
[105] Holvoet, S.; Chevallier, P.; Turgeon, S.; Mantovani, D. Toward High-Performance Coatings for Biomedical Devices: Study on Plasma-Deposited Fluorocarbon Films and Ageing in PBS. *Materials (Basel).* **2010**, *3* (3), 1515–1532.
[106] Touzin, M.; Chevallier, P.; Lewis, F.; Turgeon, S.; Holvoet, S.; Laroche, G.; Mantovani, D. Study on the Stability of Plasma-Polymerized Fluorocarbon Ultra-Thin Coatings on Stainless Steel in Water. *Surf. Coatings Technol.* **2008**, *202* (19), 4884–4891.
[107] Xi, T.; Gao, R.; Xu, B.; Chen, L.; Luo, T.; Liu, J.; Wei, Y.; Zhong, S. In Vitro and in Vivo Changes to PLGA/Sirolimus Coating on Drug Eluting Stents. *Biomaterials* **2010**, *31* (19), 5151–5158.
[108] Kang, C. K.; Lee, Y. S. Carbohydrate Polymer Grafting on Stainless Steel Surface and Its Biocompatibility Study. *J. Ind. Eng. Chem.* **2012**, *18* (5), 1670–1675.
[109] Song, S.-J.; Park, Y. J.; Park, J.; Cho, M. D.; Kim, J.-H.; Jeong, M. H.; Kim, Y. S.; Cho, D. L. Preparation of a Drug-Eluting Stent Using a TiO2 Film Deposited by Plasma Enhanced Chemical Vapour Deposition as a Drug-Combining Matrix. *J. Mater. Chem.* **2010**, *20* (23), 4792.

[110] Zhong, Q.; Yan, J.; Qian, X.; Zhang, T.; Zhang, Z.; Li, A. Atomic Layer Deposition Enhanced Grafting of Phosphorylcholine on Stainless Steel for Intravascular Stents. *Colloids Surfaces B Biointerfaces* **2014**, *121*, 238–247.
[111] Thiruppathi, E.; Larson, M. K.; Mani, G. Surface Modification of CoCr Alloy Using Varying Concentrations of Phosphoric and Phosphonoacetic Acids: Albumin and Fibrinogen Adsorption, Platelet Adhesion, Activation, and Aggregation Studies. *Langmuir* **2015**, *31* (1), 358–370.
[112] Klages, C.-P.; Kotula, S. Critical Remarks on Chemical Derivatization Analysis of Plasma-Treated Polymer Surfaces and Plasma Polymers. *Plasma Process. Polym.* **2016**, *13* (12), 1213–1223.
[113] Migliavacca, F.; Petrini, L.; Montanari, V.; Quagliana, I.; Auricchio, F.; Dubini, G. A Predictive Study of the Mechanical Behaviour of Coronary Stents by Computer Modelling. *Med. Eng. Phys.* **2005**, *27* (1), 13–18.
[114] Cloutier, M.; Turgeon, S.; Chevallier, P.; Mantovani, D. On the Interface between Plasma Fluorocarbon Films and 316L Stainless Steel Substrates for Advanced Coated Stents. *Adv. Mater. Res.* **2011**, *409*, 117–122.
[115] Diaz-Rodriguez, S.; Chevallier, P.; Mantovani, D. Low-Pressure Plasma Treatment for Direct Amination of L605 CoCr Alloy for the Further Covalent Grafting of Molecules. *Plasma Process. Polym.* **2018**, No. January, e1700214.
[116] Hryniewicz, T.; Rokicki, R.; Rokosz, K. Co–Cr Alloy Corrosion Behaviour after Electropolishing and "Magnetoelectropolishing" Treatments. *Mater. Lett.* **2008**, *62* (17–18), 3073–3076.
[117] Tian, Y.; Cao, H.; Qiao, Y.; Liu, X. Antimicrobial and Osteogenic Properties of Iron-Doped Titanium. *RSC Adv.* **2016**, *6* (52), 46495–46507.
[118] Ghosh, S.; Bhattacharyya, R.; Saha, H.; Chaudhuri, C. R.; Mukherjee, N. Functionalized ZnO/ZnO 2 N–N Straddling Heterostructure Achieved by Oxygen Plasma Bombardment for Highly Selective Methane Sensing. *Phys. Chem. Chem. Phys.* **2015**, *17* (41), 27777–27788.
[119] Sojitra, P.; Engineer, C.; Kothwala, D.; Raval, A.; Kotadia, H.; Mehta, G. Electropolishing of 316LVM Stainless Steel Cardiovascular Stents: An Investigation of Material Removal, Surface Roughness and Corrosion Behaviour. *Trends Biomater. Artif. Organs* **2010**, *23* (3), 115–121.
[120] Lewis, F.; Mantovani, D. Methods to Investigate the Adhesion of Soft Nano-Coatings on Metal Substrates - Application to Polymer-Coated Stents. *Macromol. Mater. Eng.* **2009**, *294* (1), 11–19.
[121] Loy, C.; Pezzoli, D.; Candiani, G.; Mantovani, D. A Cost-Effective Culture System for the In Vitro Assembly, Maturation, and Stimulation of Advanced Multilayered Multiculture Tubular Tissue Models. *Biotechnol. J.* **2018**, *13* (1), 1700359.
[122] Grisaffe, S. J.; Lowell, C. E. Examination of Oxide Scales on Heat Resisting Alloys. *NASA Tech. Note* **1969**, *D-5019*, 1–41.
[123] Wang, J.; Zhou, X.; Thompson, G. E.; Hunter, J. A.; Yuan, Y. Delamination of Near-Surface Layer on Cold Rolled AlFeSi Alloy during Sheet Forming. *Mater. Charact.* **2015**, *99*, 109–117.
[124] Mändl, S.; Díaz, C.; Gerlach, J. W.; García, J. A. Near Surface Analysis of Duplex PIII Treated CoCr Alloys. *Nucl. Instruments Methods Phys. Res. Sect. B Beam Interact. with Mater. Atoms* **2013**, *307*, 305–309.
[125] Jasaitis, D.; Beganskienė, A.; Senvaitienė1, J.; Kareiva, A.; Ramanauskas, R.; Juškėnas, R.; Selskis, A. Sol-Gel Synthesis and Characterization of Cobalt Chromium Spinel CoCr2O4. *Chemija* **2011**, *22* (2), 125–130.
[126] Tanaka, Y.; Saito, H.; Tsutsumi, Y.; Doi, H.; Imai, H.; Hanawa, T. Active Hydroxyl Groups on Surface Oxide Film of Titanium, 316L Stainless Steel, and Cobalt-Chromium-Molybdenum Alloy and Its Effect on the Immobilization of Poly(Ethylene Glycol). *Mater. Trans.* **2008**, *49* (4), 805–811.
[127] Allen, M. J.; Myer, B. J.; Millett, P. J.; Rushton, N. THE EFFECTS OF PARTICULATE COBALT, CHROMIUM AND COBALT-CHROMIUM ALLOY ON HUMAN OSTEOBLAST-LIKE CELLS IN VITRO. *J. Bone Joint Surg. Br.* **1997**, *79–B* (3), 475–482.
[128] Anissian, L.; Stark, A.; Dahlstrand, H.; Granberg, B.; Good, V.; Bucht, E. Cobalt Ions Influence Proliferation and Function of Human Osteoblast-like Cells. *Acta Orthop. Scand.* **2002**, *73* (3), 369–374.
[129] Permenter, M. G.; Dennis, W. E.; Sutto, T. E.; Jackson, D. A.; Lewis, J. A.; Stallings, J. D. Exposure to Cobalt Causes Transcriptomic and Proteomic Changes in Two Rat Liver Derived Cell Lines. *PLoS One* **2013**, *8* (12), e83751.
[130] Simonsen, L. O.; Harbak, H.; Bennekou, P. Cobalt Metabolism and Toxicology—A Brief Update. *Sci. Total Environ.* **2012**, *432*, 210–215.

[131] Rokicki, R.; Haider, W.; Maffi, S. K. Hemocompatibility Improvement of Chromium-Bearing Bare-Metal Stent Platform After Magnetoelectropolishing. *J. Mater. Eng. Perform.* **2015**, *24* (1), 345–352.
[132] Yang, Y.; Franzen, S. F.; Olin, C. L. In Vivo Comparison of Hemocompatibility of Materials Used in Mechanical Heart Valves. *J. Heart Valve Dis.* **1996**, *5* (5), 532–537.
[133] Mani, G.; Feldman, M. D.; Patel, D.; Agrawal, C. M. Coronary Stents: A Materials Perspective. *Biomaterials* **2007**, *28* (9), 1689–1710.
[134] Lange, R. A.; Willard, J. E.; Hillis, L. D. Restenosis: The Achilles Heel of Coronary Angioplasty. *Am. J. Med. Sci.* **1993**, *306* (4), 265–275.
[135] Holmes, D. R.; Schwartz, R. S.; Webster, M. W. I. Coronary Restenosis: What Have We Learned from Angiography? *J. Am. Coll. Cardiol.* **1991**, *17* (6 SUPPL. 2), 14–22.
[136] Dangas, G.; Fuster, V. Management of Restenosis after Coronary Intervention. *Am. Heart J.* **1996**, *132* (2), 428–436.
[137] Granada, J. F.; Kaluza, G. L.; Raizner, A. Drug-Eluting Stents for Cardiovascular Disorders. *Curr. Atheroscler. Rep.* **2003**, *5* (4), 308–316.
[138] Takahashi, H.; Letourneur, D.; Grainger, D. W. Delivery of Large Biopharmaceuticals from Cardiovascular Stents: A Review. *Biomacromolecules* **2007**, *8* (11), 3281–3293.
[139] Takano, M.; Yamamoto, M.; Mizuno, M.; Murakami, D.; Inami, T.; Kimata, N.; Murai, K.; Kobayashi, N.; Okamatsu, K.; Ohba, T.; et al. Late Vascular Responses from 2 to 4 Years after Implantation of Sirolimus-Eluting Stents : Serial Observations by Intracoronary Optical Coherence Tomography. *Circ. Cardiovasc. Interv.* **2010**, *3* (5), 476–483.
[140] Byrne, R. A.; Iijima, R.; Mehilli, J.; Pinieck, S.; Bruskina, O.; Schömig, A.; Kastrati, A. Durability of Antirestenotic Efficacy in Drug-Eluting Stents With and Without Permanent Polymer. *JACC Cardiovasc. Interv.* **2009**, *2* (4), 291–299.
[141] Kastrati, A.; Byrne, R. New Roads, New Ruts. *JACC Cardiovasc. Interv.* **2011**, *4* (2), 165–167.
[142] Vallières, K.; Petitclerc, É.; Laroche, G. Covalent Grafting of Fibronectin onto Plasma-Treated PTFE: Influence of the Conjugation Strategy on Fibronectin Biological Activity. *Macromol. Biosci.* **2007**, *7* (5), 738–745.
[143] Lowe, H. C.; Oesterle, S. N.; Khachigian, L. M. Coronary In-Stent Restenosis: Current Status and Future Strategies. *J. Am. Coll. Cardiol.* **2002**, *39* (2), 183–193.
[144] Kim, J. M.; Bae, I.-H.; Lim, K. S.; Park, J.-K.; Park, D. S.; Lee, S.-Y.; Jang, E.-J.; Ji, M. S.; Sim, D. S.; Hong, Y. J.; et al. A Method for Coating Fucoidan onto Bare Metal Stent and in Vivo Evaluation. *Prog. Org. Coatings* **2015**, *78*, 348–356.
[145] Mani, G.; Feldman, M. D.; Patel, D.; Agrawal, C. M. Coronary Stents: A Materials Perspective. *Biomaterials* **2007**, *28* (9), 1689–1710.
[146] Caligiuri, G.; Nicoletti, A. Patent: Use of CD31 Peptides in the Treatment of Atherothrombosis and Autoimmune Disorders. *Wo 2010/000741 a1*. January 8, 2009.
[147] Ming, Z.; Hu, Y.; Xiang, J.; Polewski, P.; Newman, P. J.; Newman, D. K. Lyn and PECAM-1 Function as Interdependent Inhibitors of Platelet Aggregation. *Blood* **2011**, *117* (14), 3903–3906.
[148] Cao, G.; O'Brien, C. D.; Zhou, Z.; Sanders, S. M.; Greenbaum, J. N.; Makrigiannakis, A.; DeLisser, H. M. Involvement of Human PECAM-1 in Angiogenesis and in Vitro Endothelial Cell Migration. *Am.J.Physiol Cell Physiol* **2002**, *282* (5), C1181–C1190.
[149] Roach, P.; Eglin, D.; Rohde, K.; Perry, C. C. Modern Biomaterials: A Review—bulk Properties and Implications of Surface Modifications. *J. Mater. Sci. Mater. Med.* **2007**, *18* (7), 1263–1277.
[150] Sydow-Plum, G.; Tabrizian, M. Review of Stent Coating Strategies: Clinical Insights. *Mater. Sci. Technol.* **2008**, *24* (9), 1127–1143.
[151] Cloutier, M.; Turgeon, S.; Chevallier, P.; Mantovani, D. On the Interface between Plasma Fluorocarbon Films and 316L Stainless Steel Substrates for Advanced Coated Stents. *Adv. Mater. Res.* **2011**, *409*, 117–122.
[152] Diaz-Rodriguez, S.; Chevallier, P.; Mantovani, D. Low-Pressure Plasma Treatment for Direct Amination of L605 CoCr Alloy for the Further Covalent Grafting of Molecules. *Plasma Process. Polym.* **2018**, No. January, e1700214.

[153] John, A. A.; Subramanian, A. P.; Vellayappan, M. V.; Balaji, A.; Jaganathan, S. K.; Mohandas, H.; Paramalinggam, T.; Supriyanto, E.; Yusof, M. Review: Physico-Chemical Modification as a Versatile Strategy for the Biocompatibility Enhancement of Biomaterials. *RSC Adv.* **2015**, *5* (49), 39232–39244.
[154] Honari, G.; Ellis, S. G.; Wilkoff, B. L.; Aronica, M. A.; Svensson, L. G.; Taylor, J. S. Hypersensitivity Reactions Associated with Endovascular Devices. *Contact Dermatitis* **2008**, *59* (1), 7–22.
[155] Hu, Y.; Winn, S. R.; Krajbich, I.; Hollinger, J. O. Porous Polymer Scaffolds Surface-Modified with Arginine-Glycine-Aspartic Acid Enhance Bone Cell Attachment and Differentiationin Vitro. *J. Biomed. Mater. Res.* **2003**, *64A* (3), 583–590.
[156] Montaño-machado, V.; Hugoni, L.; Díaz-rodríguez, S.; Tolouei, R.; Pauthe, E.; Mantovani, D. A Comparison of Adsorbed and Grafted Fibronectin Coatings under Static and Dynamic Conditions. *Phys. Chem. Chem. Phys.* **2016**, *18* (35), 1–29.
[157] Holmes, C.; Tabrizian, M. Surface Functionalization of Biomaterials. In *Stem Cell Biology and Tissue Engineering in Dental Sciences*; Elsevier, 2015; pp 187–206.
[158] Campelo, C. S.; Chevallier, P.; Vaz, J. M.; Vieira, R. S.; Mantovani, D. Sulfonated Chitosan and Dopamine Based Coatings for Metallic Implants in Contact with Blood. *Mater. Sci. Eng. C* **2017**, *72*, 682–691.
[159] Vaz, J. M.; Taketa, T. B.; Hernandez-Montelongo, J.; Chevallier, P.; Cotta, M. A.; Mantovani, D.; Beppu, M. M. Antibacterial Properties of Chitosan-Based Coatings Are Affected by Spacer-Length and Molecular Weight. *Appl. Surf. Sci.* **2018**, *445*, 478–487.
[160] Loy, C.; Meghezi, S.; Lévesque, L.; Pezzoli, D.; Kumra, H.; Reinhardt, D.; Kizhakkedathu, J. N.; Mantovani, D. A Planar Model of the Vessel Wall from Cellularized-Collagen Scaffolds: Focus on Cell–matrix Interactions in Mono-, Bi- and Tri-Culture Models. *Biomater. Sci.* **2017**, *5* (1), 153–162.
[161] Dangas, G.; Fuster, V. Management of Restenosis after Coronary Intervention. *Am. Heart J.* **1996**, *132* (2), 428–436.
[162] Dejana, E.; Corada, M.; Lampugnani, M. G. Endothelial Cell-to-Cell Junctions. *FASEB J.* **1995**, *9* (10), 910–918.
[163] Dong, B.; Jiang, H.; Manolache, S.; Wong, A. C. L.; Denes, F. S. Plasma-Mediated Grafting of Poly(Ethylene Glycol) on Polyamide and Polyester Surfaces and Evaluation of Antifouling Ability of Modified Substrates. *Langmuir* **2007**, *23* (13), 7306–7313.
[164] Michel, E. C.; Montaño-Machado, V.; Chevallier, P.; Labbé-Barrère, A.; Letourneur, D.; Mantovani, D. Dextran Grafting on PTFE Surface for Cardiovascular Applications. *Biomatter* **2014**, *4* (1), F28805.
[165] Adams, M. R.; Kinlay, S.; Blake, G. J.; Orford, J. L.; Ganz, P.; Selwyn, a P. Pathophysiology of Atherosclerosis: Development, Regression, Restenosis. *Curr. Atheroscler. Rep.* **2000**, *2* (3), 251–258.
[166] Montaño-Machado, V.; Sikora-Jasinska, M.; Bortolan, C. C.; Chevallier, P.; Mantovani, D. Medical Devices: Coronary Stents. In *Reference Module in Biomedical Sciences*; Elsevier, 2017; pp 386–398.
[167] Kavey, R.-E. W. American Heart Association Guidelines for Primary Prevention of Atherosclerotic Cardiovascular Disease Beginning in Childhood. *Circulation* **2003**, *107* (11), 1562–1566.
[168] Mani, G.; Feldman, M. D.; Patel, D.; Agrawal, C. M. Coronary Stents: A Materials Perspective. *Biomaterials* **2007**, *28* (9), 1689–1710.
[169] Lange, R. A.; Willard, J. E.; Hillis, L. D. Restenosis: The Achilles Heel of Coronary Angioplasty. *Am. J. Med. Sci.* **1993**, *306* (4), 265–275.
[170] Granada, J. F.; Kaluza, G. L.; Raizner, A. Drug-Eluting Stents for Cardiovascular Disorders. *Curr. Atheroscler. Rep.* **2003**, *5* (4), 308–316.
[171] Byrne, R. A.; Iijima, R.; Mehilli, J.; Pinieck, S.; Bruskina, O.; Schömig, A.; Kastrati, A. Durability of Antirestenotic Efficacy in Drug-Eluting Stents With and Without Permanent Polymer. *JACC Cardiovasc. Interv.* **2009**, *2* (4), 291–299.
[172] Foin, N.; Lee, R. D.; Torii, R.; Guitierrez-Chico, J. L.; Mattesini, A.; Nijjer, S.; Sen, S.; Petraco, R.; Davies, J. E.; Di Mario, C.; et al. Impact of Stent Strut Design in Metallic Stents and Biodegradable Scaffolds. *Int. J. Cardiol.* **2014**, *177* (3), 800–808.
[173] Piccolo, R.; Pilgrim, T. How These Stent Design Characteristics May Affect PCI Outcomes Going Forward. The Impact of Thin-Strut, Biodegradable Polymer Stent Designs. *Card. Interv. today* **2017**, *11* (1), 43–46.
[174] Pache, J.; Kastrati, A.; Mehilli, J.; Schühlen, H.; Dotzer, F.; Hausleiter, J.; Fleckenstein, M.; Neuman, F. J.; Sattelberger, U.; Schmitt, C.; et al. Intracoronary Stenting and Angiographic Results: Strut Thickness Effect on Restenosis Outcome (ISAR-STEREO-2) Trial. *J. Am. Coll. Cardiol.* **2003**, *41* (8), 1283–1288.

[175] Diaz-Rodriguez, S.; Chevallier, P.; Mantovani, D. Low-Pressure Plasma Treatment for Direct Amination of L605 CoCr Alloy for the Further Covalent Grafting of Molecules. *Plasma Process. Polym.* **2018**, No. January, e1700214.
[176] Honari, G.; Ellis, S. G.; Wilkoff, B. L.; Aronica, M. A.; Svensson, L. G.; Taylor, J. S. Hypersensitivity Reactions Associated with Endovascular Devices. *Contact Dermatitis* **2008**, *59* (1), 7–22.
[177] Cao, G.; O'Brien, C. D.; Zhou, Z.; Sanders, S. M.; Greenbaum, J. N.; Makrigiannakis, A.; DeLisser, H. M. Involvement of Human PECAM-1 in Angiogenesis and in Vitro Endothelial Cell Migration. *Am.J.Physiol Cell Physiol* **2002**, *282* (5), C1181–C1190.
[178] Ming, Z.; Hu, Y.; Xiang, J.; Polewski, P.; Newman, P. J.; Newman, D. K. Lyn and PECAM-1 Function as Interdependent Inhibitors of Platelet Aggregation. *Blood* **2011**, *117* (14), 3903–3906.
[179] Jackson, D. E. The Unfolding Tale of PECAM-1. *FEBS Lett.* **2003**, *540* (1–3), 7–14.
[180] Caligiuri, G.; Nicoletti, A. Patent: Use of CD31 Peptides in the Treatment of Atherothrombosis and Autoimmune Disorders. *WO 2010/000741 A1* **2009**.
[181] Cook-Mills, J. M.; Marchese, M. E.; Abdala-Valencia, H. Vascular Cell Adhesion Molecule-1 Expression and Signaling During Disease: Regulation by Reactive Oxygen Species and Antioxidants. *Antioxid. Redox Signal.* **2011**, *15* (6), 1607–1638.
[182] Tanaka, T.; Narazaki, M.; Kishimoto, T. IL-6 in Inflammation, Immunity, and Disease. *Cold Spring Harb. Perspect. Biol.* **2014**, *6* (10), a016295–a016295.
[183] Wood, J. P.; Ellery, P. E. R.; Maroney, S. A.; Mast, A. E. Biology of Tissue Factor Pathway Inhibitor. *Blood* **2014**, *123* (19), 2934–2943.
[184] Montaño-machado, V.; Hugoni, L.; Díaz-rodríguez, S.; Tolouei, R.; Pauthe, E.; Mantovani, D. A Comparison of Adsorbed and Grafted Fibronectin Coatings under Static and Dynamic Conditions. *Phys. Chem. Chem. Phys.* **2016**, *18* (35), 1–29.
[185] Byrom, M. J.; Bannon, P. G.; White, G. H.; Ng, M. K. C. Animal Models for the Assessment of Novel Vascular Conduits. *J. Vasc. Surg.* **2010**, *52* (1), 176–195.
[186] Galon, M. Z.; Takimura, C. K.; Figueira Chaves, M. J.; de Campos, J. C.; Eduardo Krieger, J.; Gutierrez, P. S.; Laurindo, F. R. M.; Filho, R. K.; Neto, P. A. L. Porcine Model for the Evaluation and Development of Catheter-Based Coronary Devices: An Essential Preclinical Tool. *Rev. Bras. Cardiol. Invasiva (English Ed.* **2013**, *21* (4), 378–383.
[187] Heldman, A. W.; Cheng, L.; Jenkins, G. M.; Heller, P. F.; Kim, D.; Ware, M.; Nater, C.; Hruban, R. H.; Rezai, B.; Abella, B. S.; et al. Paclitaxel Stent Coating Inhibits Neointimal Hyperplasia at 4 Weeks in a Porcine Model of Coronary Restenosis. *Circulation* **2001**, *103* (18), 2289–2295.
[188] Leica Microsystems. Leica QWin Quick Start Guide. **2002**. http://www.microimage.com.cn/uploadfile/xwjs/uploadfile/201008/20100818011455516.pdf
[189] Cicala, G.; Creatore, M.; Favia, P.; Lamendola, R.; D'Agostino, R. Modulated Rf Discharges as an Effective Tool for Selecting Excited Species. *Appl. Phys. Lett.* **1999**, *75* (1), 37–39.
[190] Shahidzadeh, N.; Chehimi, M. M.; Arefi-Khonsari, F.; Amouroux, J.; Delamar, M. Evaluation of Acid-Base Properties of Ammonia Plasma-Treated Polypropylene by Means of XPS. *Plasmas Polym.* **1996**, *1* (1), 27–45.
[191] Chollet, C.; Chanseau, C.; Remy, M.; Guignandon, A.; Bareille, R.; Labrugère, C.; Bordenave, L.; Durrieu, M.-C. The Effect of RGD Density on Osteoblast and Endothelial Cell Behavior on RGD-Grafted Polyethylene Terephthalate Surfaces. *Biomaterials* **2009**, *30* (5), 711–720.